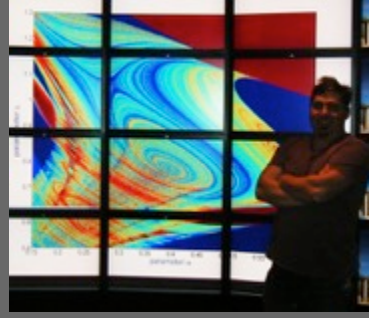

symbolic QUEST into Homoclinic Chaos

Andrey Shilnikov & Tingli Xing

Neuroscience Institute
Mathematics & Statistics
GSU Atlanta

when Shilnikov meets Lorenz

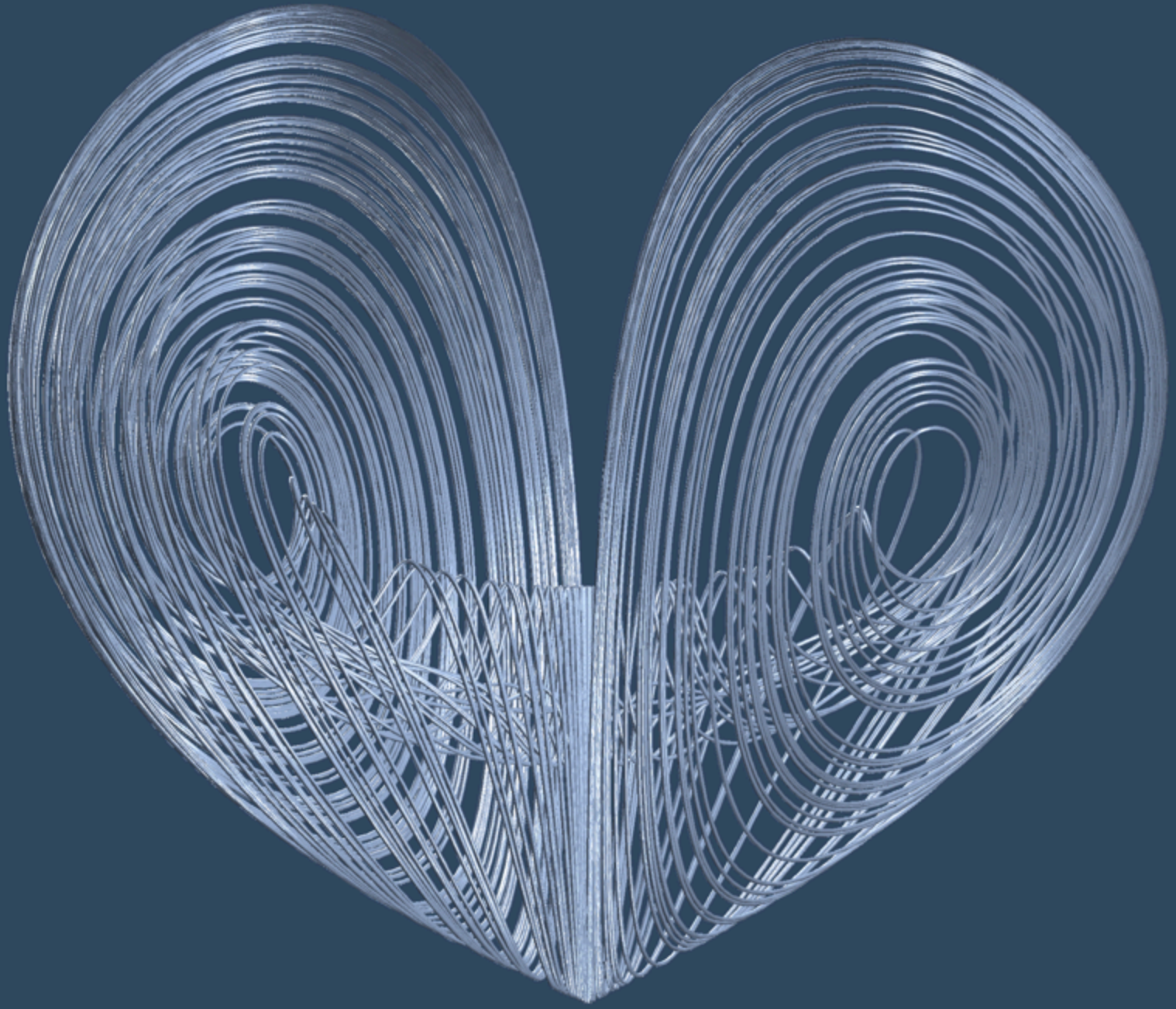

Kneadings
Symbolic dynamics
in unimodal 1D maps

isolated periodic points of f for each i, except in the case $i = p < \infty$, where it may also be a finite union of intervals. The basic sets are mutually disjoint except for the possibility that $\Omega_{p-1} \cap \Omega_p \neq \emptyset$ when $p < \infty$.

The renormalization of a unimodal map f can be understood on a symbolic level by means of kneading theory [14]. If $x \in I$ is not a pre-image of c, then the *kneading sequence* $k(x) = \{k_i(x)\}_{i \in N} \in \{-1, +1\}^N$ of x is defined by

$$k_0(x) = \begin{cases} +1 & \text{if } x < c \\ -1 & \text{if } x > c \end{cases}$$

and $k_i(x) = k_{i-1}(x) k_0(f^i(x))$ for each $i > 0$. For general $x \in I$, we can define upper and lower kneading sequences $k(x^+) = \lim_{y \searrow x} k(y)$ and $k(x^-) = \lim_{y \nearrow x} k(y)$, where the limits are taken in the product topology through points y which are not pre-images of c. It is clear that these limits exist, and are equal if and only if x is not a pre-image of c (in which case they are equal to $k(x)$). It is often convenient in dealing with particular examples to abbreviate the symbols $+1$ and -1 to $+$ and $-$ respectively. The *kneading invariant* of f is the sequence $k = k(c^-)$. From it we can construct a formal power series

$$P(t) = \sum_{i=0}^{\infty} k_i(c^-) t^i \qquad \textbf{t=1/2}$$

which will also be referred to as the kneading invariant of f.

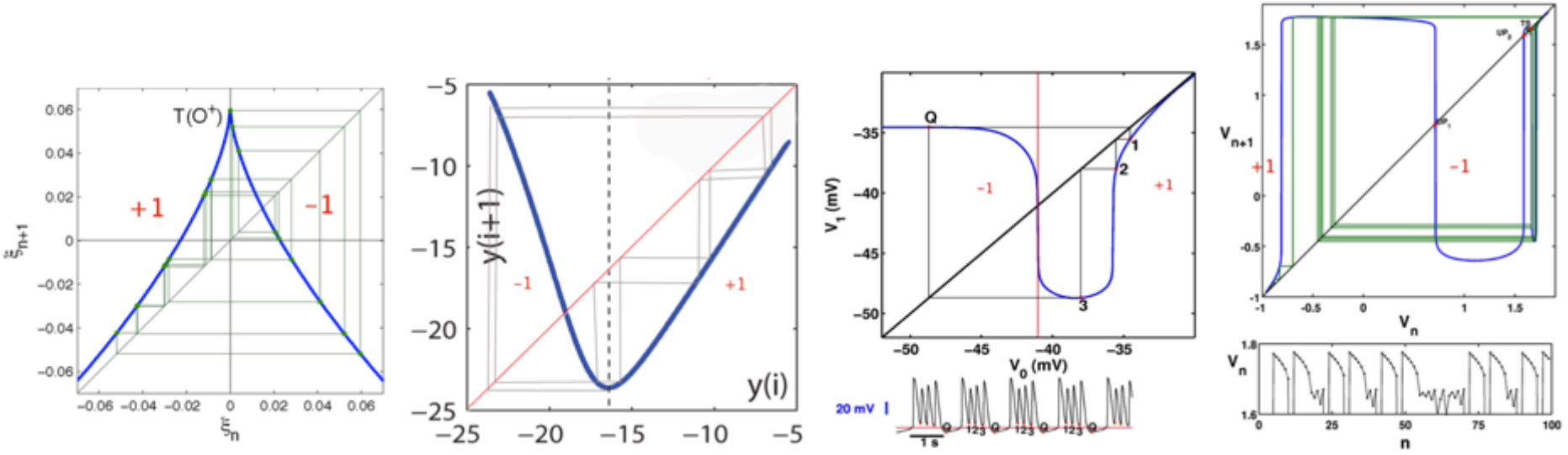

Figure 1: **1D unimodal maps admitting universal binary** $\{1, -1\}$ **description** for the forward iterates of the critical point, which are generated by trajectories of the following models: (a) Lorenz, (b) Rössler, (c) leech heart interneuron of a square-wave burster, and (d) phenomenological Fitzhugh-Nagumo-Rinzel elliptic burster displaying chaotic mixed-mode oscillations.

(1) $A = 0$, т. е.

(2) $\Gamma \not\subset W^{ss}$, т

(3) $\frac{1}{2} < \nu < 1$,

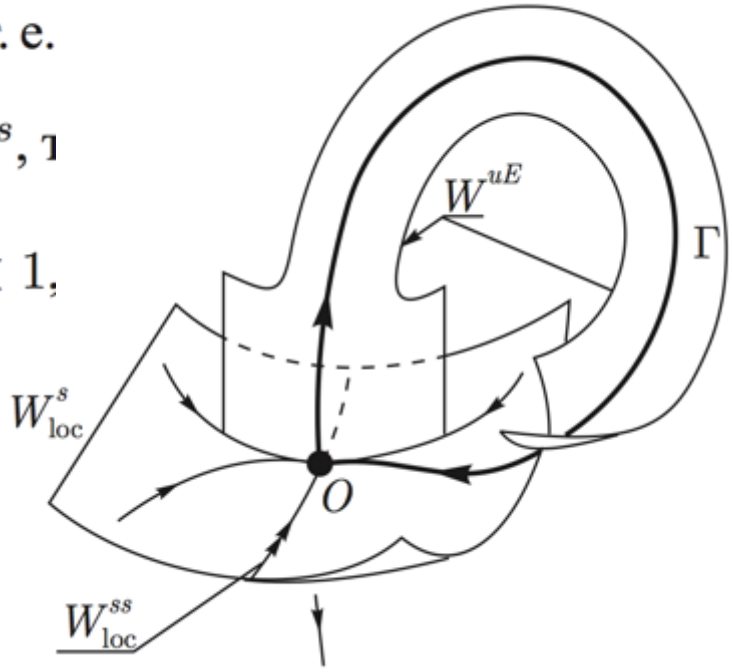

PhD. Part 1. 1962

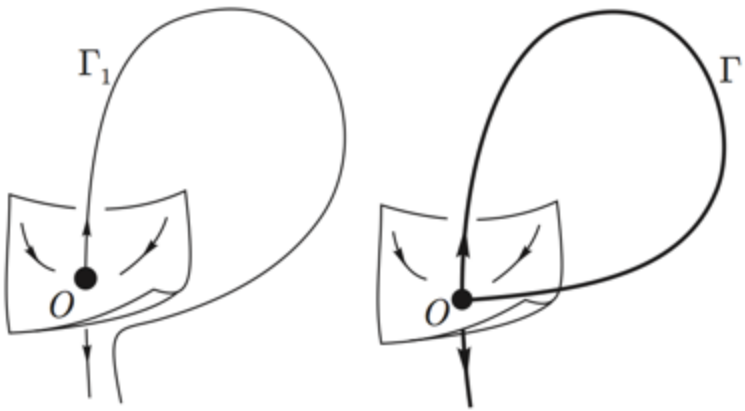

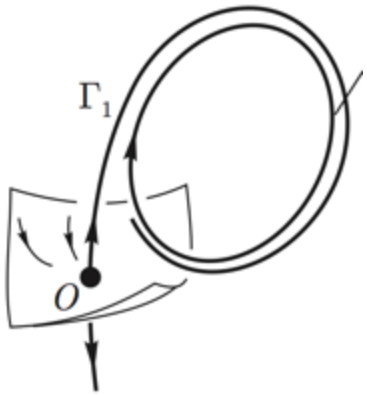

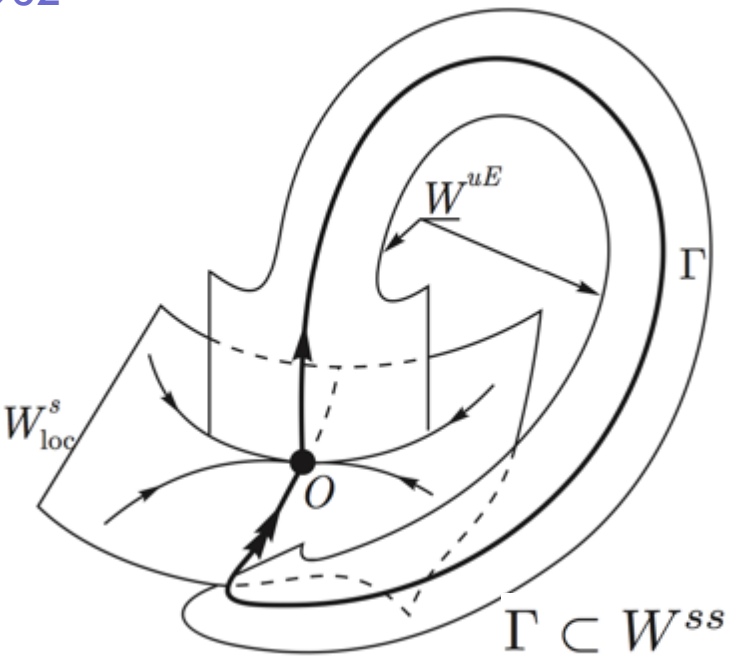

kneading sequence $\{\kappa_n\}$ is defined as follows:

$$\kappa_n = \begin{cases} +1, & \text{when } \Gamma^+ \text{ turns around the right saddle-focus } O_1, \\ 0, & \text{when } \Gamma^+ \text{ turns around the left saddle-focus } O_2. \end{cases} \quad (1)$$

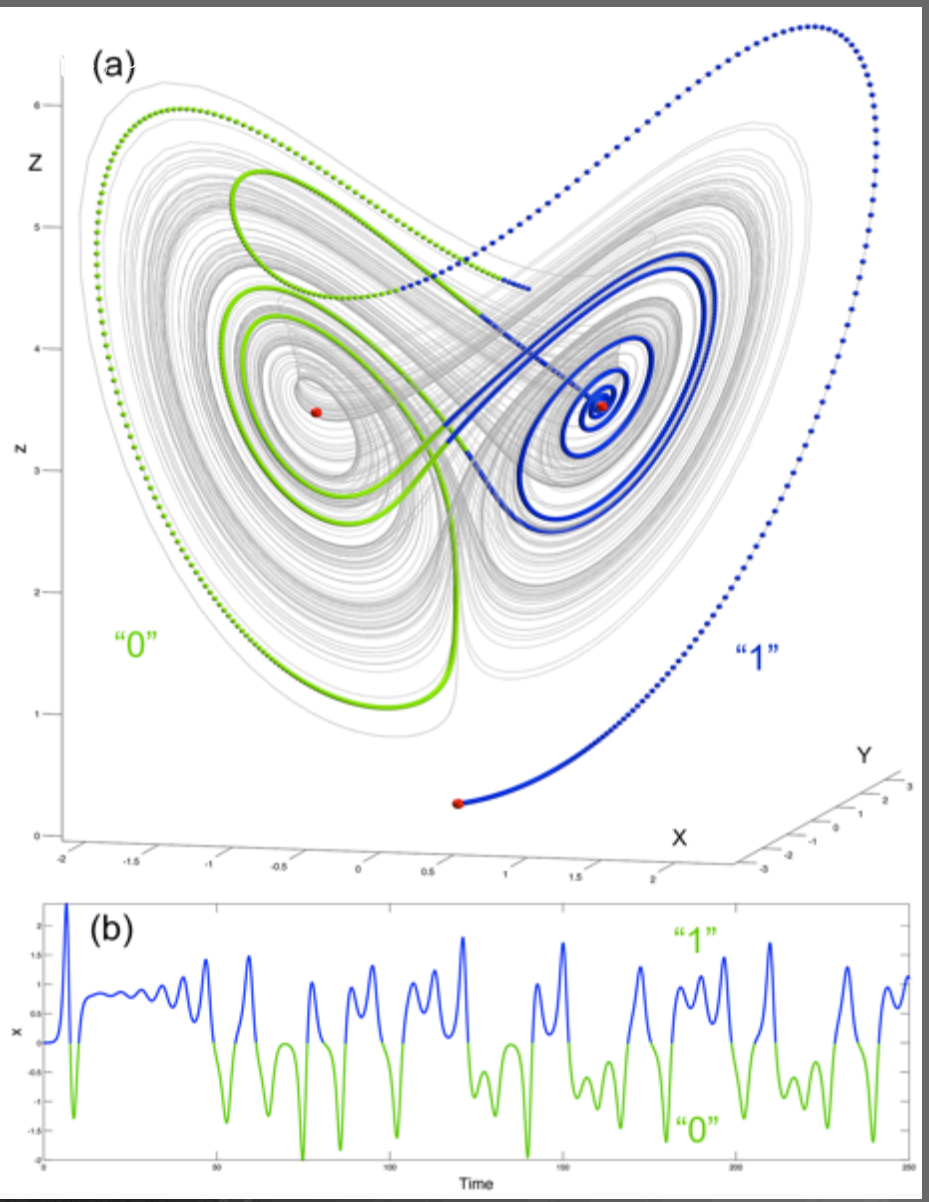

$$\{1, 0, 1, 1, 1, 1, 1, 0, 1, 0, 0 \dots\}$$

$$K(q, \mu) = \sum_{n=0}^{\infty} \kappa_n \, q^n,$$

The Homoclinic Garden (HG) model

$$\begin{aligned} \dot{x} &= -x + y, \\ \dot{y} &= (3 + \mu_1)x + y(1 + \mu_2) - xz \\ \dot{z} &= -(2 + \mu_3)z + xy; \end{aligned}$$

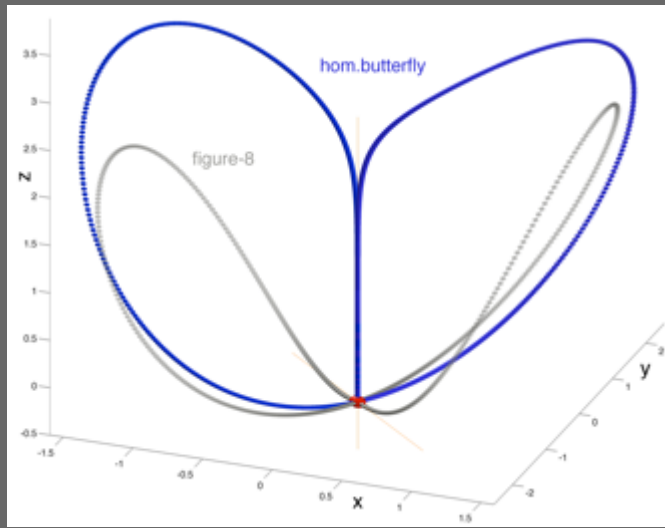

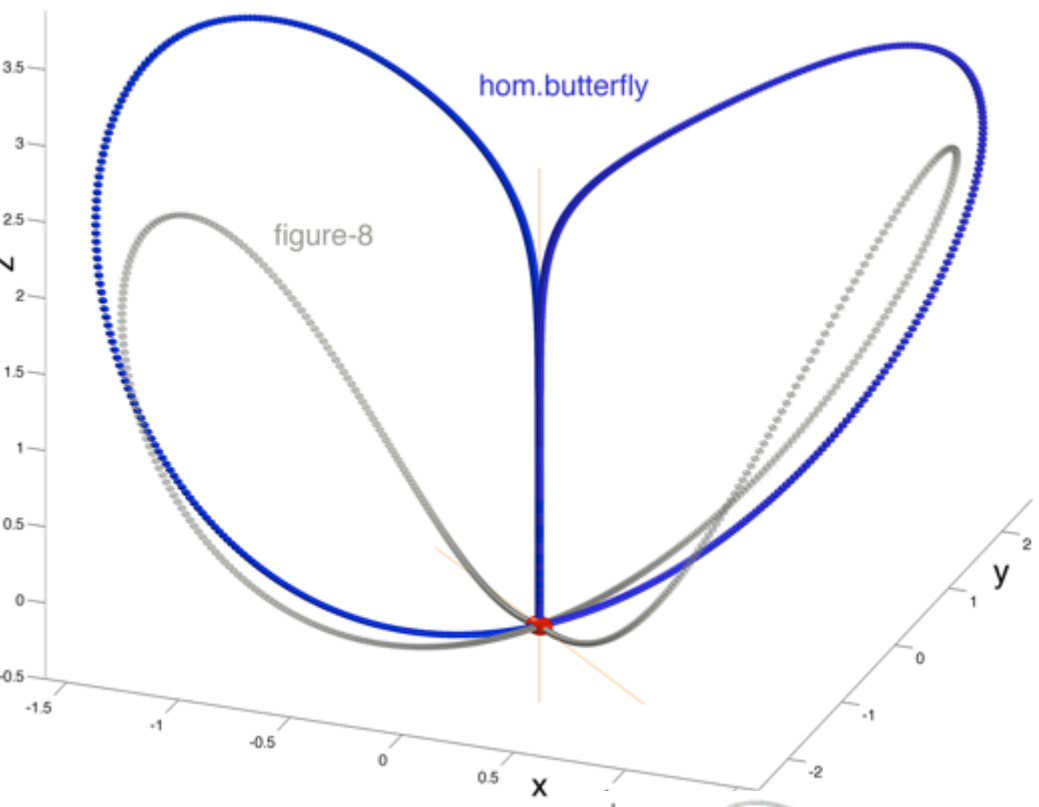
hom.butterfly
figure-8
x
y
z

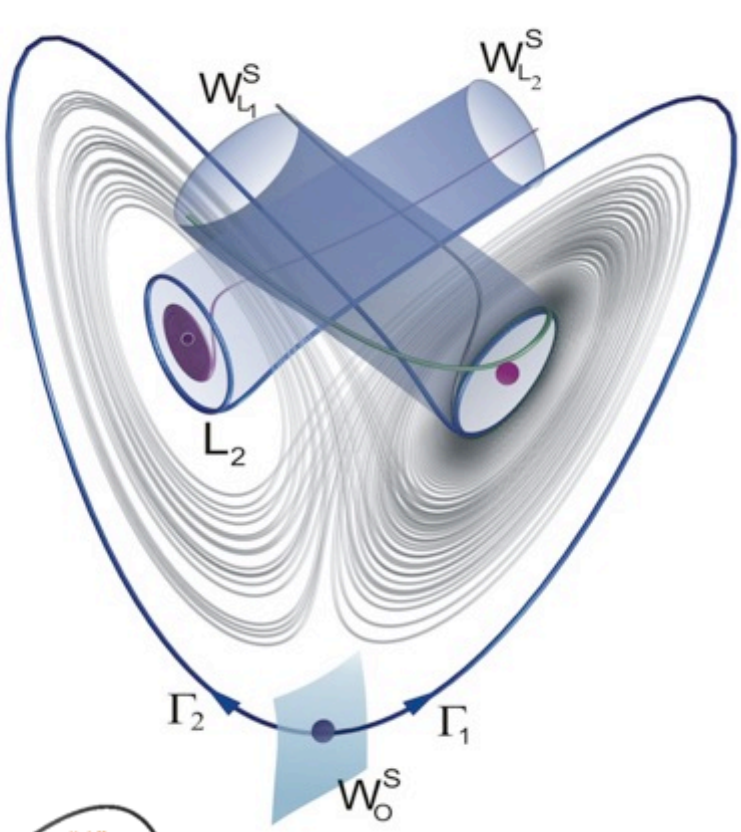
$W^s_{L_1}$
$W^s_{L_2}$
L_2
Γ_2
Γ_1
W^s_O

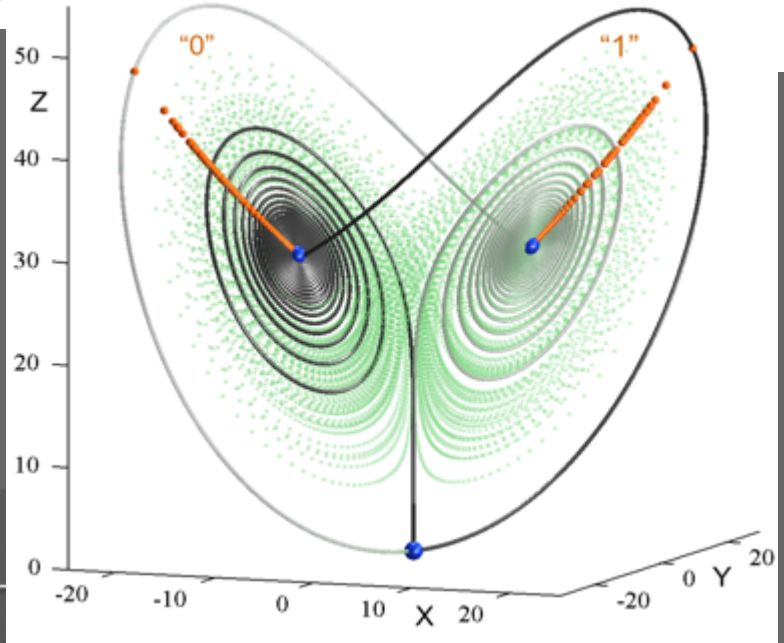
"0"
"1"
Z
X
Y

Department of Mathematics & Statistics
College of Arts & Sciences

Lorenz attractor in the Shimizu-Morioka model

$$\dot{x} = y, \quad \dot{y} = x - \alpha y - xz, \quad \dot{z} = -\beta z + x^2.$$

Bifurcation parameter continuation

Content, Auto, MatCont

Lyapunov exp. Sweeping

Morse-Smale vs. chaotic dynamics

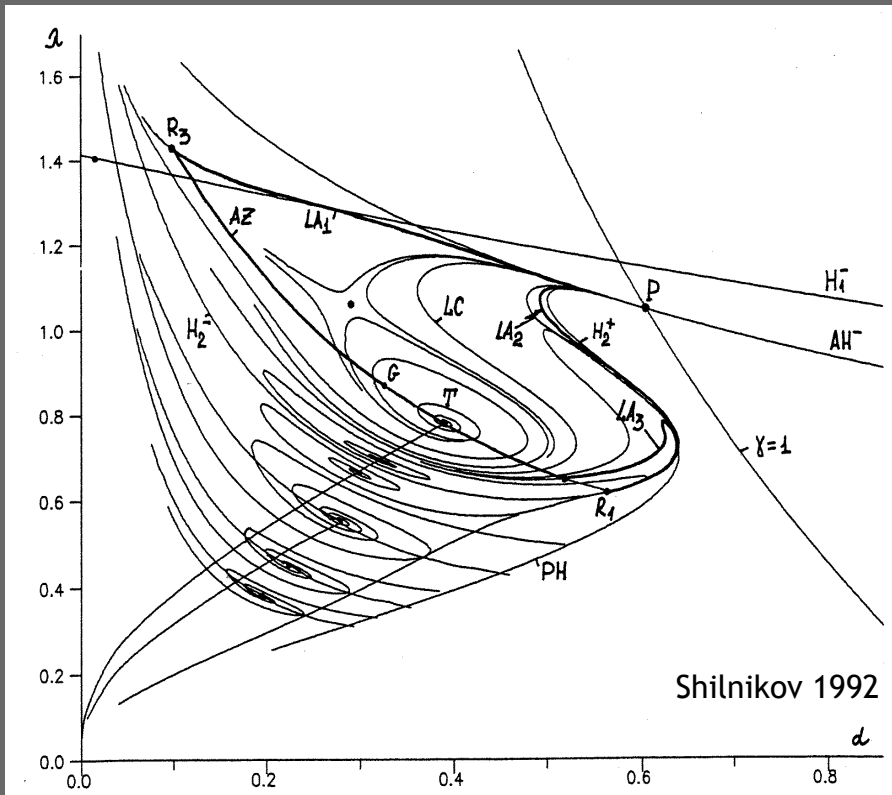

Fig. 13. The (α, λ) bifurcation diagram for $B = 0$.

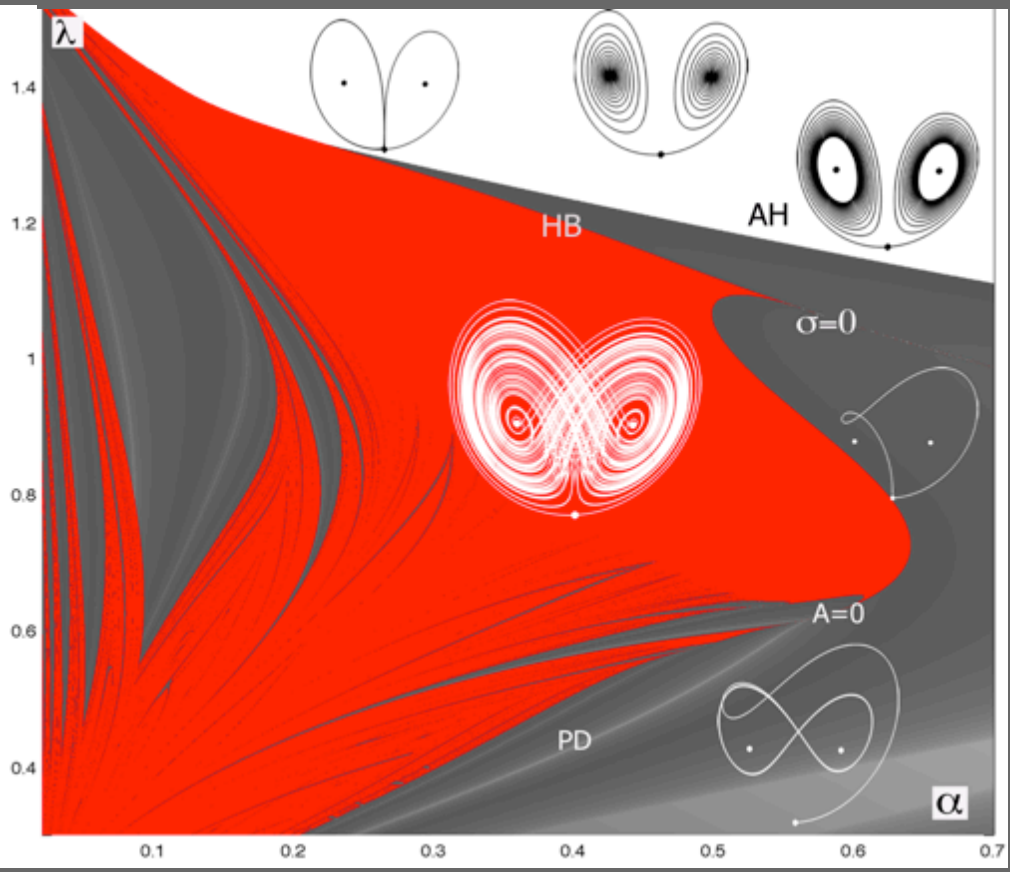

Shimizu-Morioka model

bi-parametric kneading scans

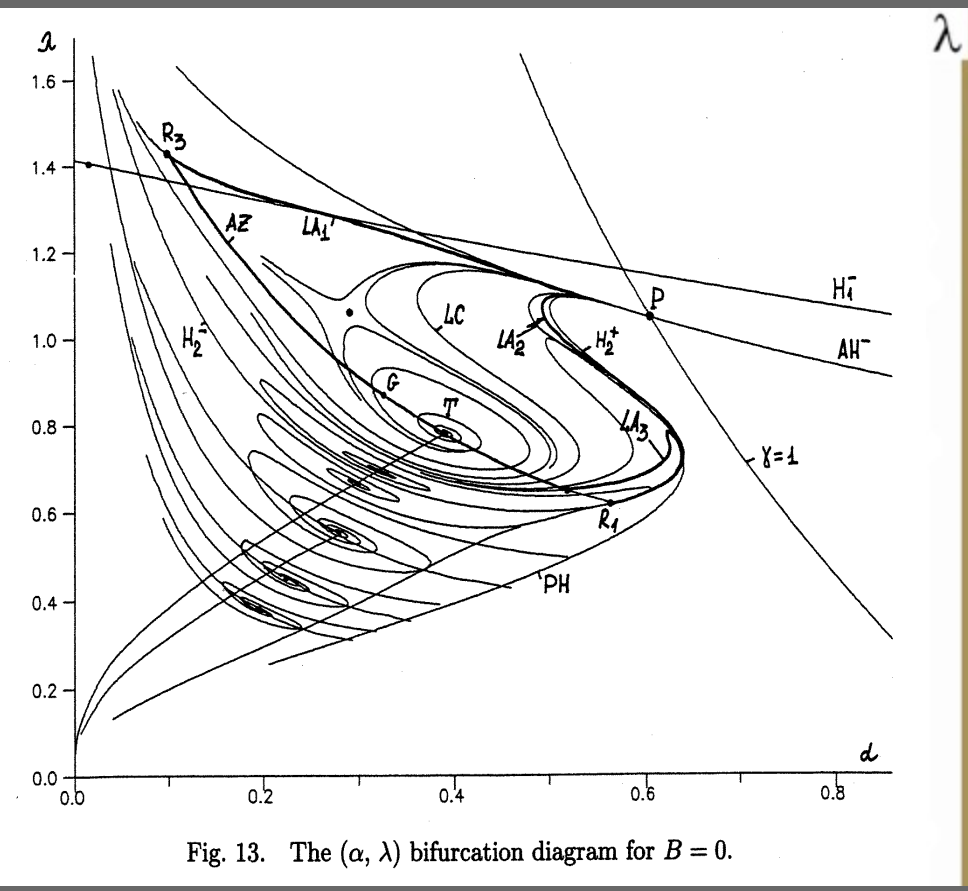

Fig. 13. The (α, λ) bifurcation diagram for $B = 0$.

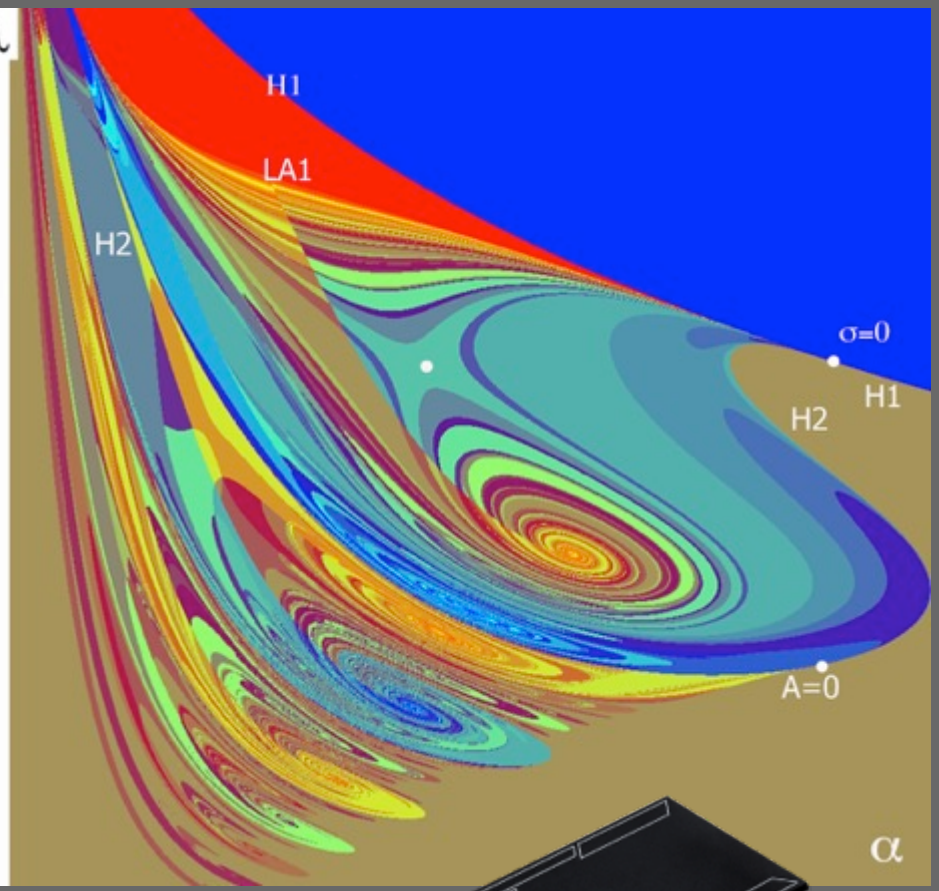

Depth of symbolic scanning: “homoclinic hunting”

single kneading 2-2

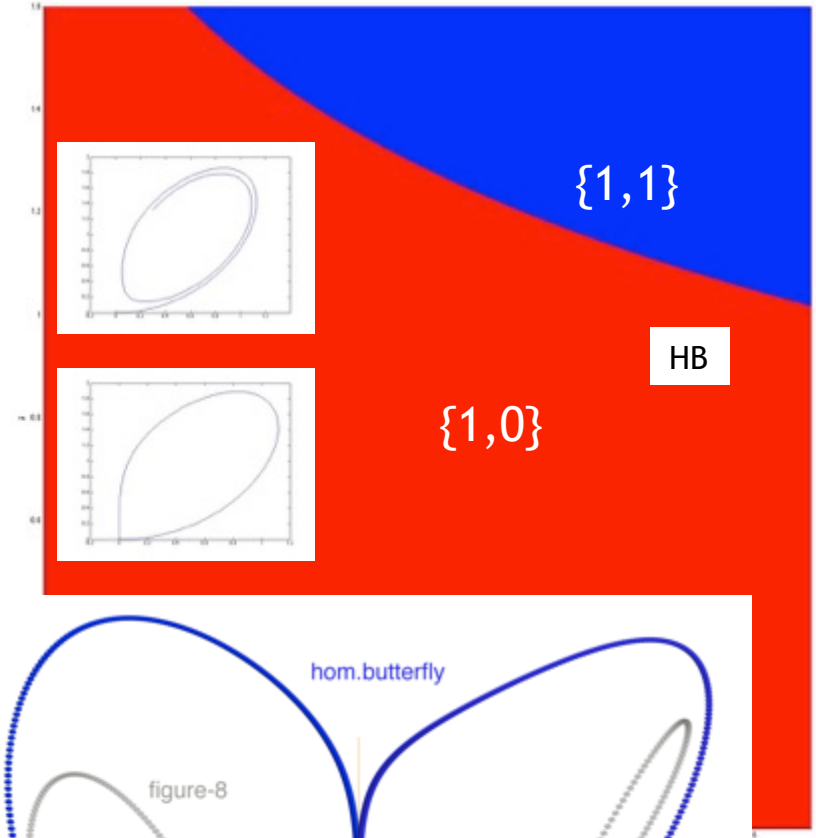

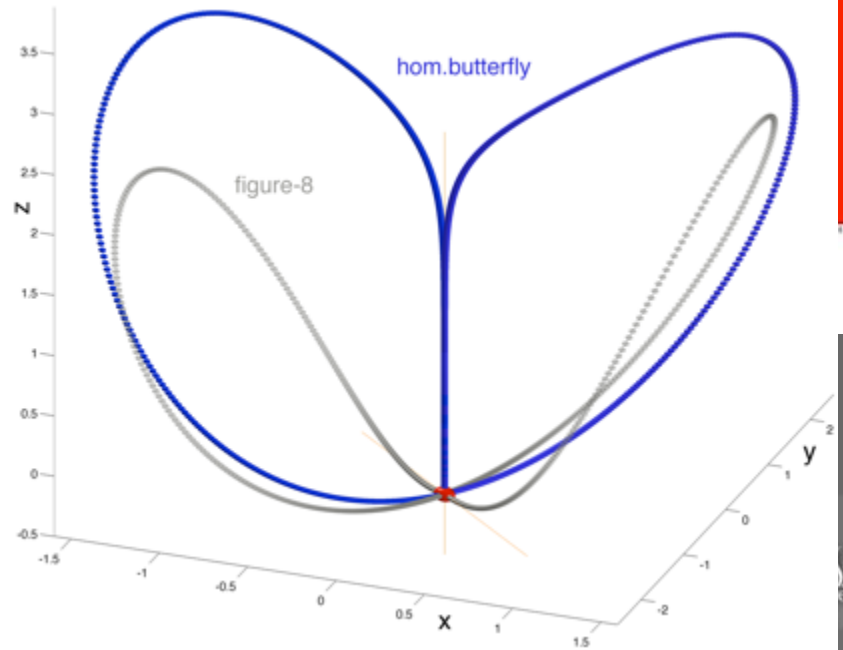

Two kneading: 2-3

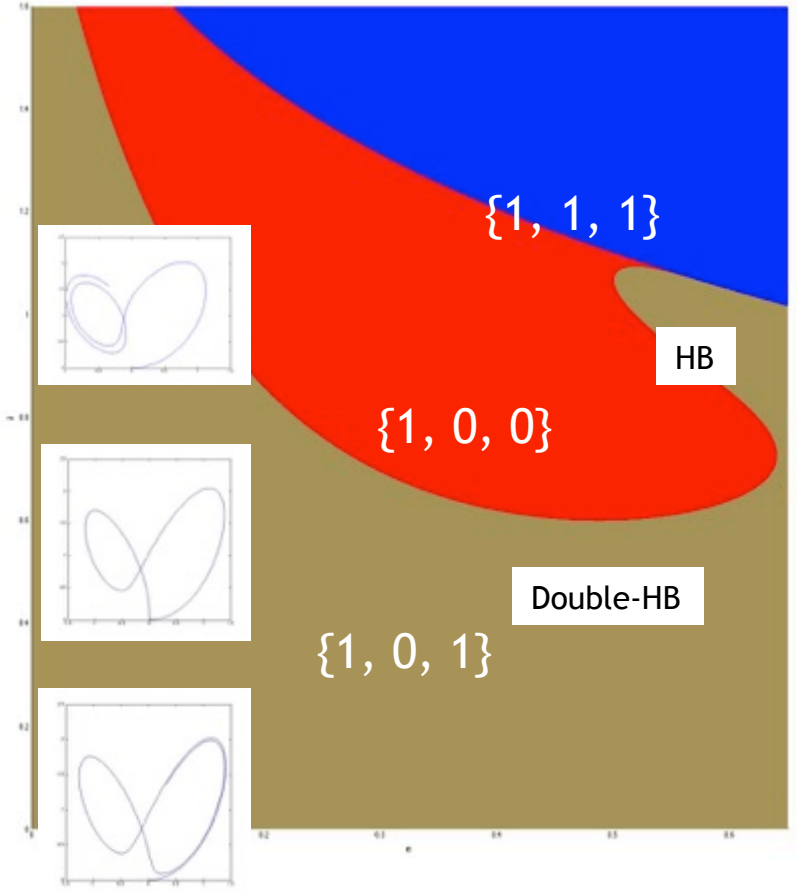

Depth of symbolic scanning: from 2 through 30 kneadings

2-4

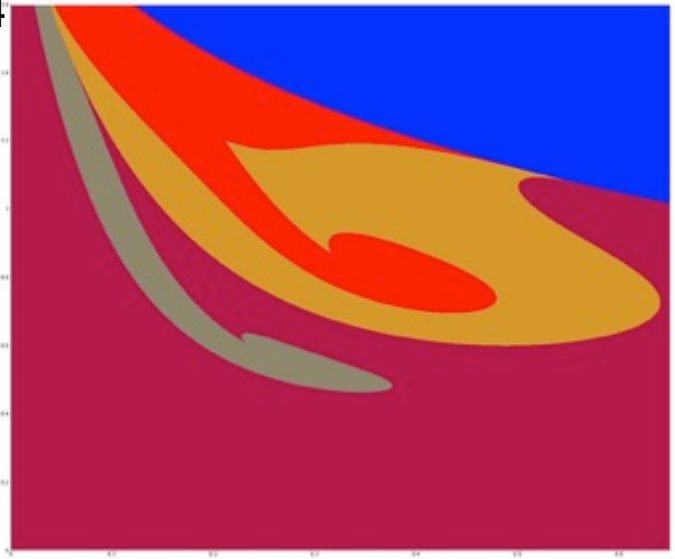

2-5

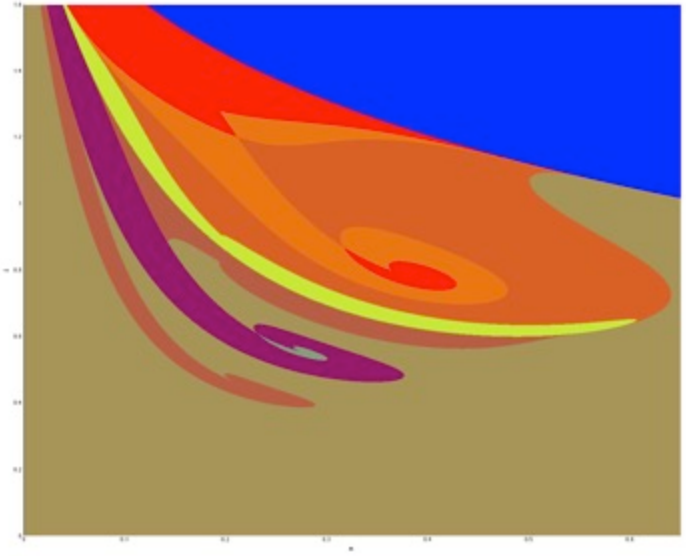

2-7

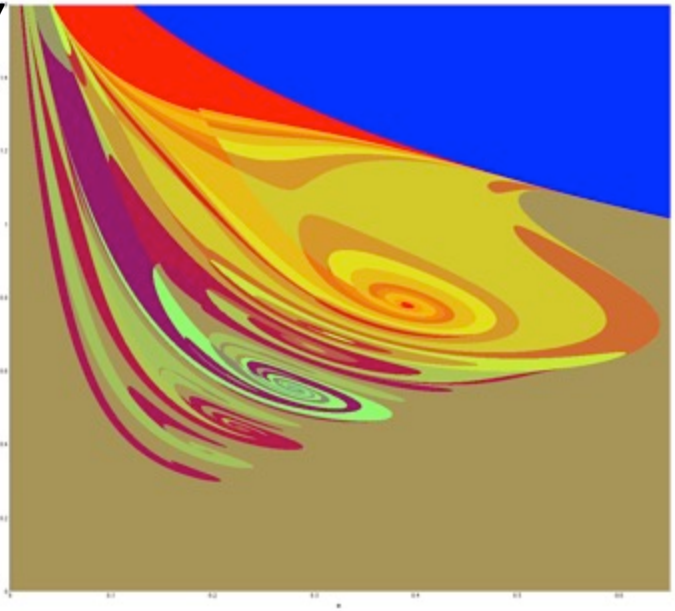

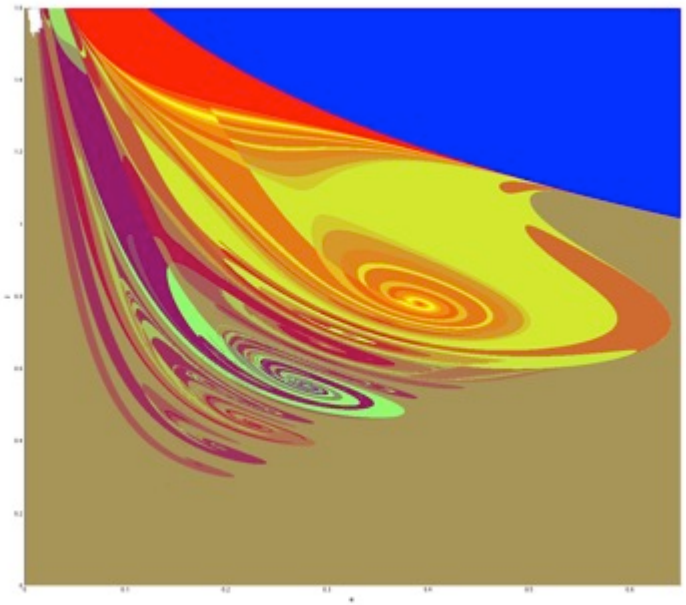

3-30

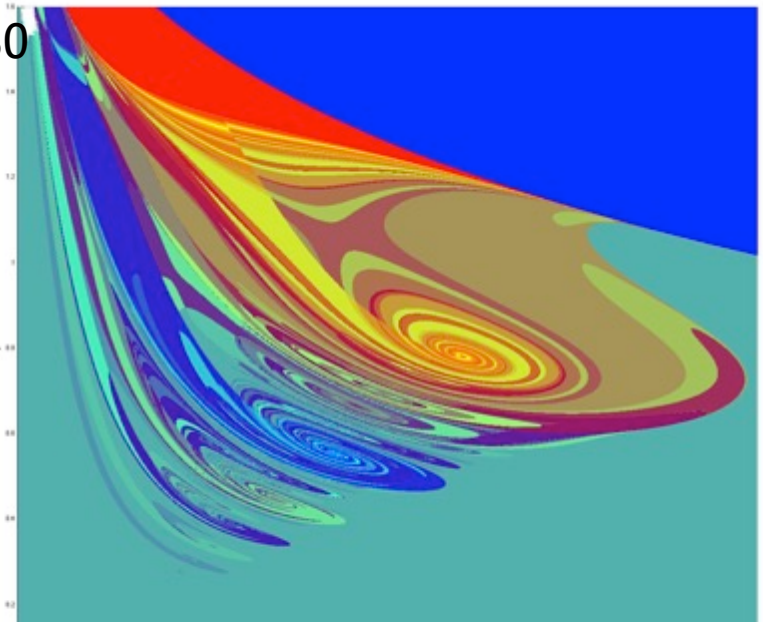

5-30

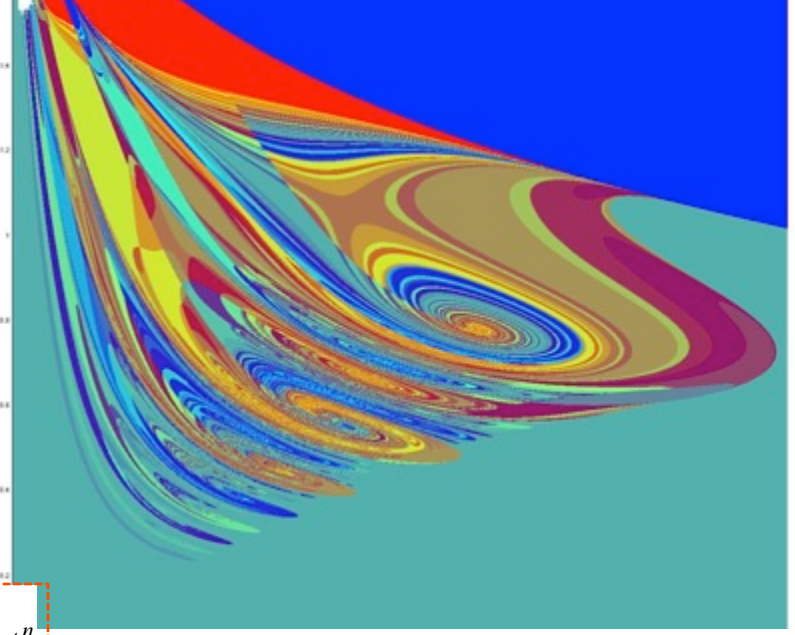

$$P = \sum_{n=1}^{\infty} k_{n+i} t^n$$

7-30

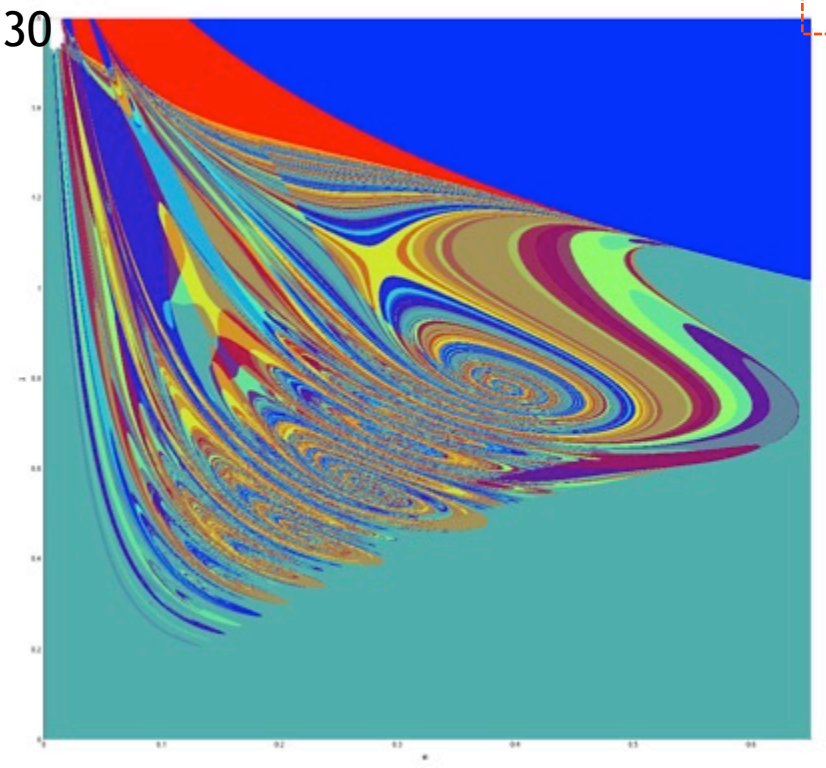

9-30

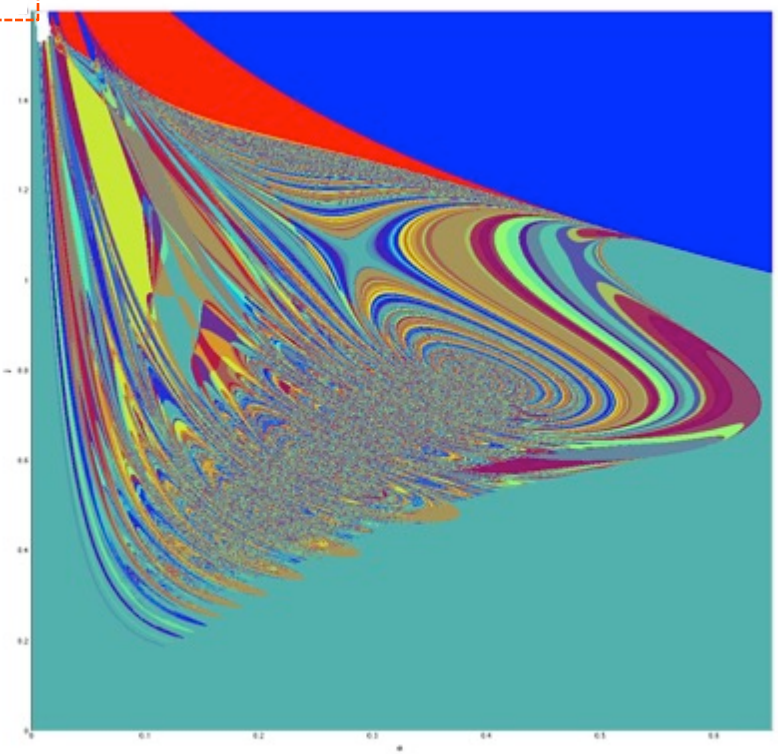

Step 2: 1-to-1 color-mapping

3D kneading potential

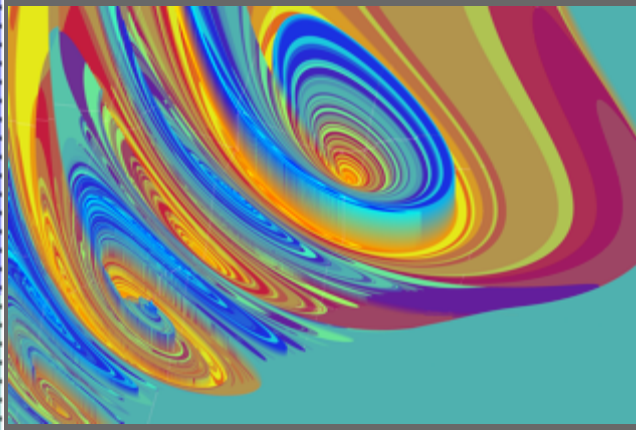

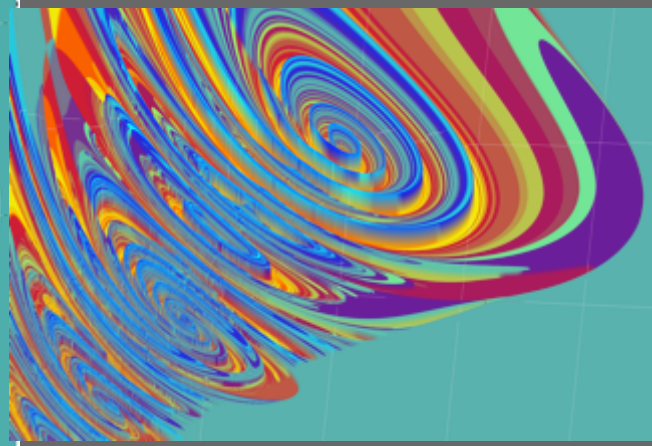

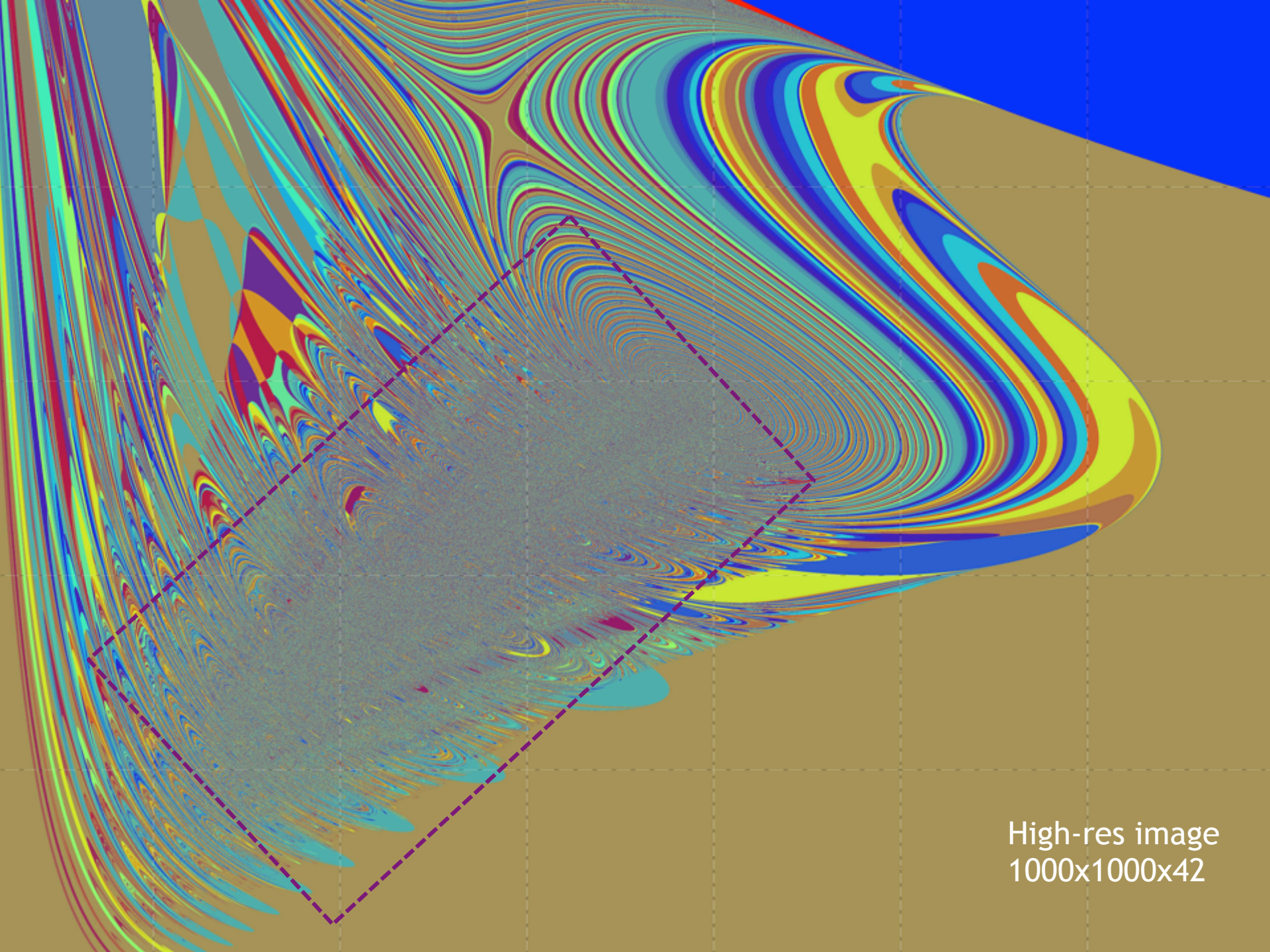
High-res image
1000x1000x42

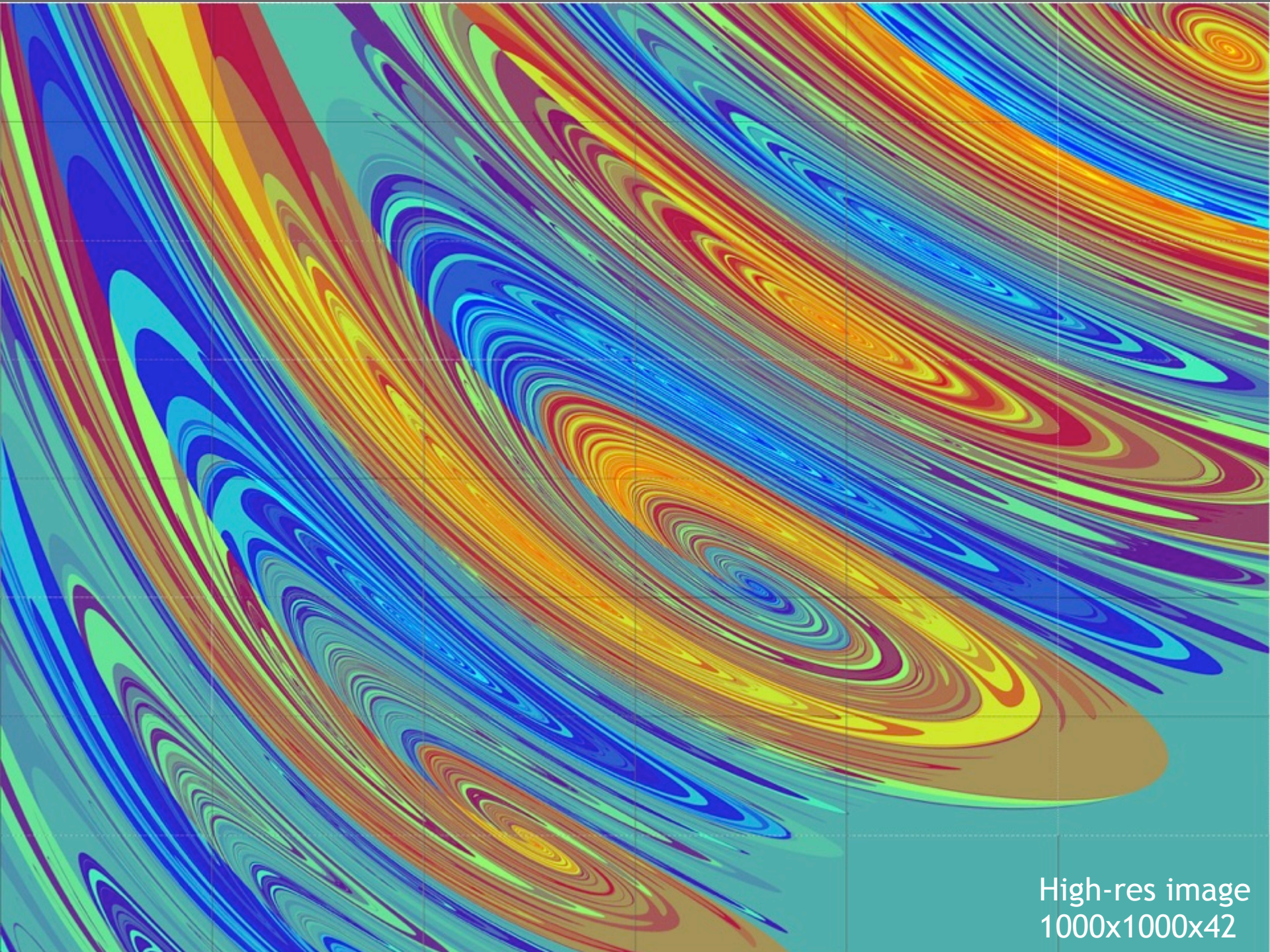
High-res image
1000x1000x42

Bykov T-point

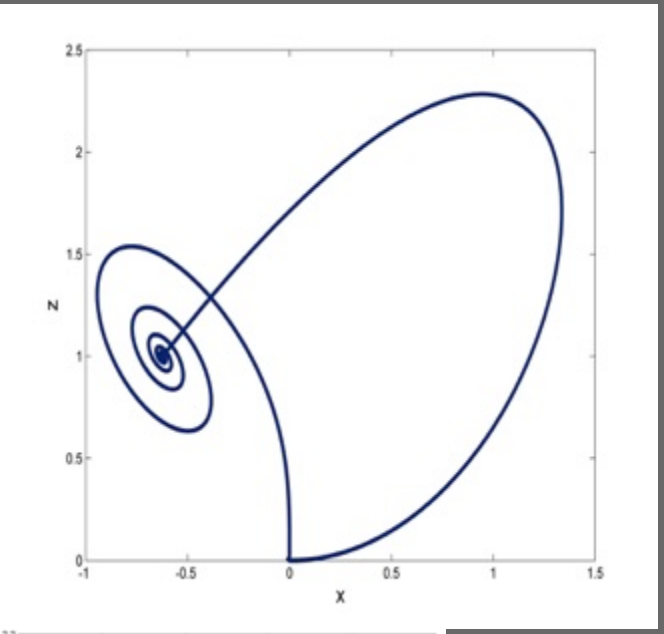

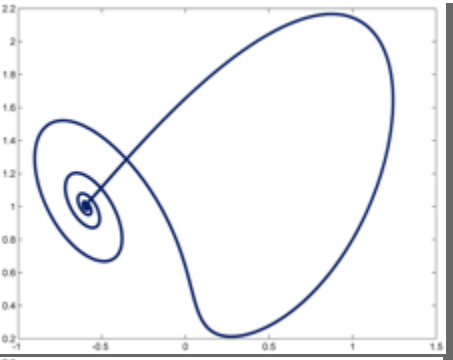

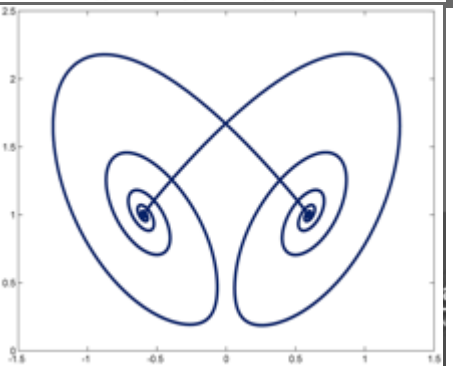

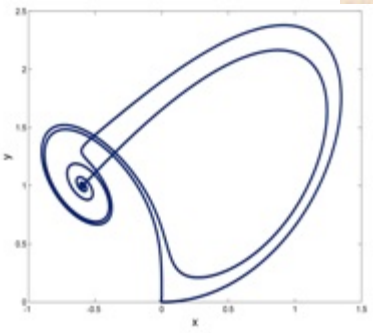

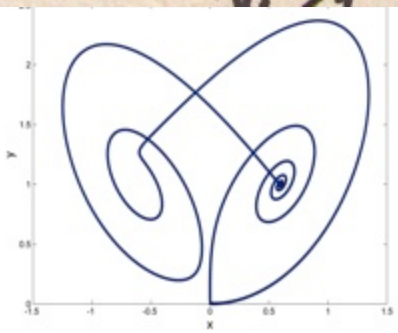

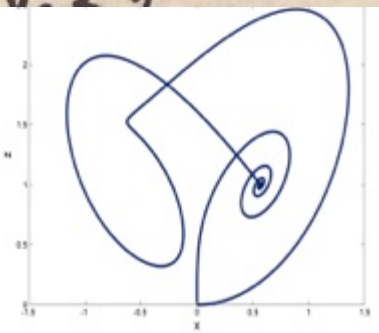

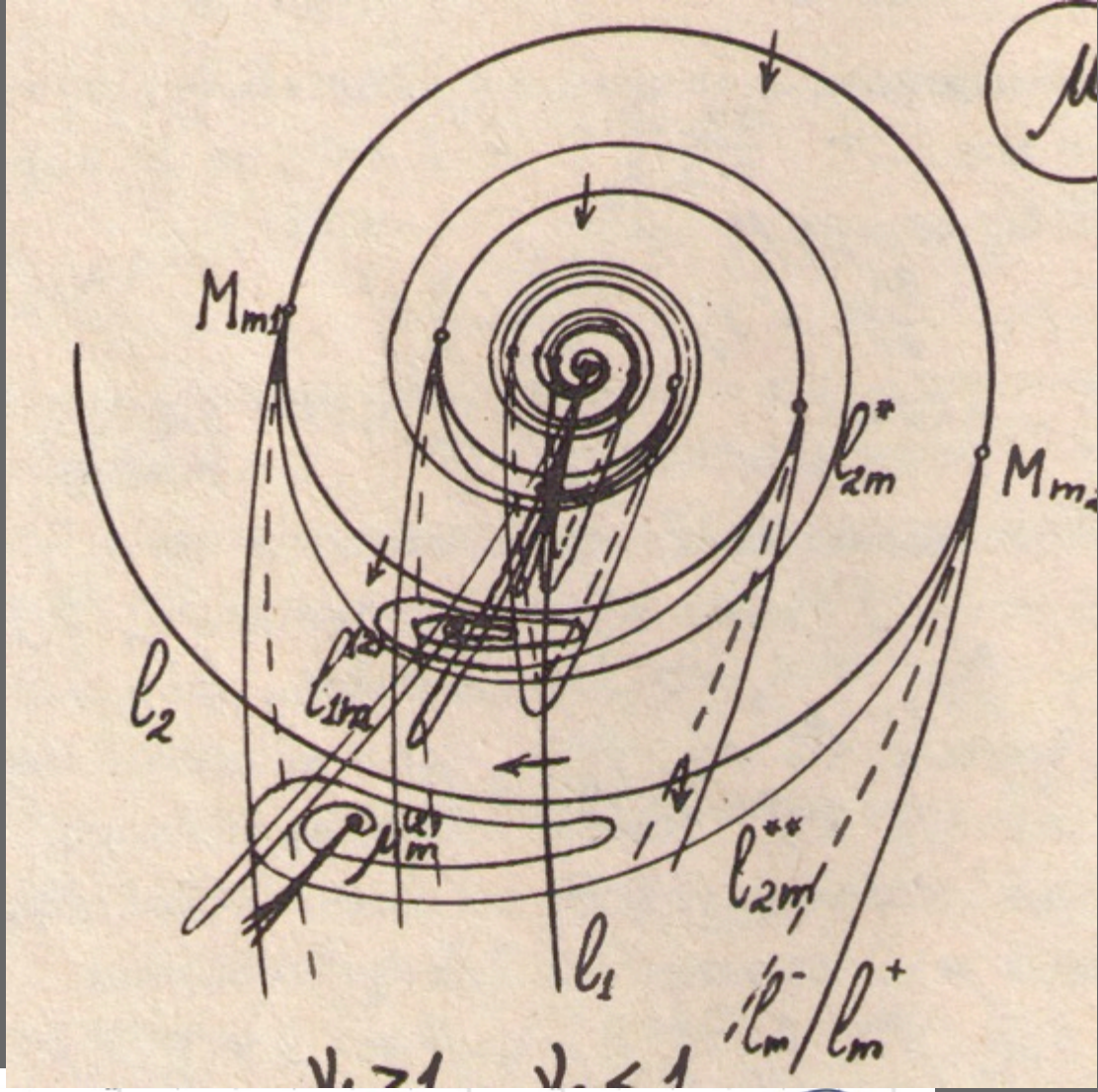

Self-similarity of T-points

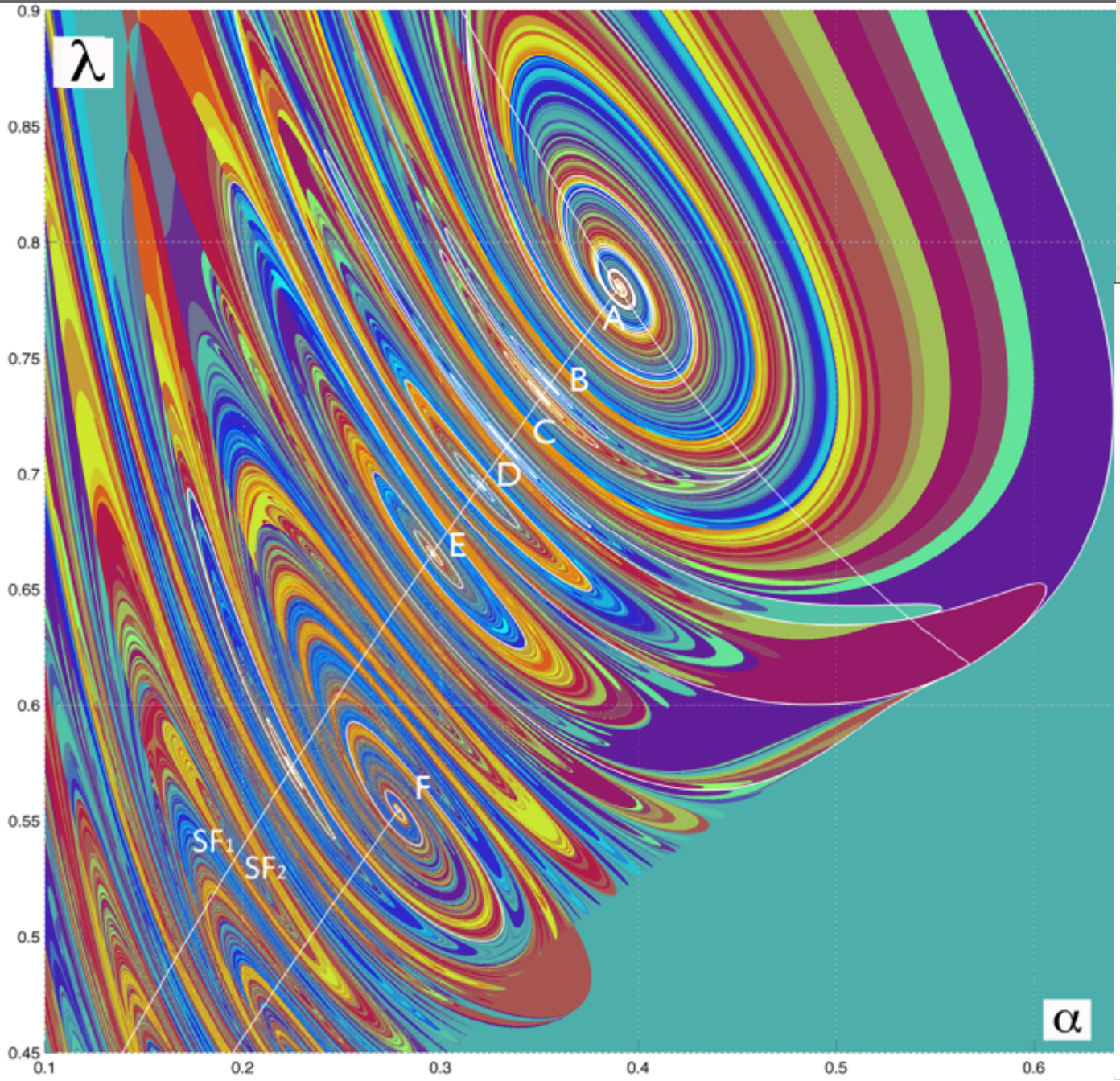

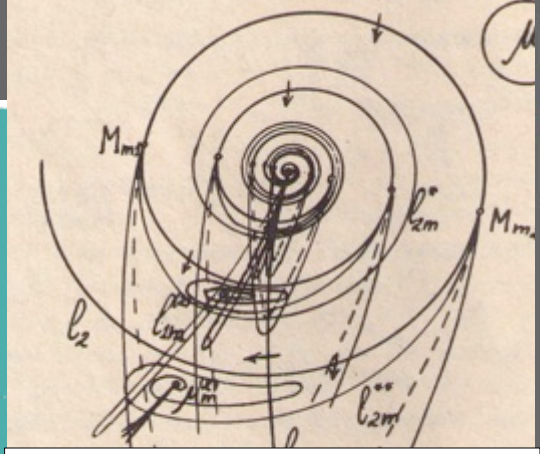

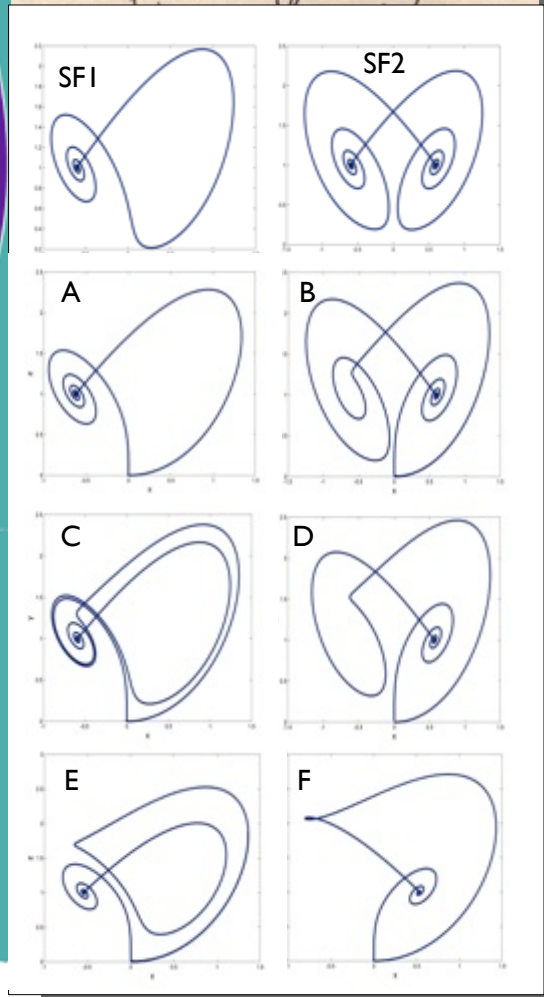

Self-similarity of T-points on the saddle-focus pathway SF_1

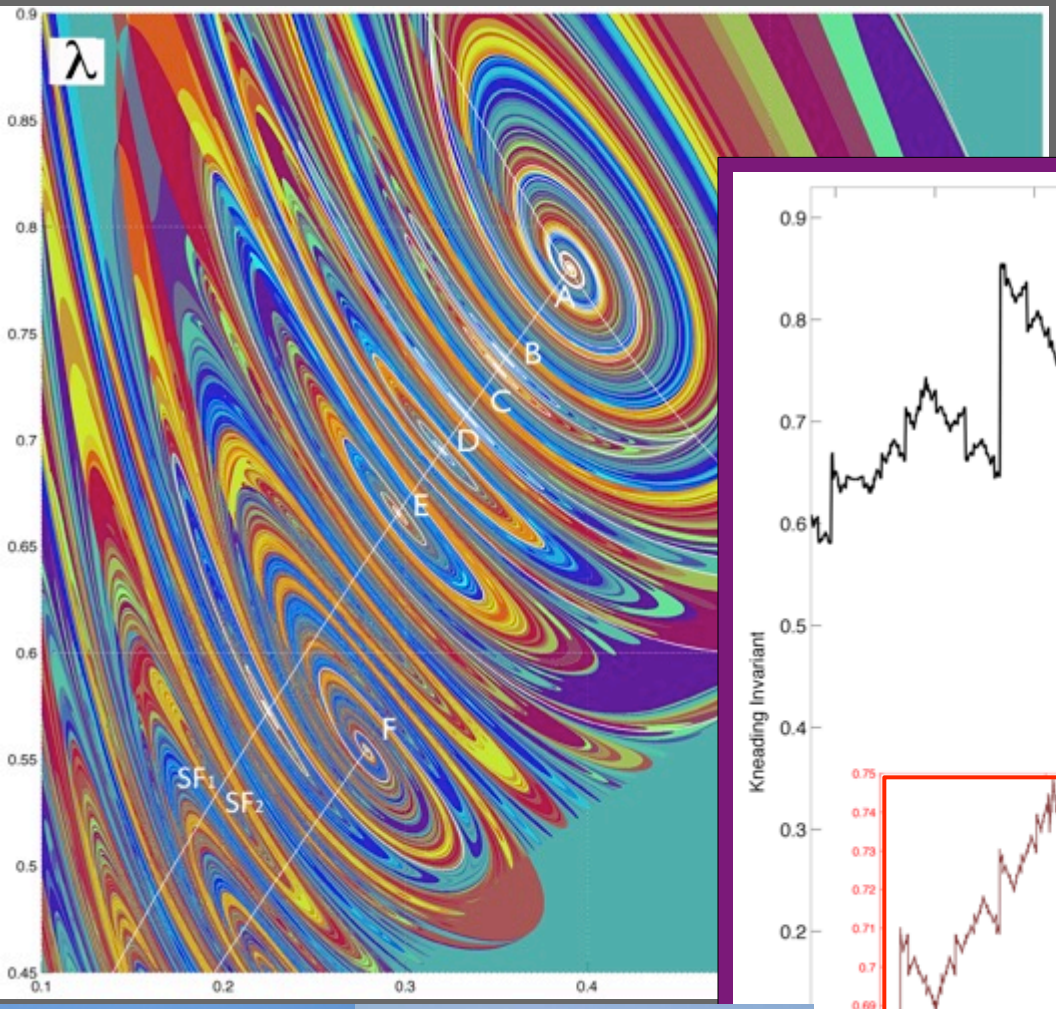

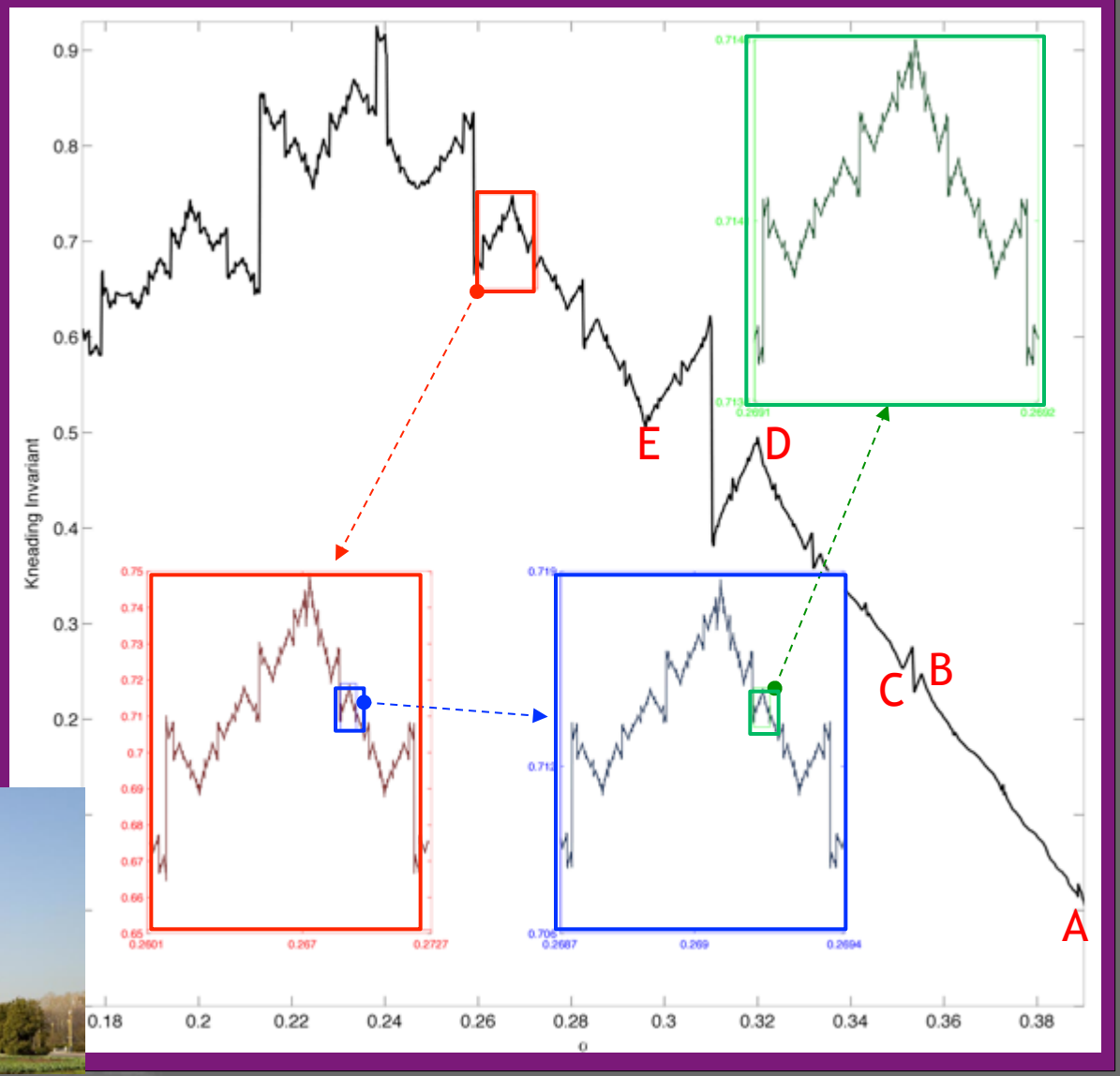

SHILNIKOV flames

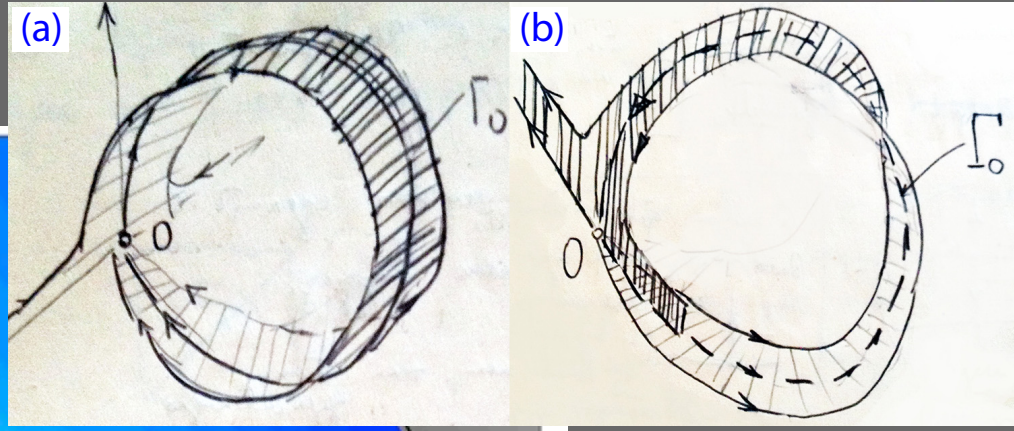

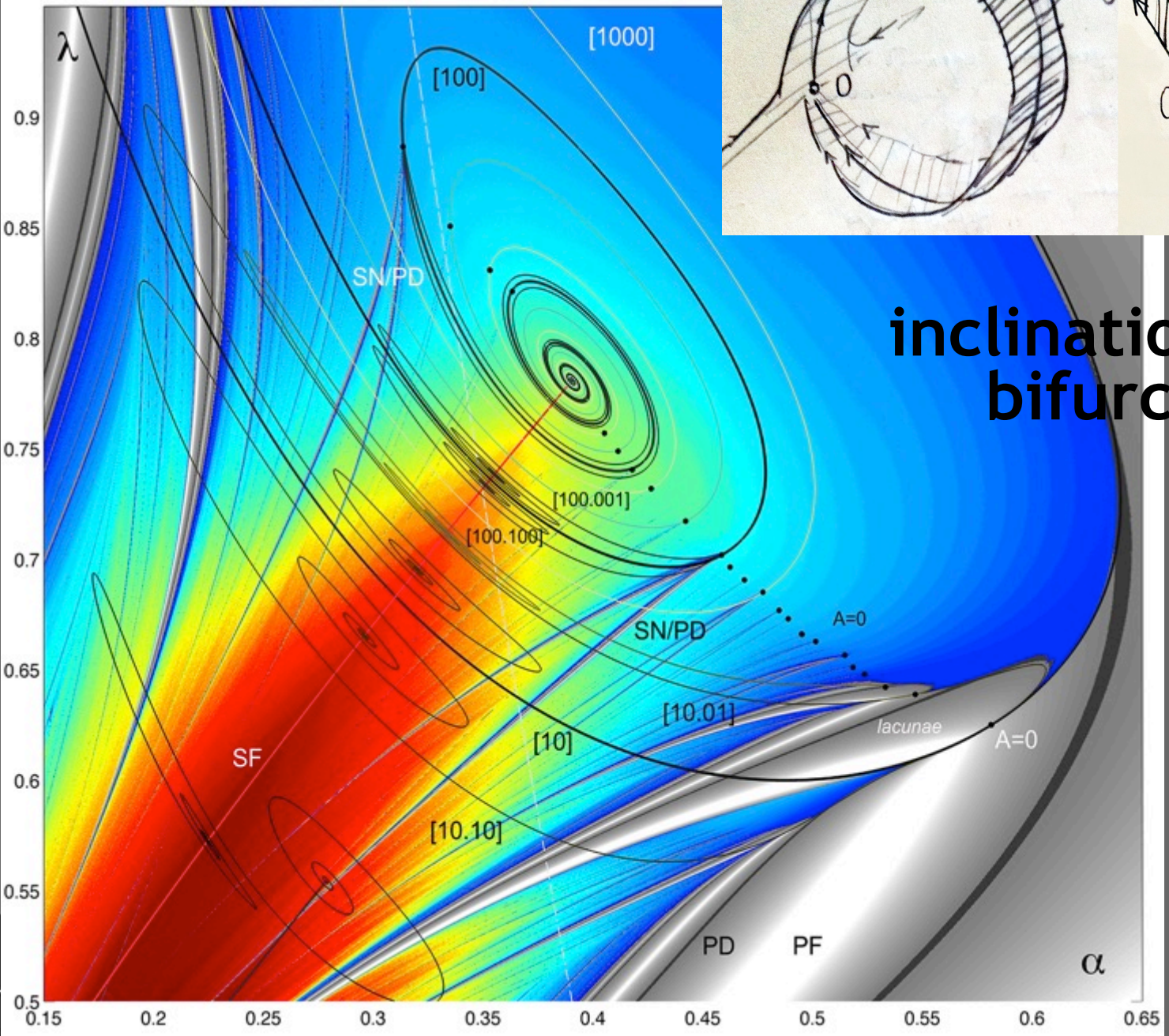

inclination switch bifurcations

Inclination switch: A=0

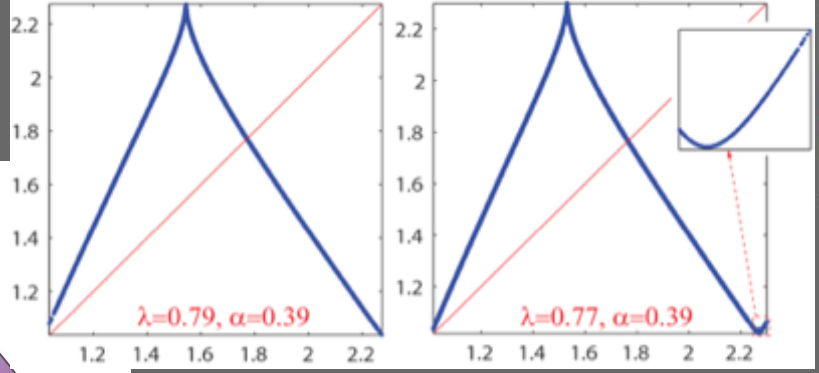

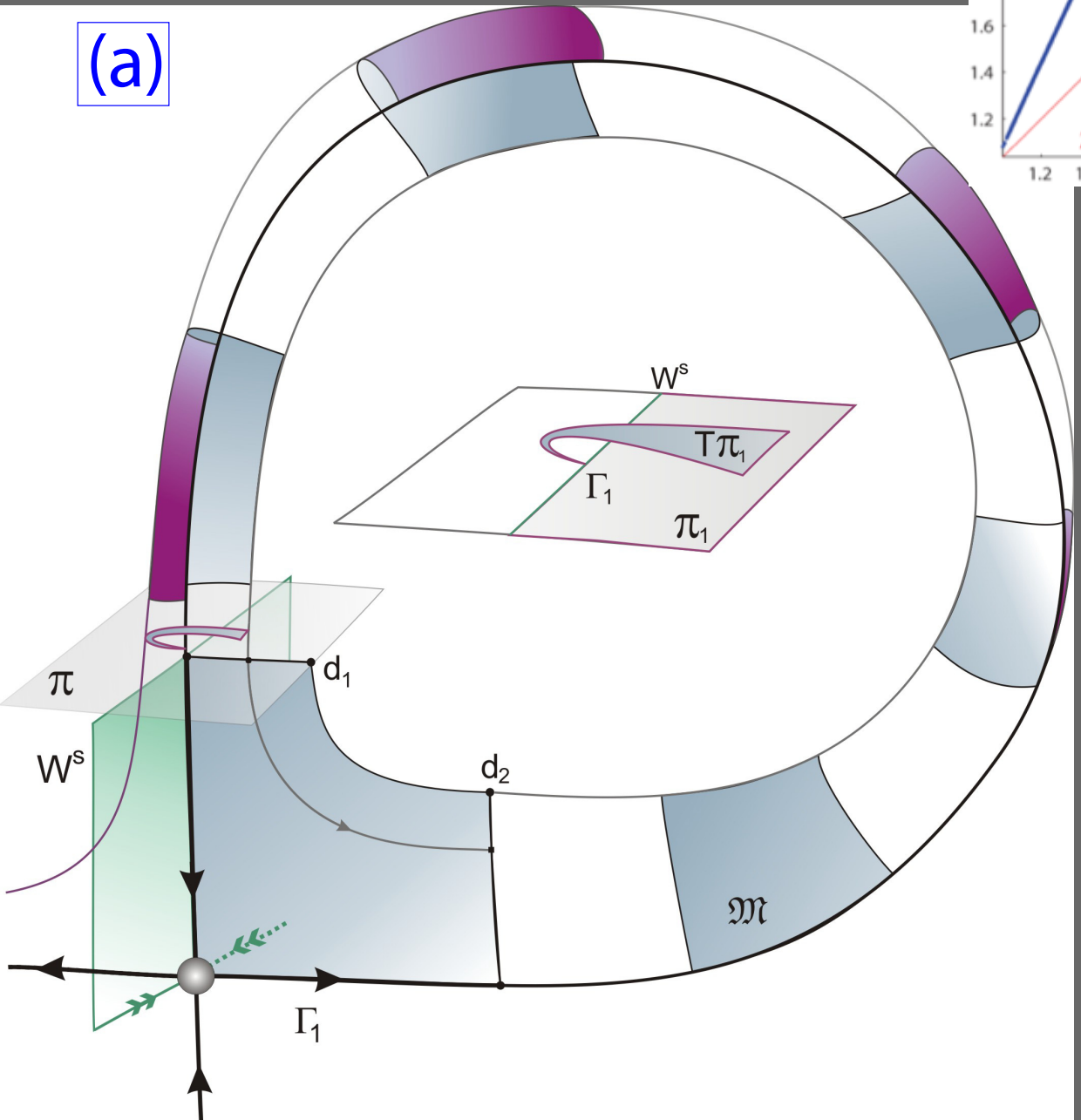

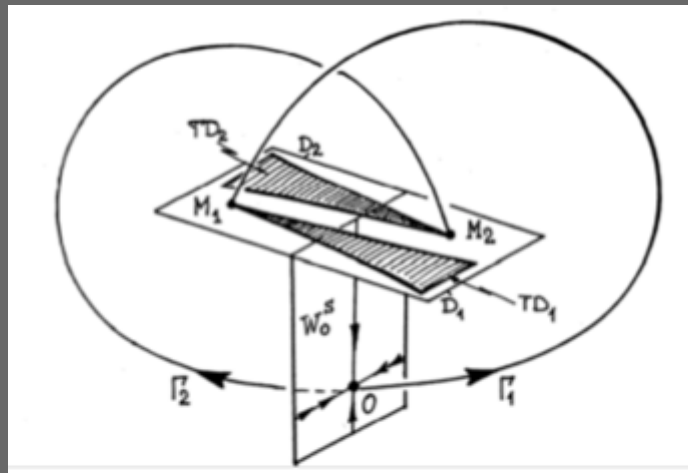

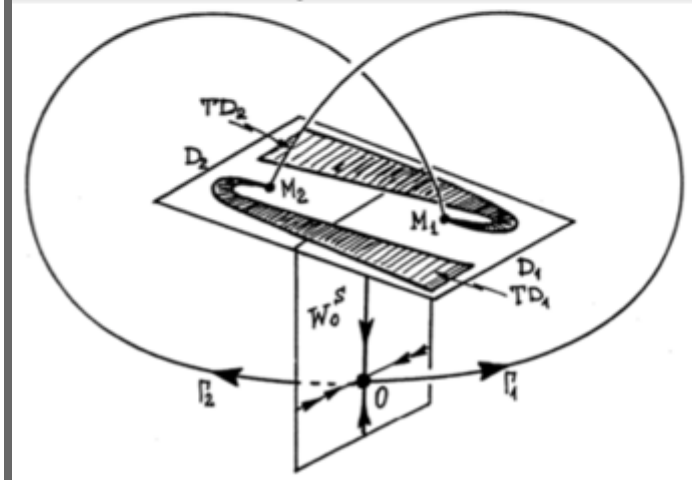

SHILNIKOV flames

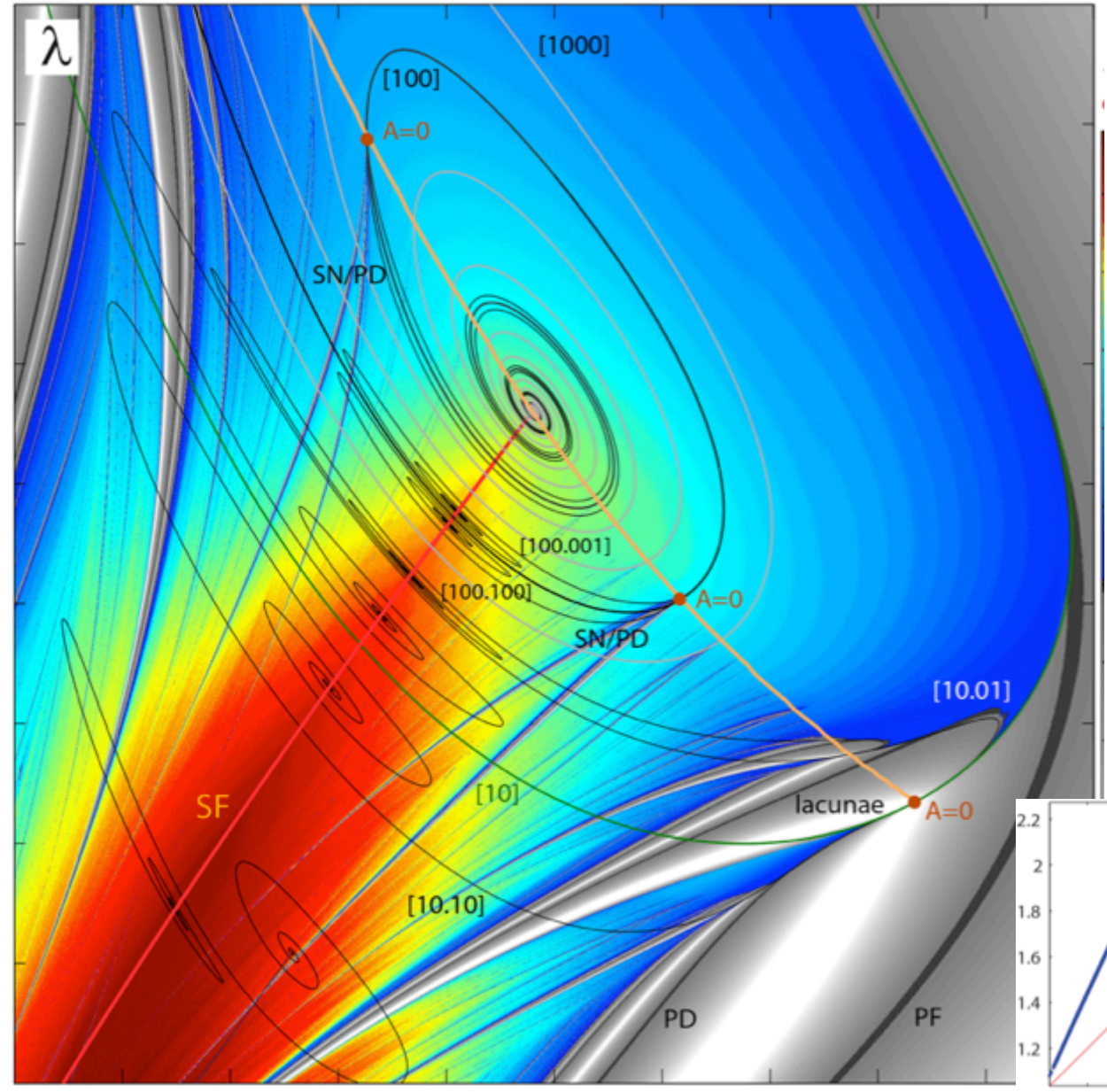

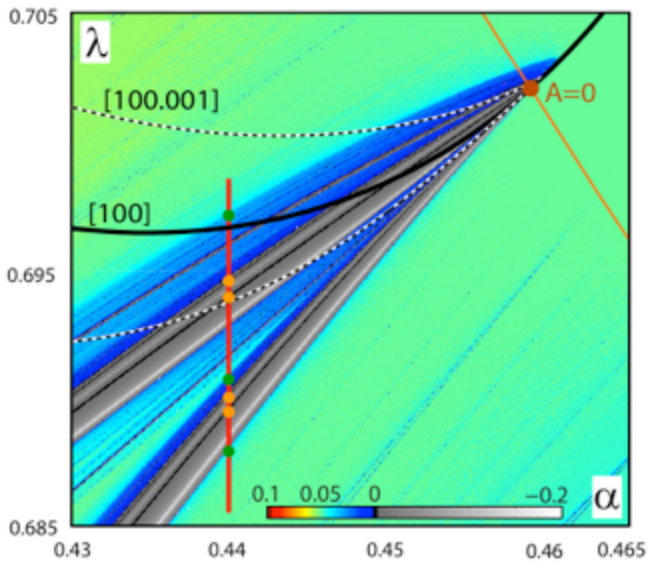

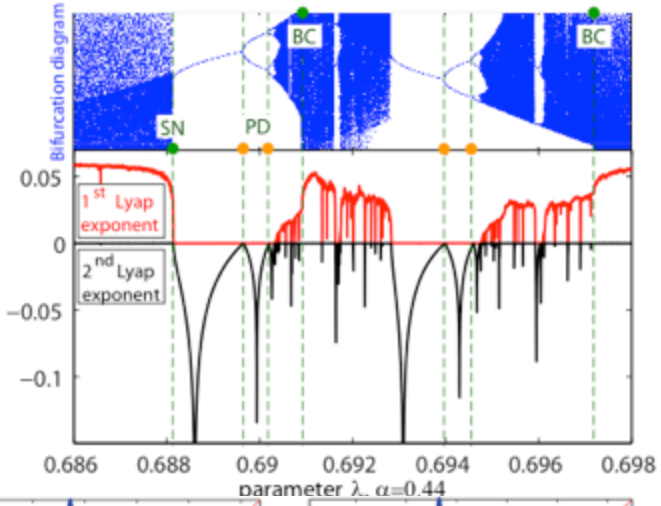

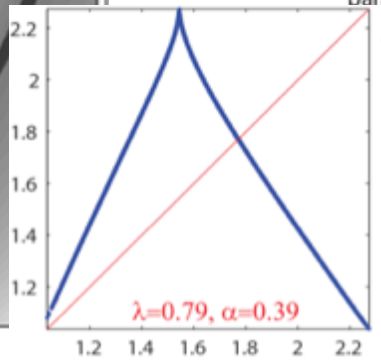

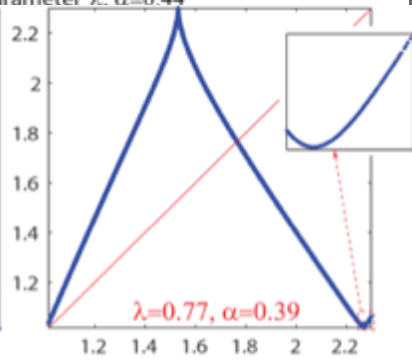

$$\frac{dx}{dt} = y, \qquad \frac{dy}{dt} = x(1-z) - \lambda y - Bx^3, \qquad \frac{dz}{dt} = -\alpha z + x^2$$

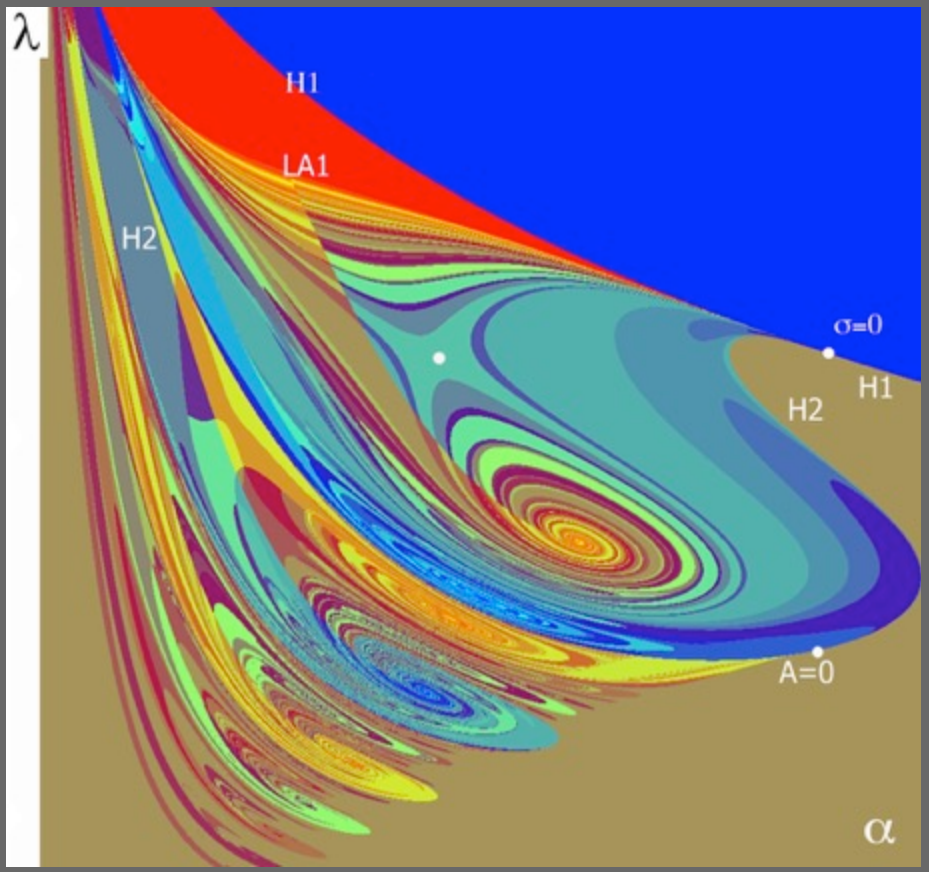

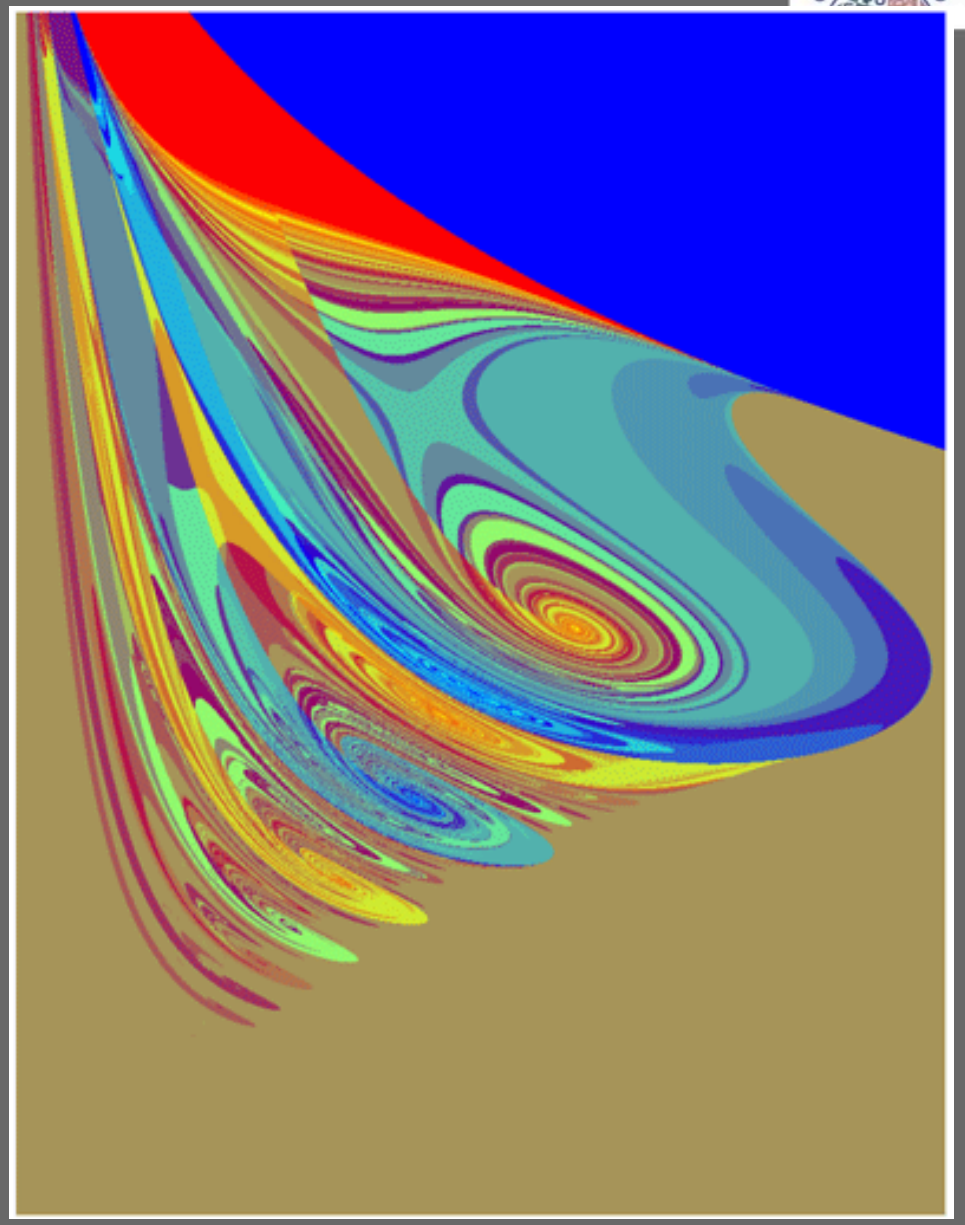

The Lorenz attractor in OP 3-level laser model

Local bifurcations of a three-level optically pumped laser

W. Forysiak, R. G. Harrison, and J. V. Moloney
Department of Physics, Heriot–Watt University, Riccarton, Edinburgh EH14 4AS, United Kingdom
(Received 24 June 1988)

We report on a linear-stability analysis of a three-level, resonantly optically pumped, homogeneously broadened, single-mode laser. We identify the relatively simple nature of the local bifurcations on the nonlasing branch comprising pitchfork, Hopf, and codimension-2 bifurcations. Their use is demonstrated in identifying regions of parameter space in which we may expect steady, periodic, and more complex dynamical behavior.

Optically pumped lasers (OPL's) have emerged as highly attractive systems for experimental investigation of nonlinear laser dynamics.[1–4] They have attracted particular attention as perhaps providing systems most closely resembling that of the Haken-Lorenz model for a single-mode, resonant two-level laser with a homogeneously broadened gain.[3] While conditions have been determined by which these lasers may be reduced to that of the Haken model[5] such a mode of operation provides but a limited aspect of their more general nonlinear dynamical behavior.[6–11] The notable distinguishing feature of these systems is the two-photon coherent interaction associated with the coupled pump and lasing transitions. In this report we present a linear-stability analysis of a resonantly pumped three-level system. We determine analytical expressions defining pitchfork bifurcations describing the onset and termination of lasing action, Hopf bifurcations marking the onset of spontaneous pulsations, and the parameter set for codimension-2 bifurcations. Our physical model of the OPL comprises a three-level system (Fig. 1 inset) in which transition $1\rightarrow 2$ is resonantly optically pumped by a field of magnitude α and lasing, of strength β, occurs from transition $2\rightarrow 3$.

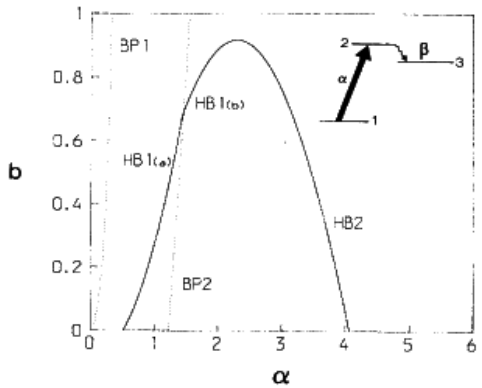

The equations governing the system dynamics are fully discussed in Refs. 5–7 and given by

$$
\begin{aligned}
\dot{\beta} &= -(\sigma\beta + ig\rho_{23}) ,\\
\dot{\rho}_{21} &= -(1-i\delta_p)\rho_{21} + i\alpha D_{21} - i\beta\rho_{31} ,\\
\dot{\rho}_{23} &= -(1-i\delta_s)\rho_{23} + i\beta D_{23} - i\alpha\rho_{31}^* ,\\
\dot{\rho}_{31} &= -[1+i(\delta_p+\delta_s)]\rho_{31} - i\beta^*\rho_{21} + i\alpha\rho_{23}^* ,\\
\dot{D}_{21} &= -b(1+D_{21}) - 4\,\mathrm{Im}(\alpha^*\rho_{21}) - 2\,\mathrm{Im}(\beta^*\rho_{23}) ,\\
\dot{D}_{23} &= -bD_{23} - 2\,\mathrm{Im}(\alpha^*\rho_{21}) - 4\,\mathrm{Im}(\beta^*\rho_{23}) .
\end{aligned}
\tag{1}
$$

Here β refers to the lasing field magnitude, ρ_{ij} are the off-diagonal matrix elements for the levels i and j, and D_{ij} refer to the pump and signal population inversions. The parameters of the system are α the pump laser magnitude, σ the cavity damping constant, g the unsaturated gain, $b=\Gamma/\gamma$ the ratio of deenergization to dipole dephasing rates, and δ_p (δ_s) the detuning of the pump (laser) from resonance. All parameters and the time t are scaled to the dipole dephasing width γ.

Specialization to the case of resonant pump and emission ($\delta_s=\delta_p=0$) enables the reduction of the above set of ten coupled ordinary differential equations (ODE's) to the following set of six,

$$
\begin{aligned}
\dot{x}_1 &= -\sigma x_1 + g x_3 ,\\
\dot{x}_2 &= -x_2 - x_1 x_4 + \alpha x_5 ,\\
\dot{x}_3 &= -x_3 + x_1 x_6 - \alpha x_4 ,\\
\dot{x}_4 &= -x_4 + x_1 x_2 + \alpha x_3 ,\\
\dot{x}_5 &= -b(1+x_5) - 2x_1 x_3 - 4\alpha x_2 ,\\
\dot{x}_6 &= -b x_6 - 4x_1 x_3 - 2\alpha x_2 ,
\end{aligned}
\tag{2}
$$

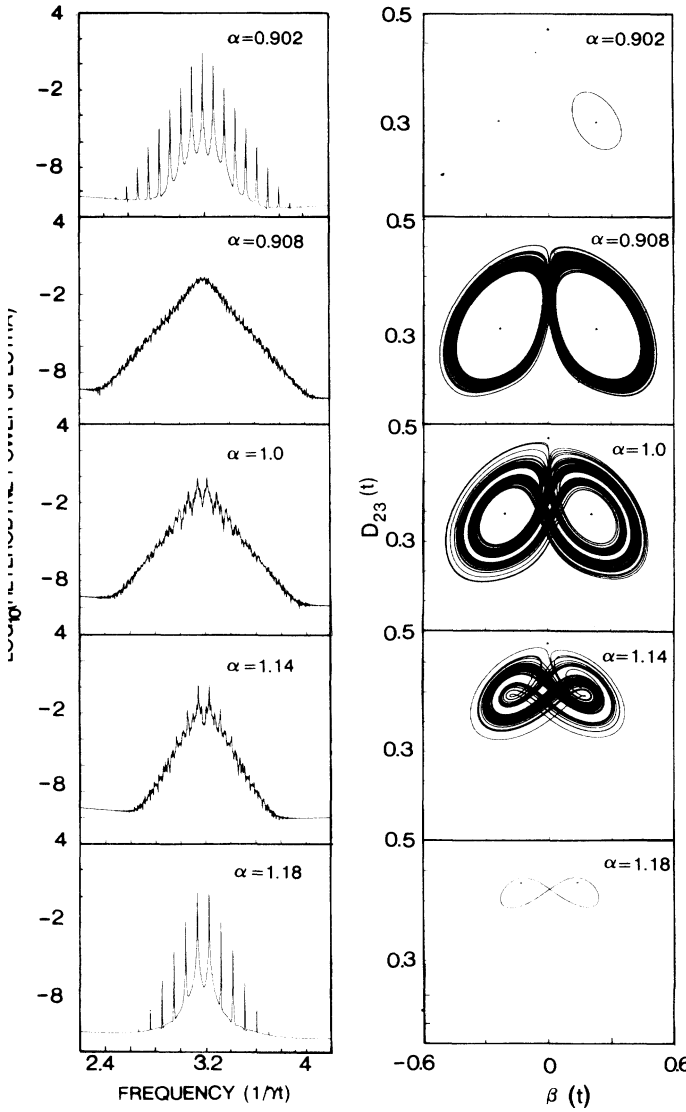

FIG. 9. Heterodyne power spectra and 2D (two-dimensional ase portraits (D_{23} vs β) for $\alpha=0.902$, 0.908, 1.0, 1.14, an 18. The frequency offset between the local oscillator and th sing field is $10/\pi$ (approximately 3.18) normalized frequenc its. The stars on the phase portraits mark projections of th stable stationary solutions onto the (β, D_{23}) plane.

Lorenz attractor in the OP 3 level laser

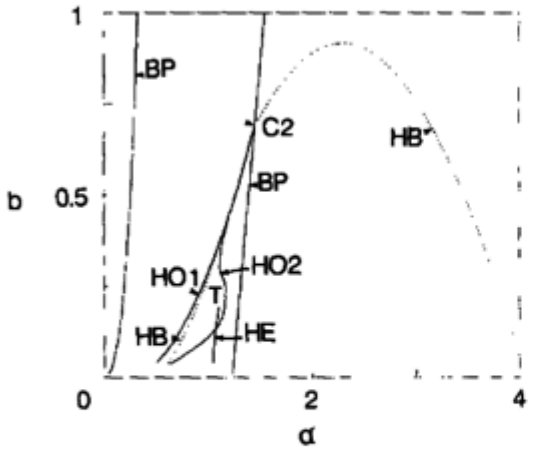

Fig. 4.1. Two-parameter (α, b) diagram of principal bifurcations for $g = 50$ and $\sigma = 10$. Notation of equilibrium bifurcations is as in section 3. C2 is the codimension-two equilibrium bifurcation. Branches of principal homoclinic orbits are marked HO1 (x) and HO2 (xy). A branch of principal heteroclinic orbits, HE, emerges from the terminal point, T.

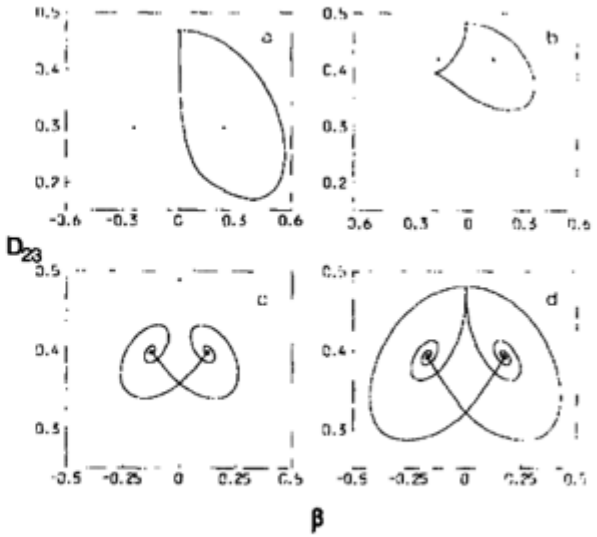

Fig. 4.2. (B, D_{23}) phase portraits corresponding to points in the (α, b) plane for $g = 50$ and $\sigma = 10$: (a) on HO1 at $b = 0.2$, (b) on HO2 at $b = 0.2$, (c) on HE at $b = 0.15$ and (d) at T.

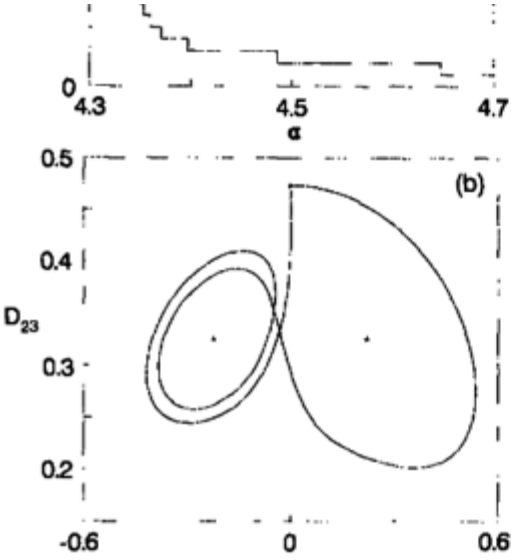

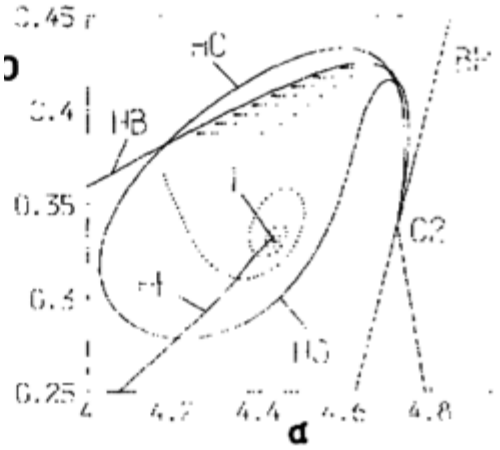

Fig. 5.7. As fig. 5.1, but additional points mark the locations of homoclinic orbits to N of type xy^n.

non-lasing stationary state spiral towards or away from stable lasing steady states, whereas in the OPL system, these trajectories spiral towards or away from stable limit cycles. Moreover, the transition window is terminated by the limit points of the branches of non-symmetric periodic orbits, rather than by subcritical Hopf bifurcations.

Lorenz attractor for OP 3 level laser

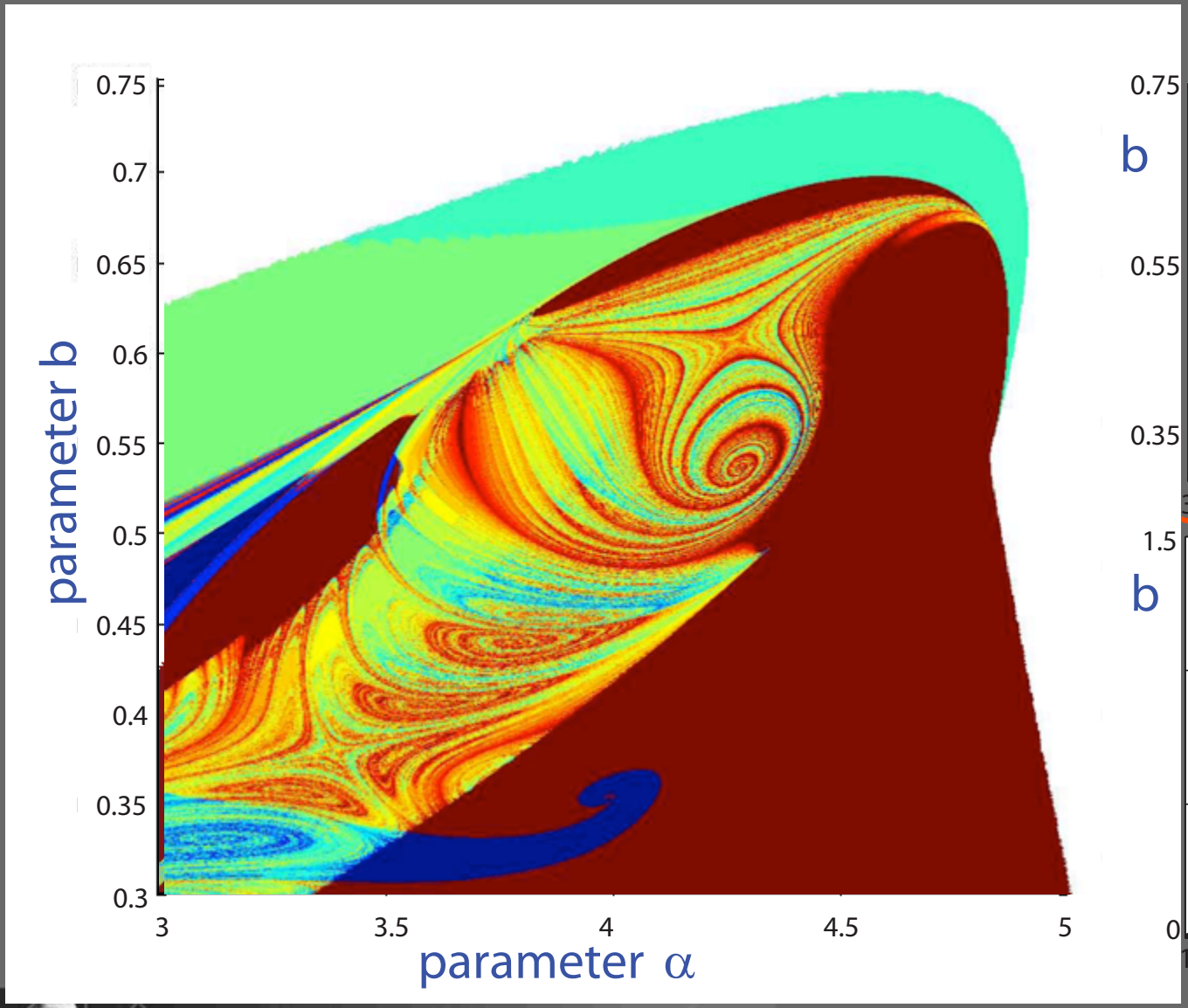

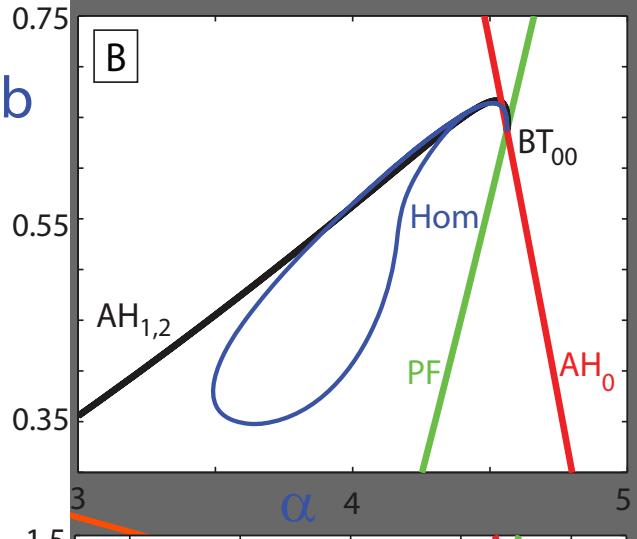

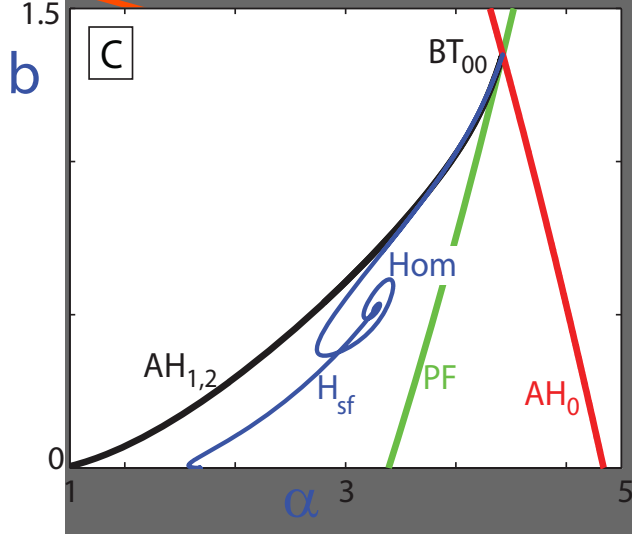

Shilnikov saddle-focus

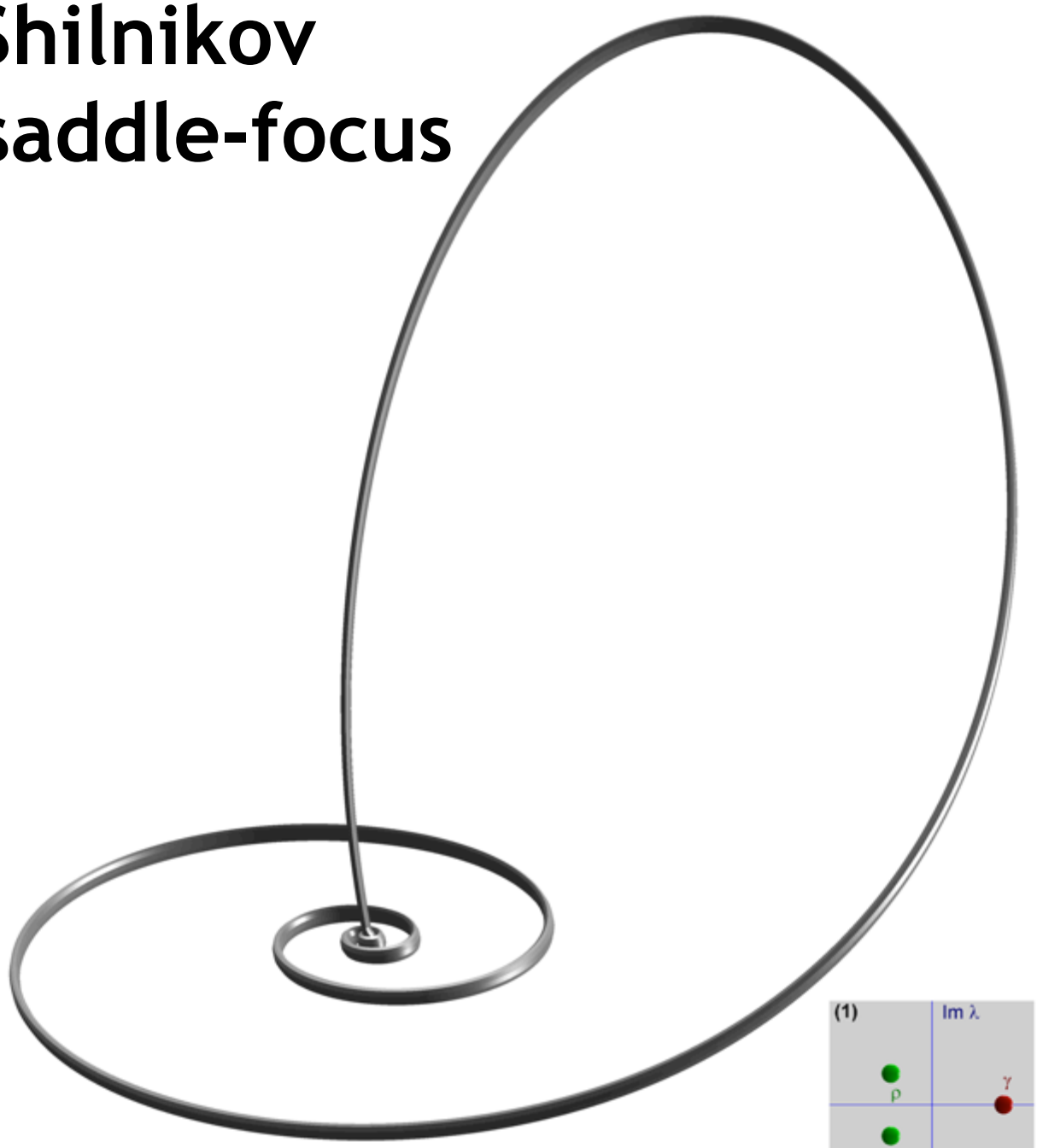

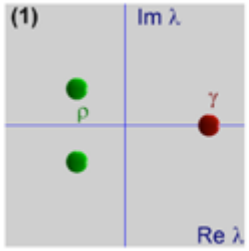

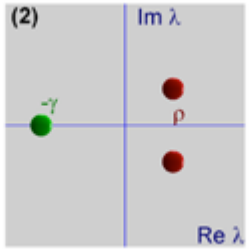

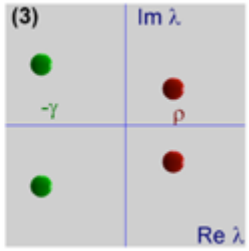

Shilnikov saddle-focus

$$\begin{aligned}
\dot{x} &= -\rho x - \omega y + F_1(x,y,z),\\
\dot{y} &= \omega x - \rho y + F_2(x,y,z),\\
\dot{z} &= \gamma z + F_3(x,y,z),
\end{aligned}$$

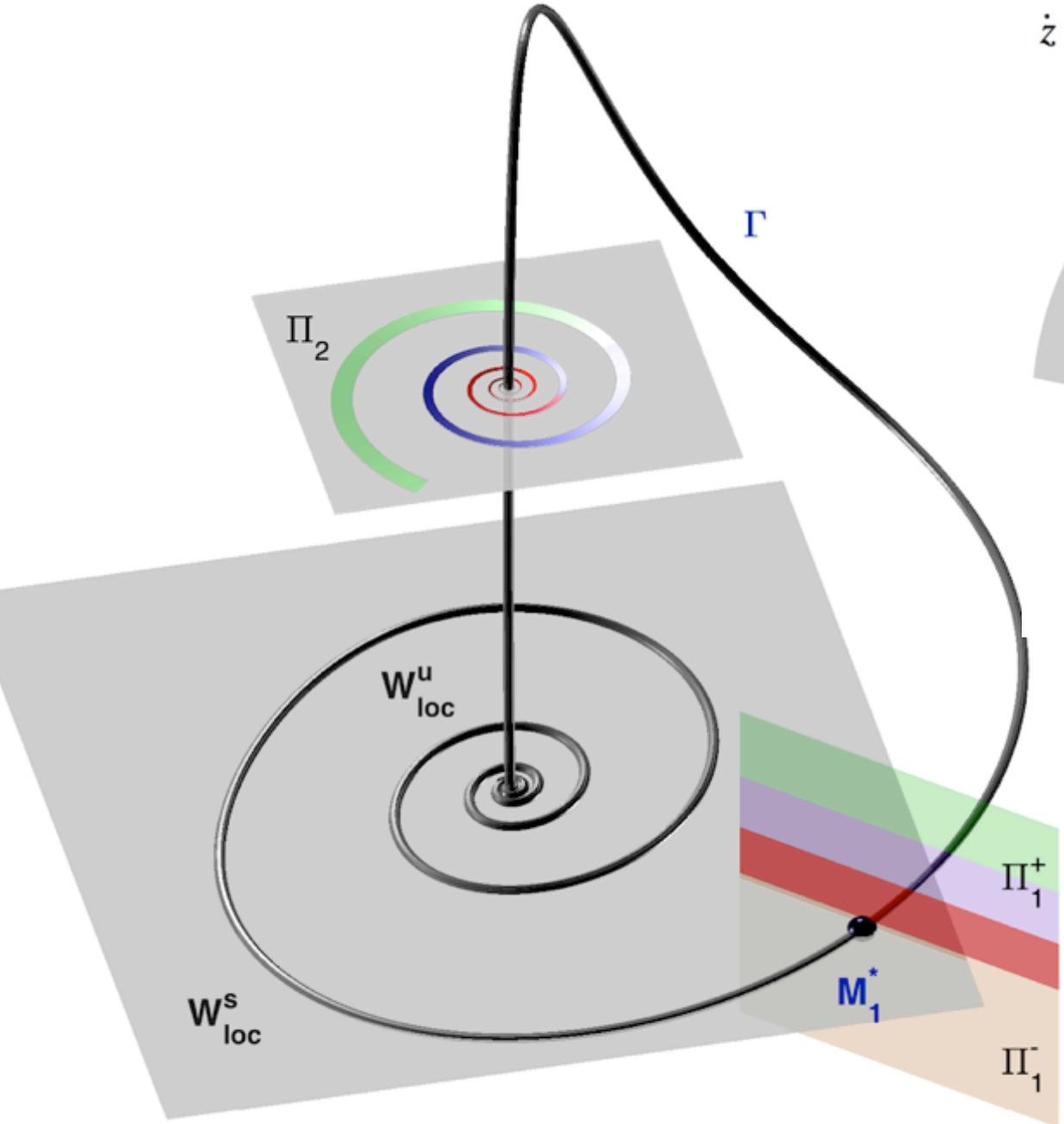

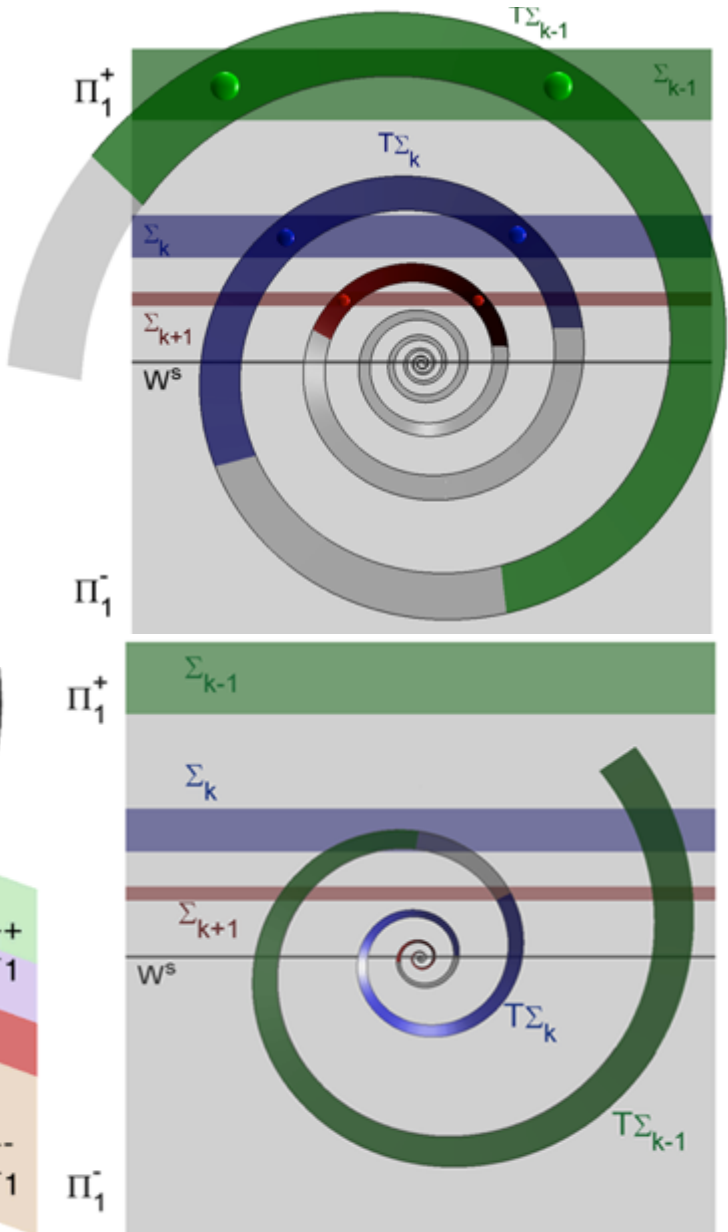

Saddle-focus: 1 or ∞ periodic orbits

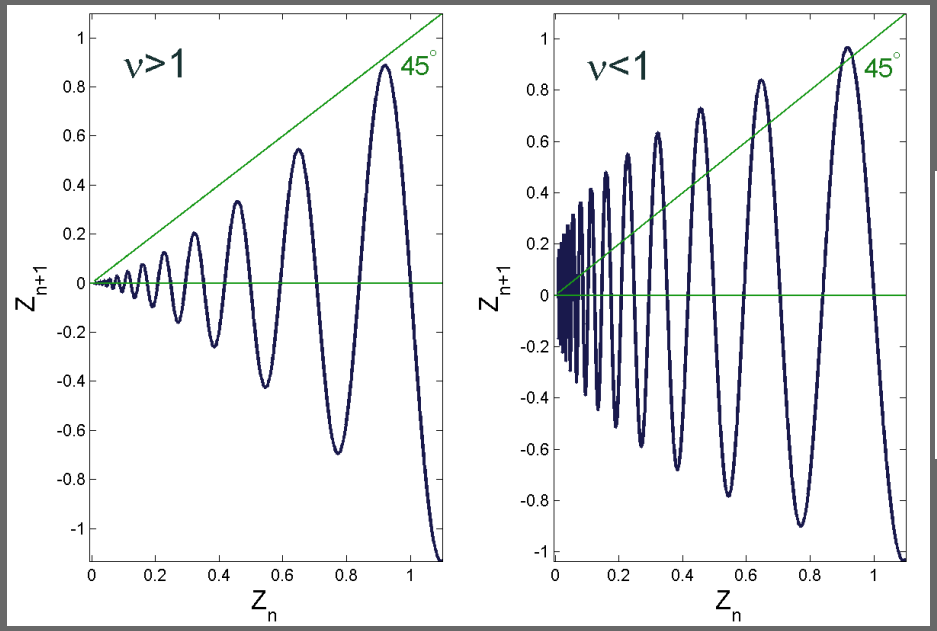

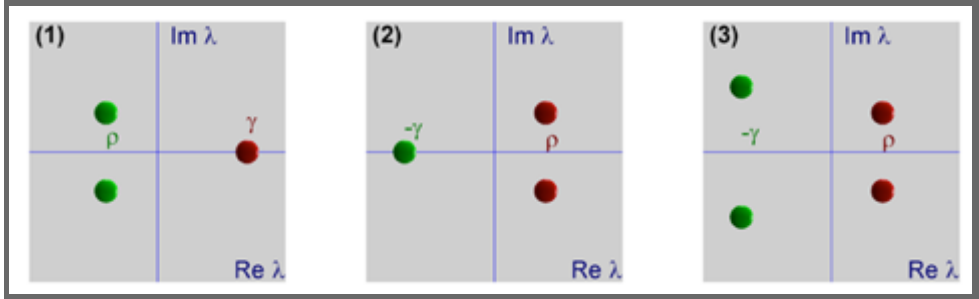

∞ Smale horseshoes

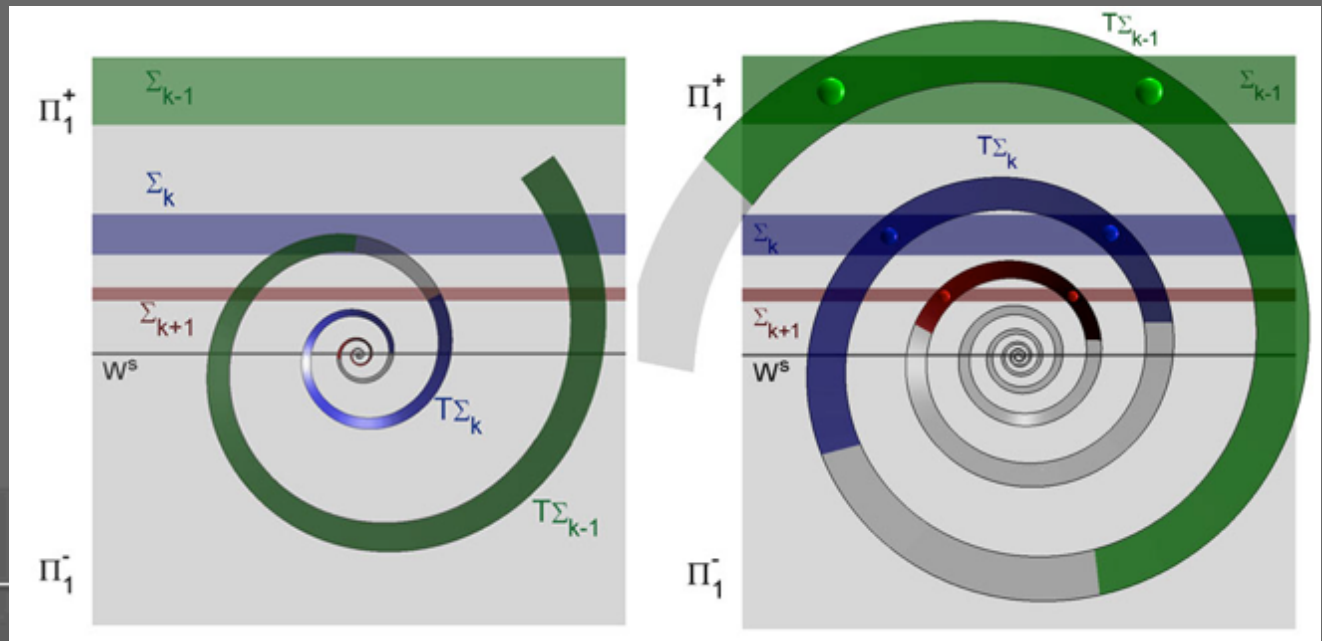

Z_2 symmetric saddle-focus homoclinics

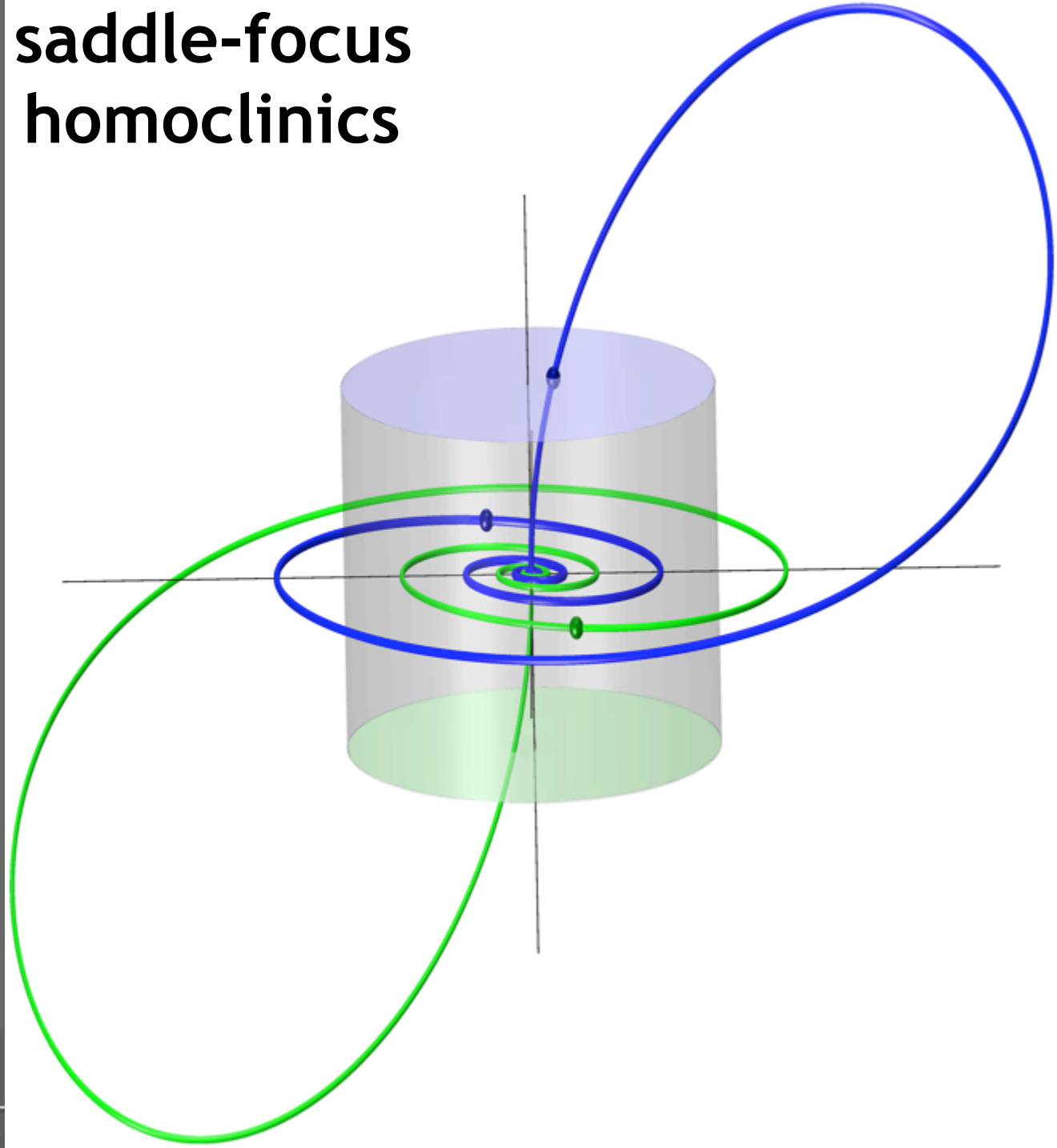

Secondary homoclinics

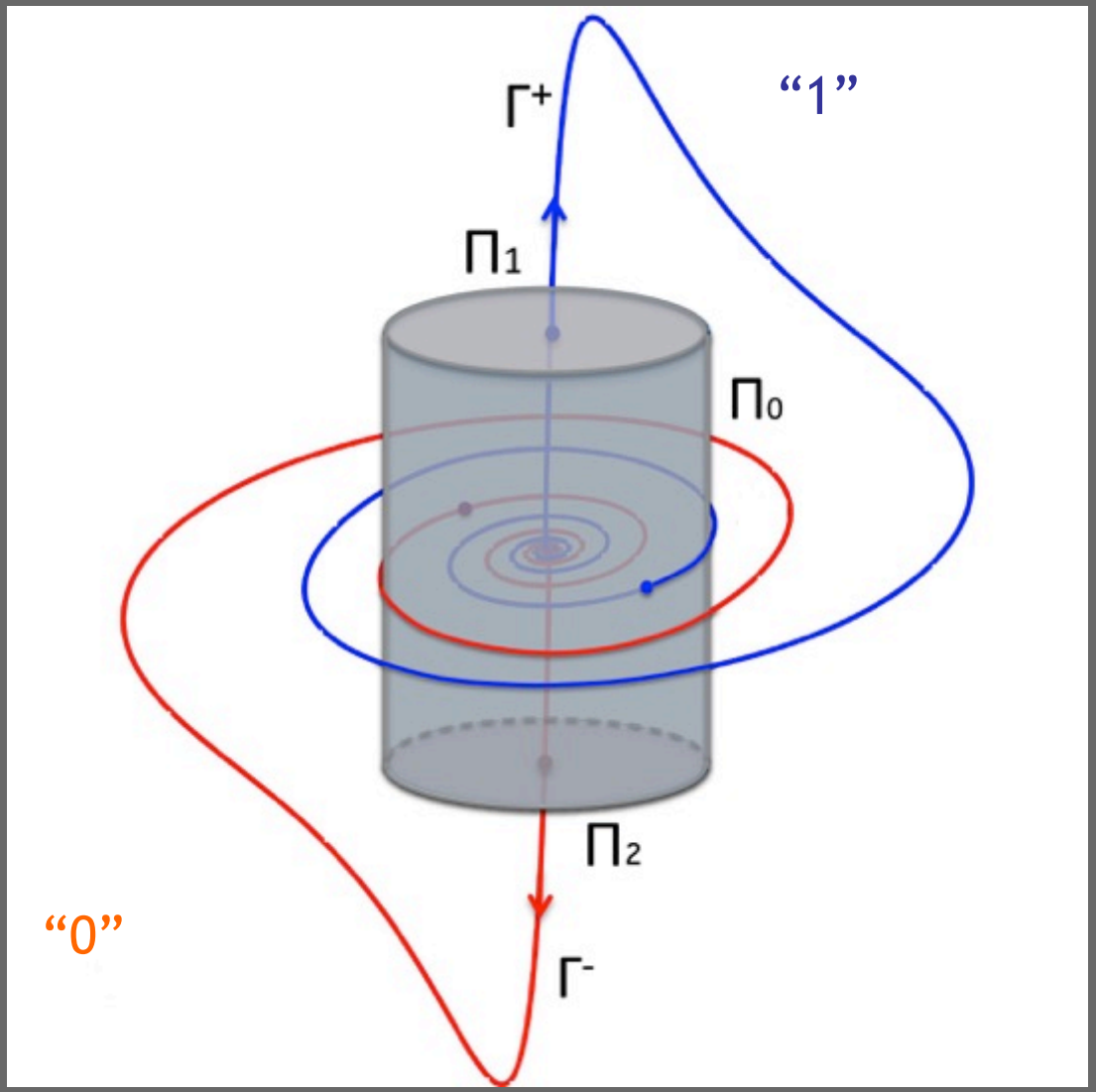

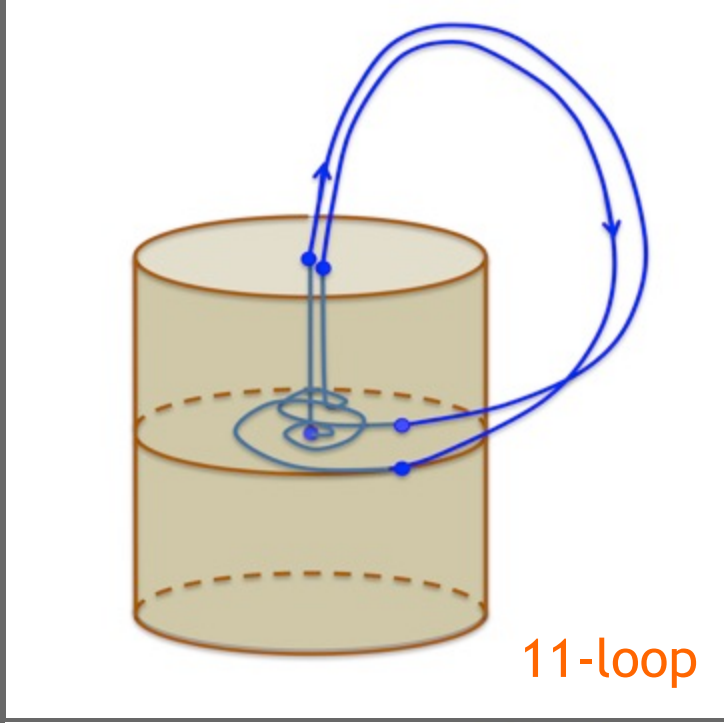

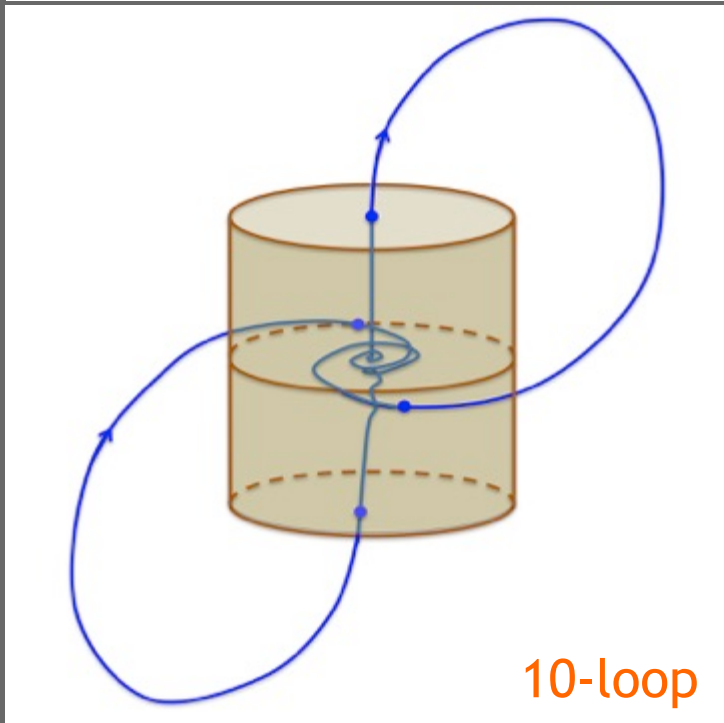

Secondary homoclinics

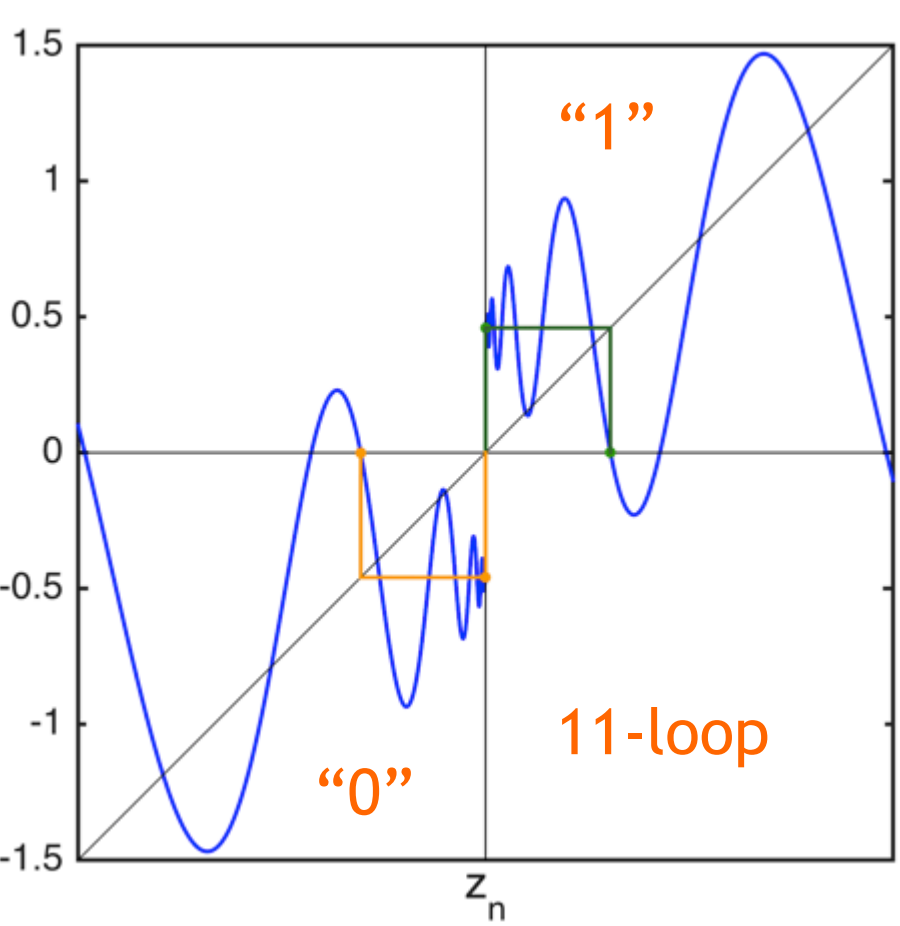

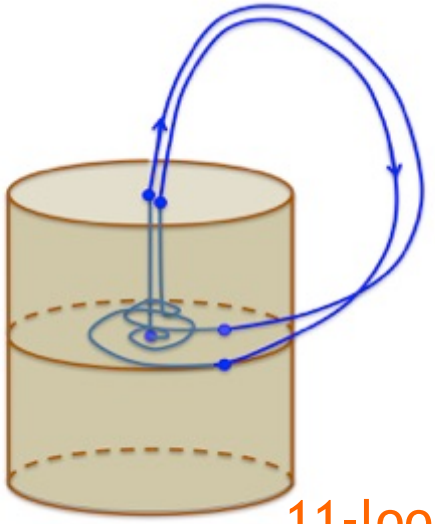

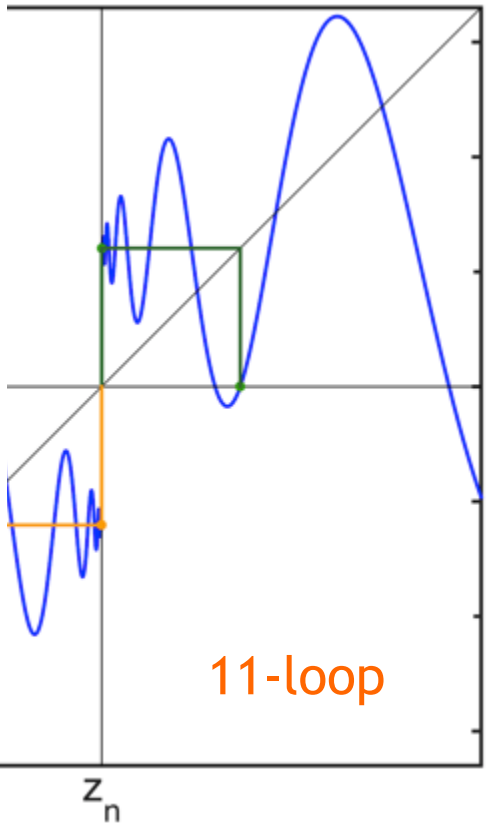

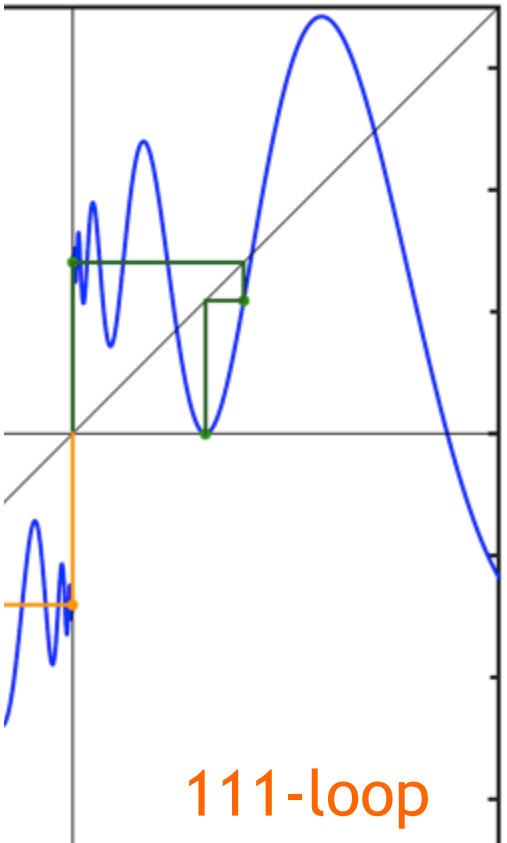

Secondary homoclinics

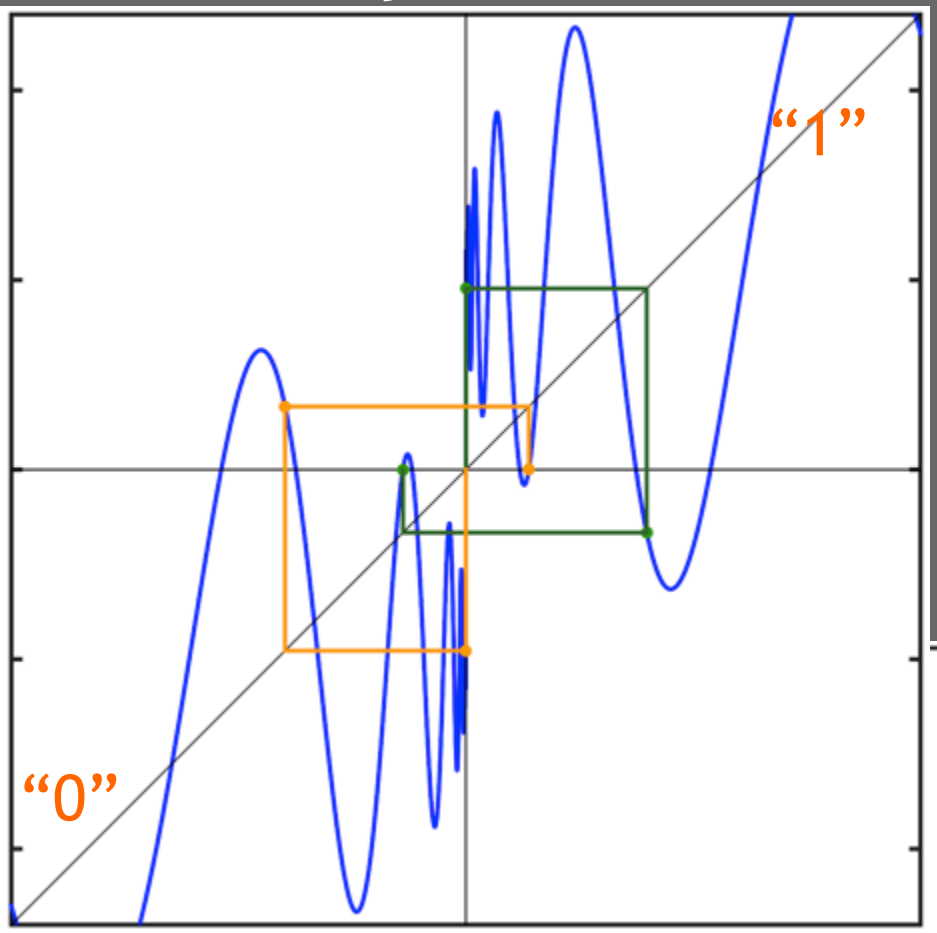

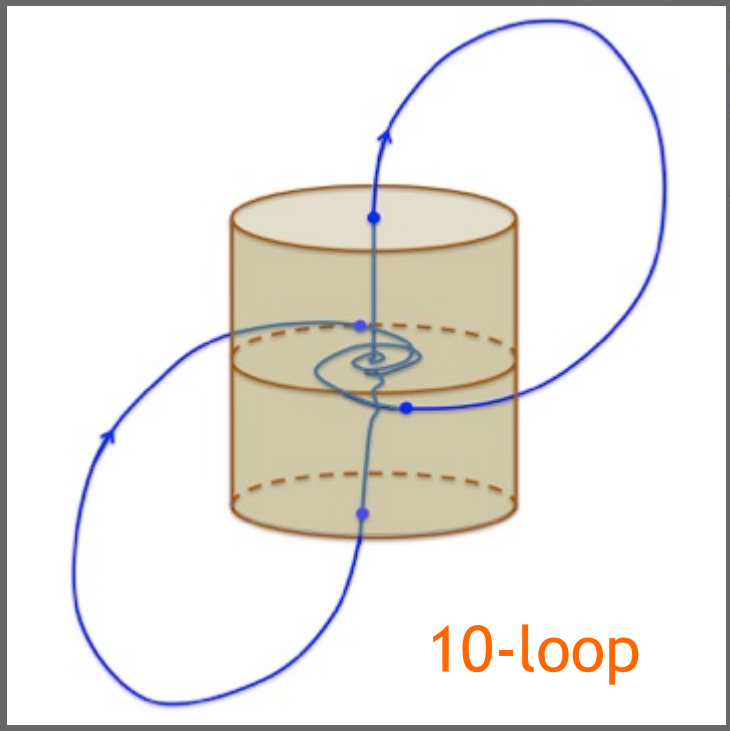

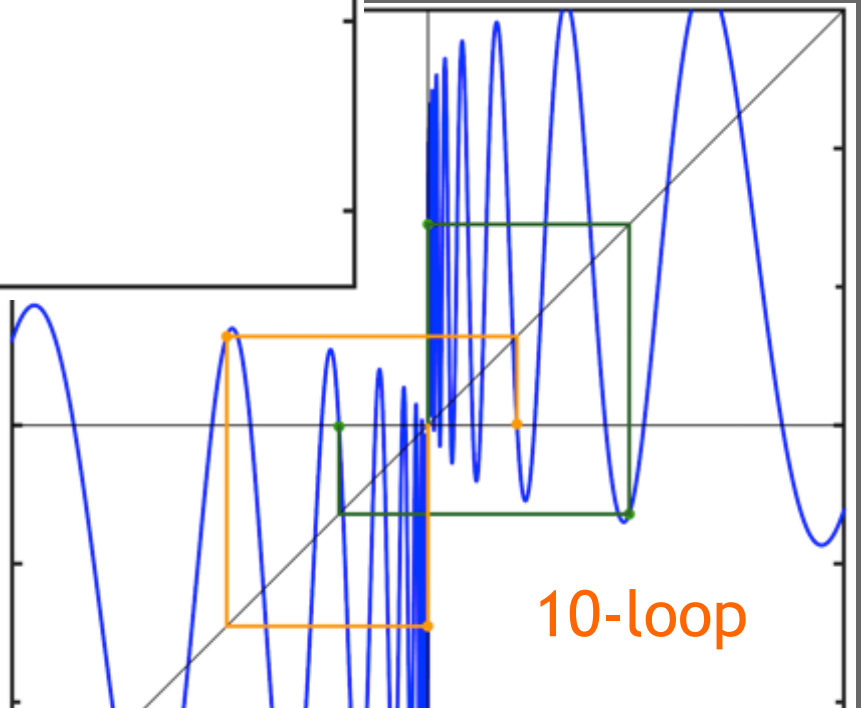

Department of Mathematics & Statistics
College of Arts & Sciences

$$\dot{x} = -\rho(\mu)x - \omega(\mu)y + P(x, y, z, \mu),$$
$$\dot{y} = \omega(\mu)x - \rho(\mu)y + Q(x, y, z, \mu),$$
$$\dot{z} = \lambda(\mu)z + R(x, y, z, \mu).$$

$$\nu(\mu) = \frac{\rho(\mu)}{\lambda(\mu)} < 1$$

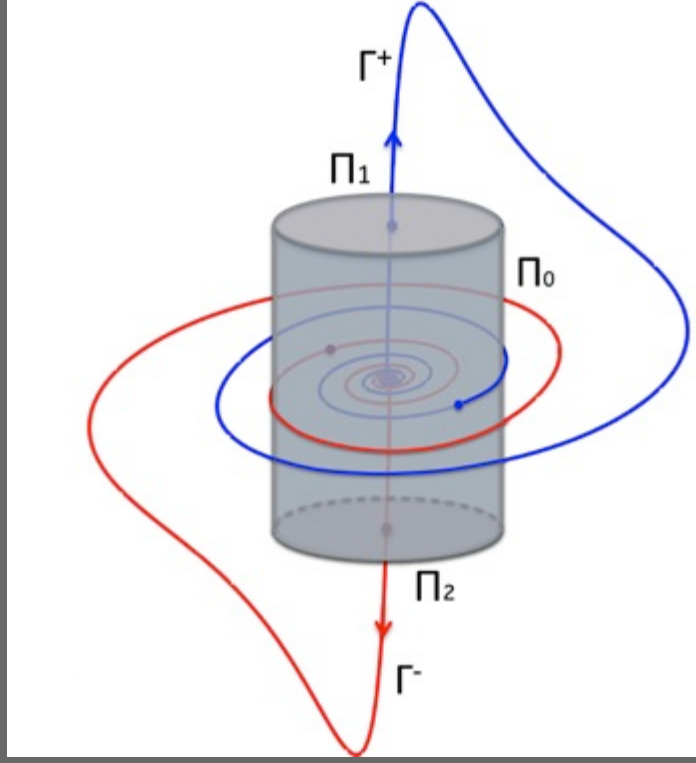

$$T(\Pi_0 \mapsto \Pi_0, \text{ if } z_0 > 0)$$

$$\tilde{\varphi}_0 = a_1\mu + A_0 R^{1-\nu_0} z_0^{\nu_0} \cos(\Omega_0 \ln z_0 + \phi_1 - \varphi_0) + O(z_0^{2\nu_0}),$$
$$\tilde{z}_0 = \mu - B_0 R^{1-\nu_0} z_0^{\nu_0} \sin(\Omega_0 \ln z_0 + \phi_2 - \varphi_0) + O(z_0^{2\nu_0}).$$

$$T'(\Pi_0 \mapsto \Pi_0, \text{ if } z_0 < 0)$$

$$\tilde{\varphi}_0 = \pi + a_1\mu - A_0 R^{1-\nu_0} (-z_0)^{\nu_0} \cos(\Omega_0 \ln(-z_0) + \phi_1 - \varphi_0) + O(z_0^{2\nu_0}),$$
$$\tilde{z}_0 = -\mu - B_0 R^{1-\nu_0} (-z_0)^{\nu_0} \sin(\Omega_0 \ln(-z_0) + \phi_2 - \varphi_0) + O(z_0^{2\nu_0}).$$

Structure of subsequent homoclinics

(1,1) or right double-loop homoclinic bifurcation

$$\varphi_1 = a_1\mu + A_0 R^{1-\nu_0}\mu^{\nu_0}\cos(\Omega_0 \ln\mu + \phi_1) + O(\mu^{2\nu_0}),$$
$$z_1 = \mu - B_0 R^{1-\nu_0}\mu^{\nu_0}\sin(\Omega_0 \ln\mu + \phi_2) + O(\mu^{2\nu_0}),$$

(1,1) double-loop homoclinic orbit occurs when $z_1 = 0$

$$\mu^{1-\nu_0} + O(\mu^{\nu_0}) = B_0 R^{1-\nu_0}\sin(\Omega_0 \ln\mu + \phi_2)$$

(1,0) or left double-loop homoclinic bifurcation

$$\varphi_1 = \pi + a_1\mu - A_0 R^{1-\nu_0}(-\mu)^{\nu_0}\cos(\Omega_0 \ln(-\mu) + \phi_1) + O((-\mu)^{2\nu_0}),$$
$$z_1 = -\mu - B_0 R^{1-\nu_0}(-\mu)^{\nu_0}\sin(\Omega_0 \ln(-\mu) + \phi_2) + O((-\mu)^{2\nu_0}).$$

(1,0) double-loop homoclinic orbit occurs when $z_1 = 0$

$$(-\mu)^{1-\nu_0} + O((-\mu)^{\nu_0}) = B_0 R^{1-\nu_0}\sin(\Omega_0 \ln(-\mu) + \phi_2)$$

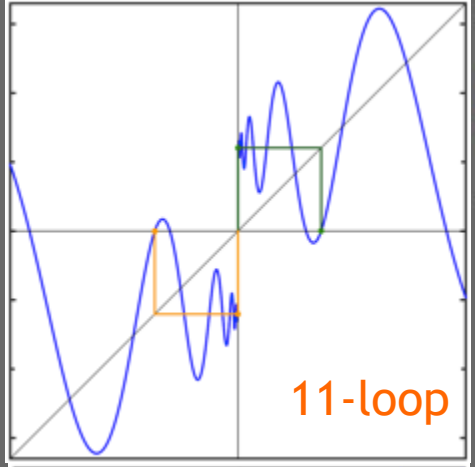

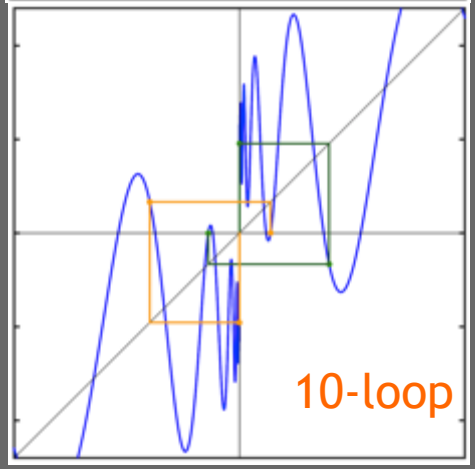

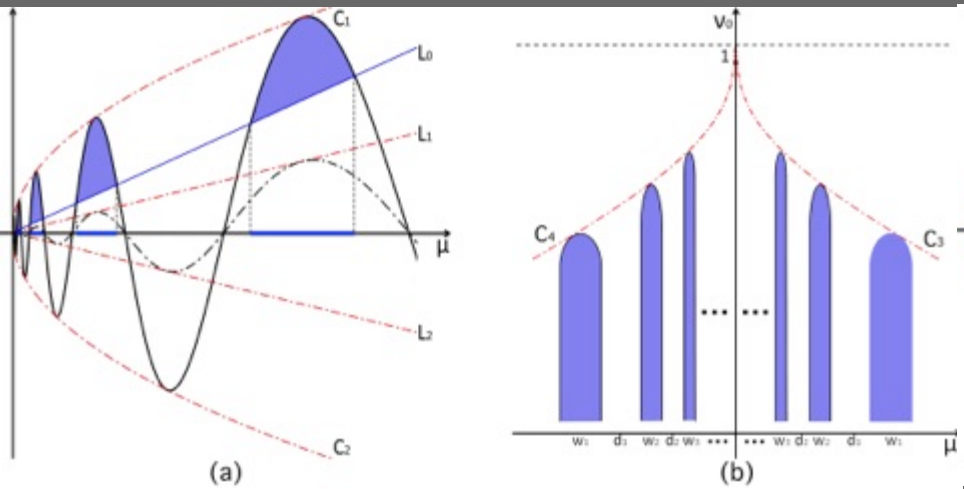

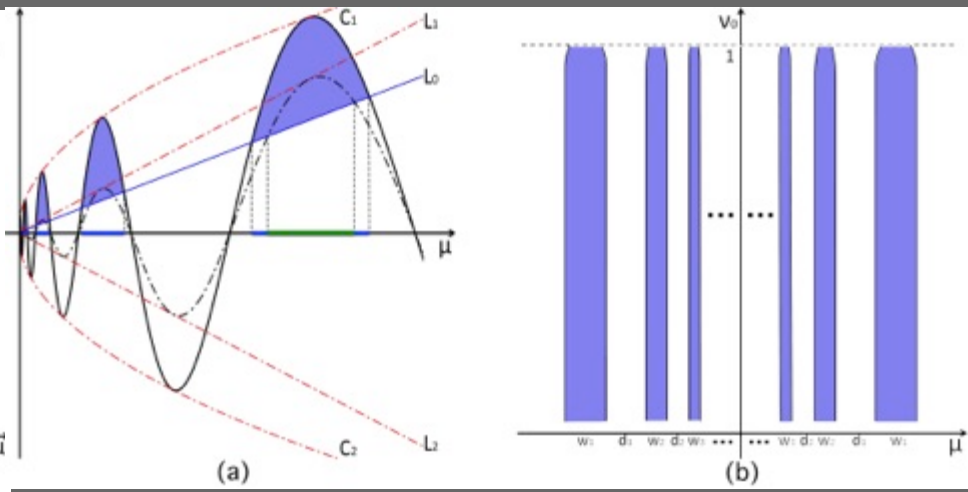

(1,1,1) or right triple-loop homoclinics

$$z_1 = \mu - B_0 R^{1-\nu_0} \mu^{\nu_0} \sin(\Omega_0 \ln \mu + \phi_2) + O(\mu^{2\nu_0}),$$
$$z_2 = \mu - B_0 R^{1-\nu_0} z_1^{\nu_0} \sin(\Omega_0 \ln z_1 + \phi_2) + O(z_1^{2\nu_0}).$$

The second equation is reduced to $sin(\Omega_0 ln z_1 + \phi_2) = 0$

$$z_1 \in I_m = (e^{-\frac{2m\pi}{\Omega_0} - \frac{\phi_2}{\Omega_0}}, e^{-\frac{2m\pi}{\Omega_0} + \frac{\pi}{\Omega_0} - \frac{\phi_2}{\Omega_0}})$$

where *m* is sufficiently large $\frac{|I_{m+1}|}{|I_m|} = e^{-\frac{2\pi}{\Omega_0}}$

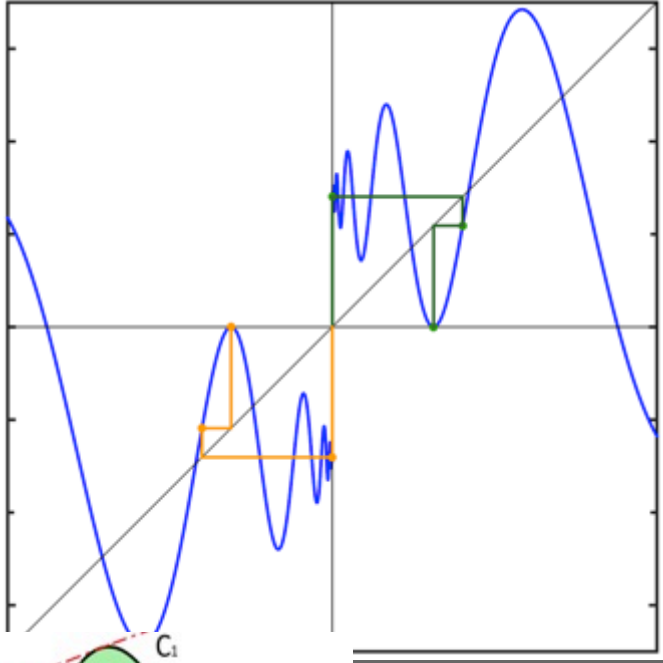

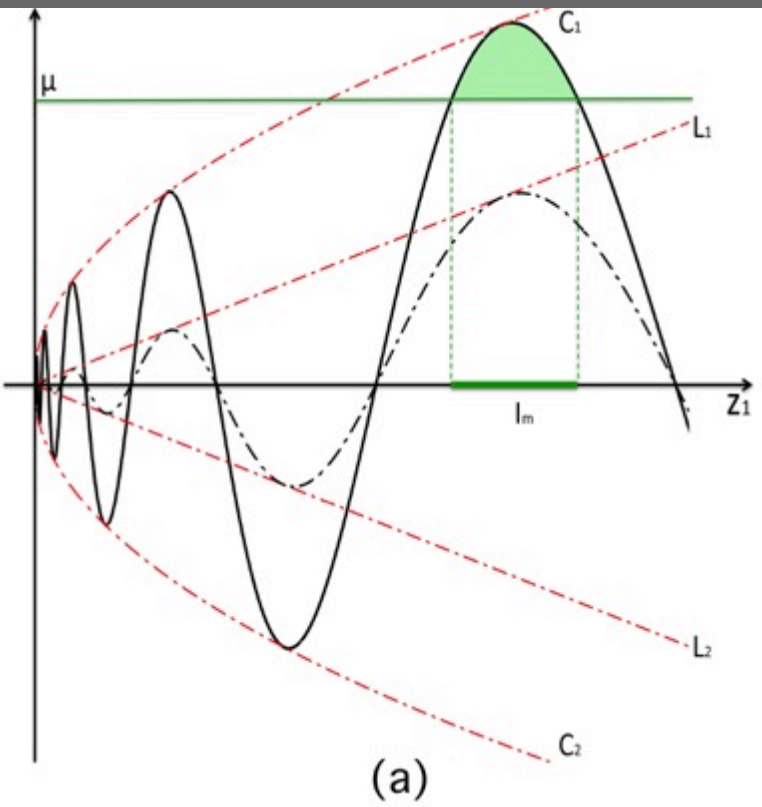

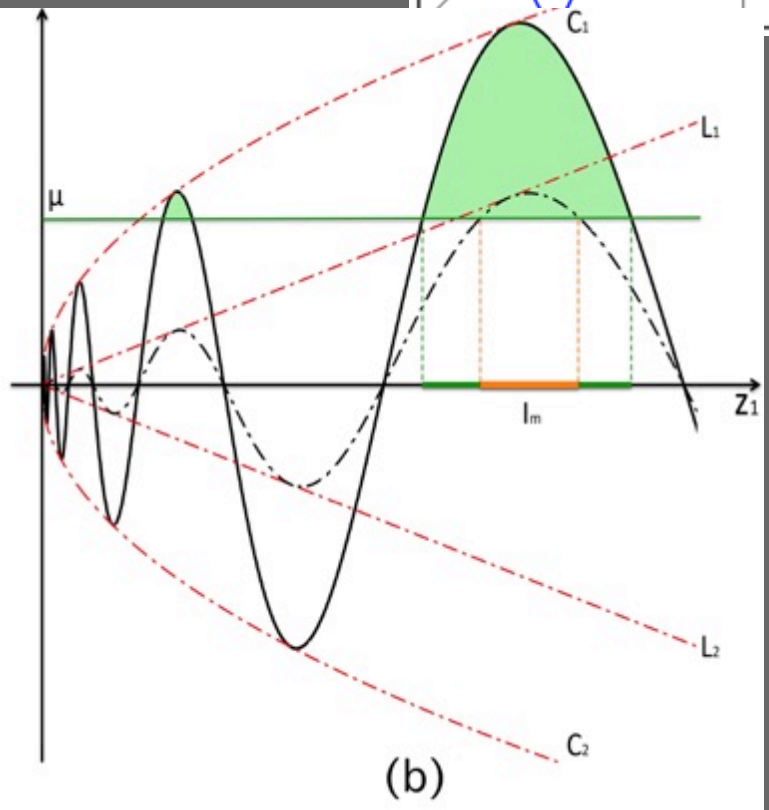

$$\mu - I_m = B_0 R^{1-\nu_0} \mu^{\nu_0} \sin(\Omega_0 \ln \mu + \phi_2)$$

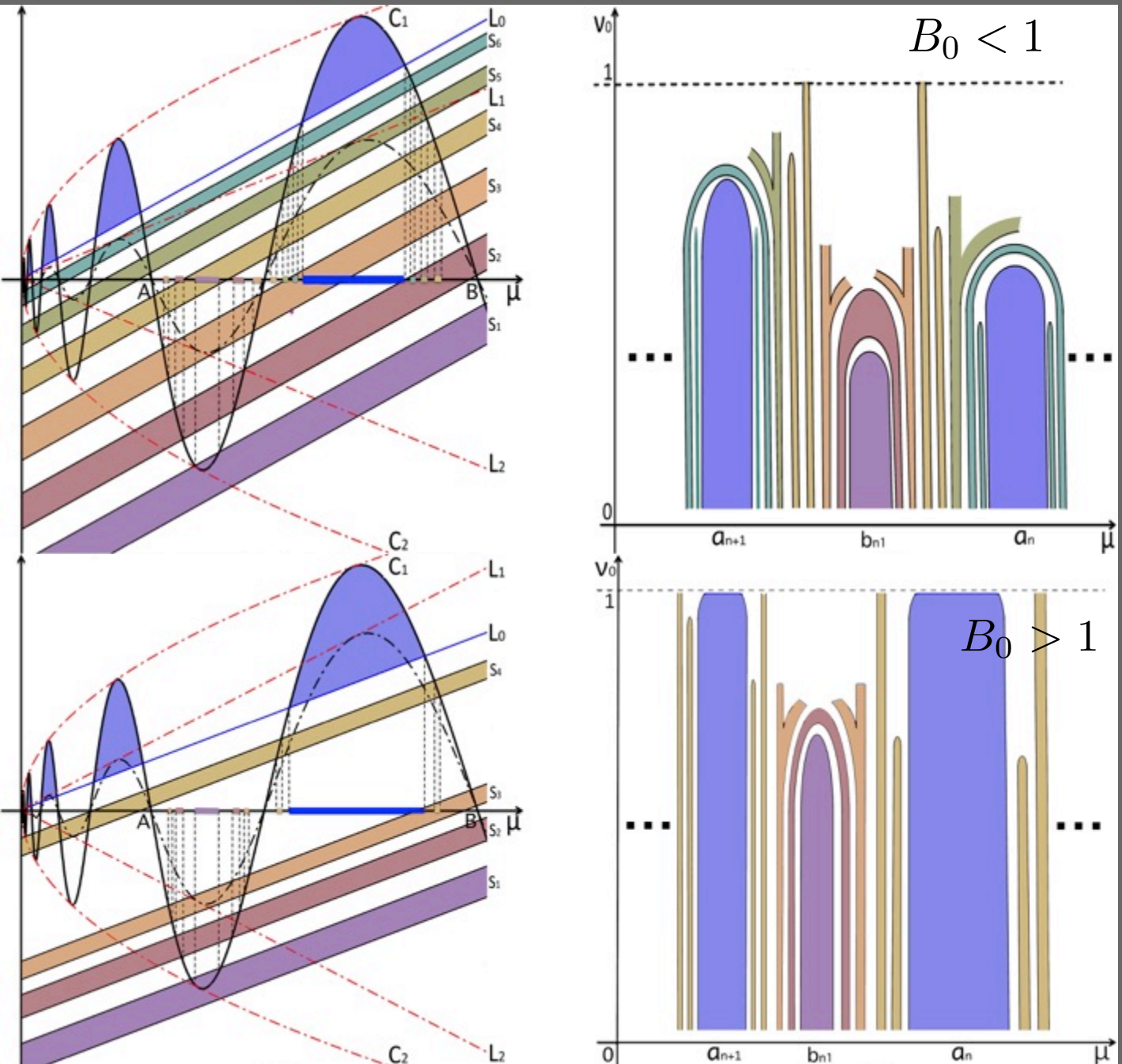

Secondary *versus* Ternary

Homoclinics

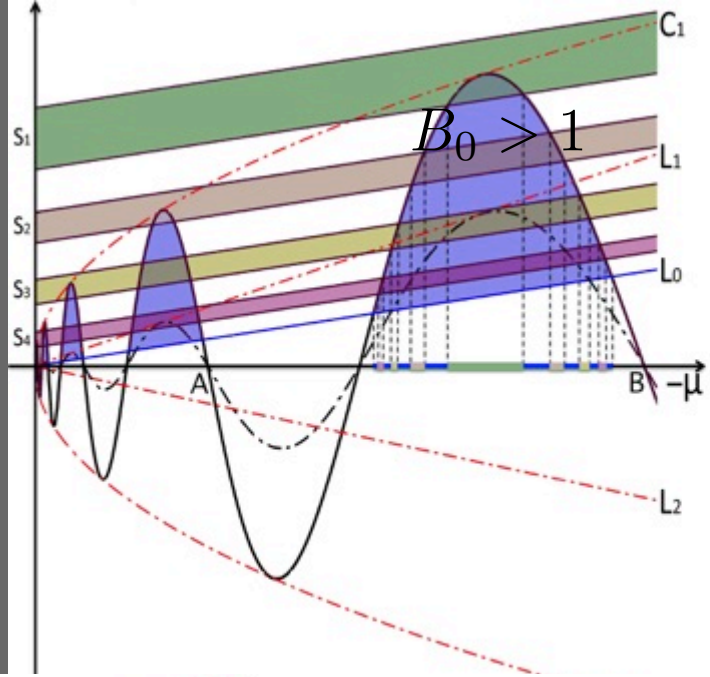

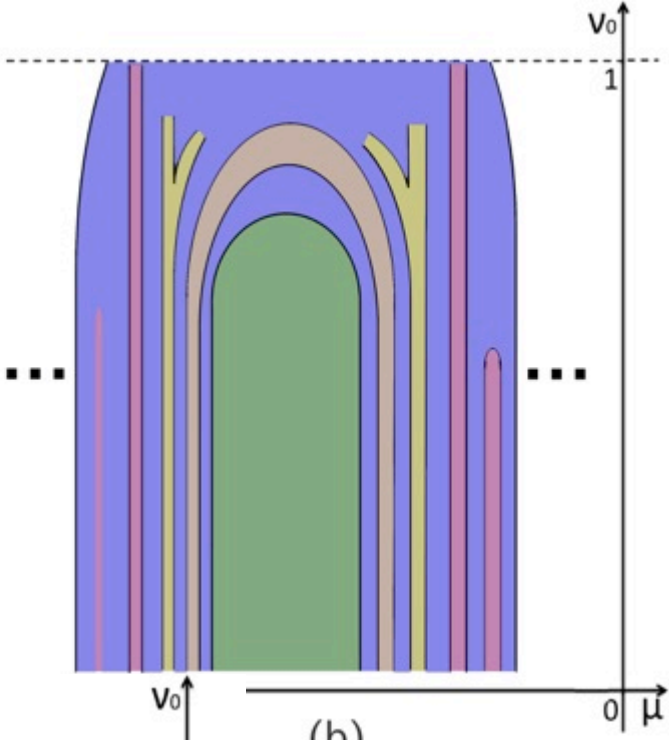

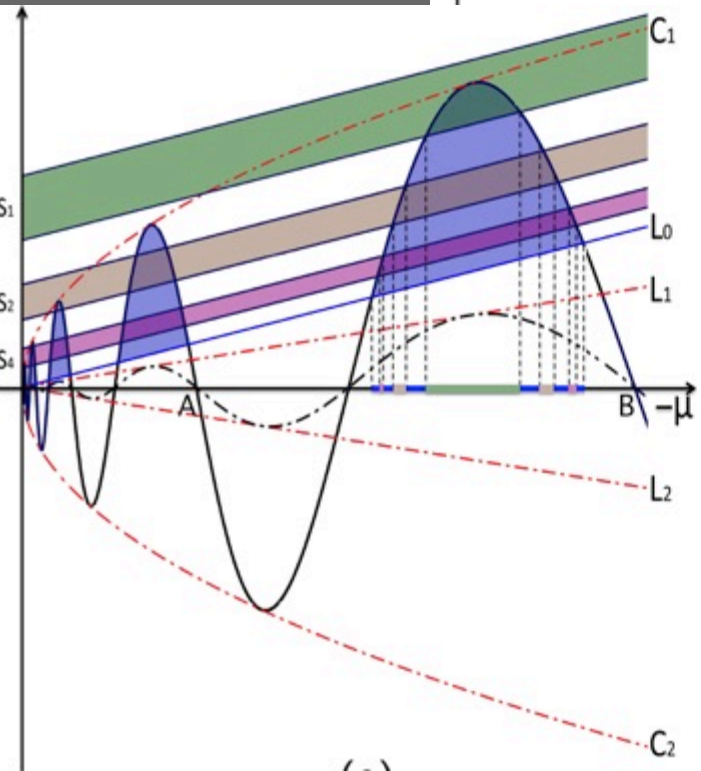

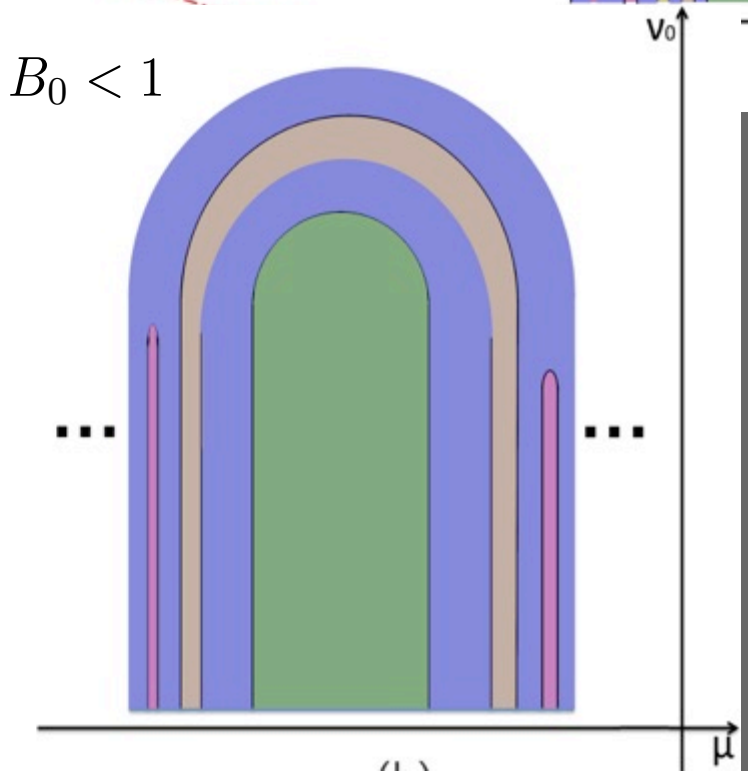

saddle-foci in the Chua circuit

$$\dot{x} = a(y + \frac{x}{6} - \frac{x^3}{6}),$$
$$\dot{y} = x - y + z,$$
$$\dot{z} = -by.$$

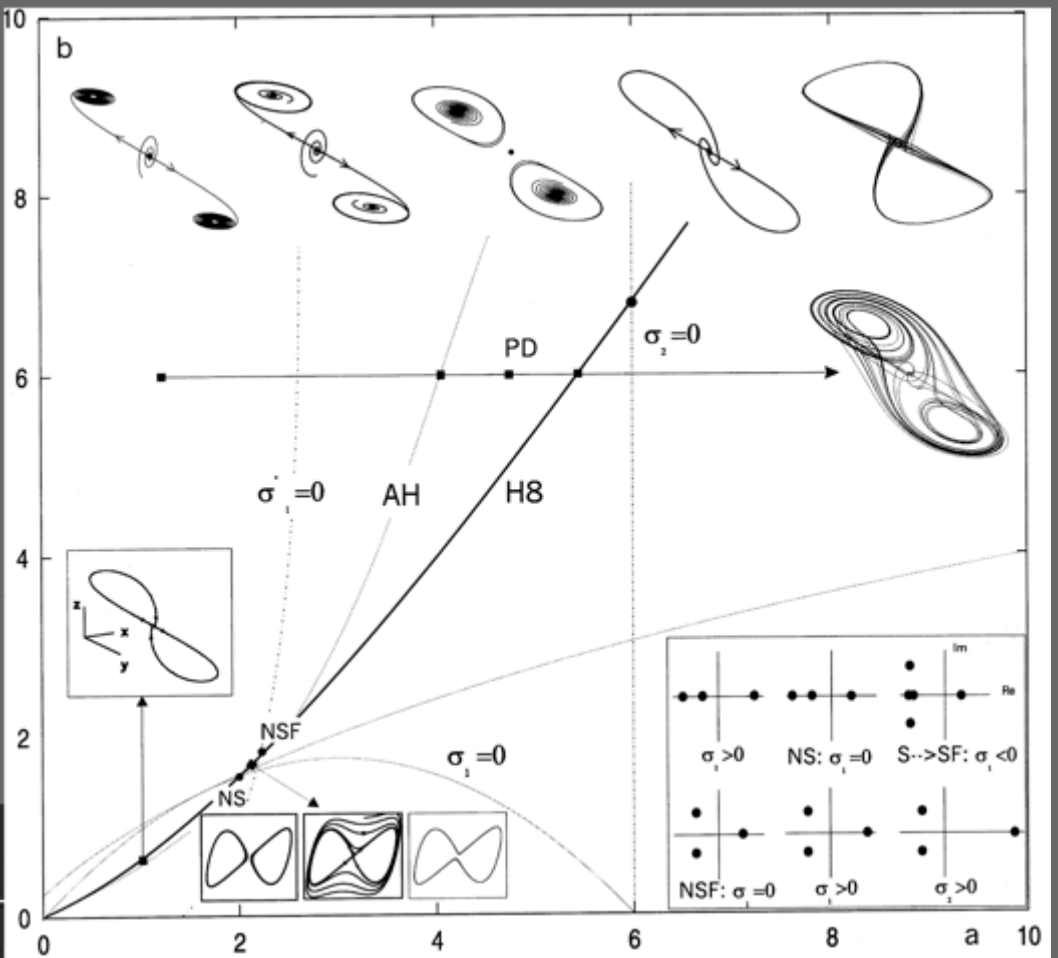

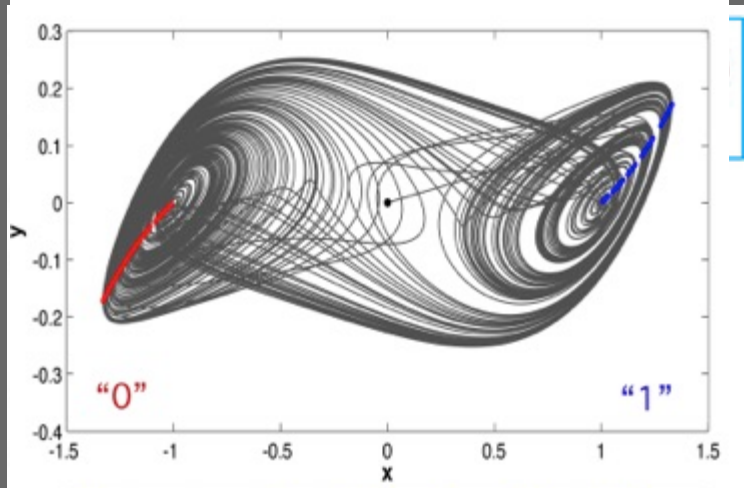

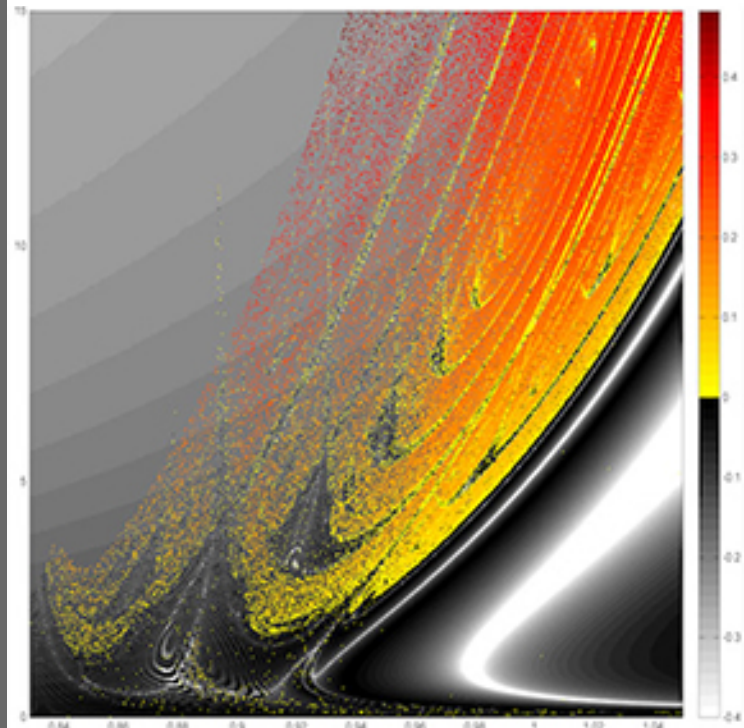

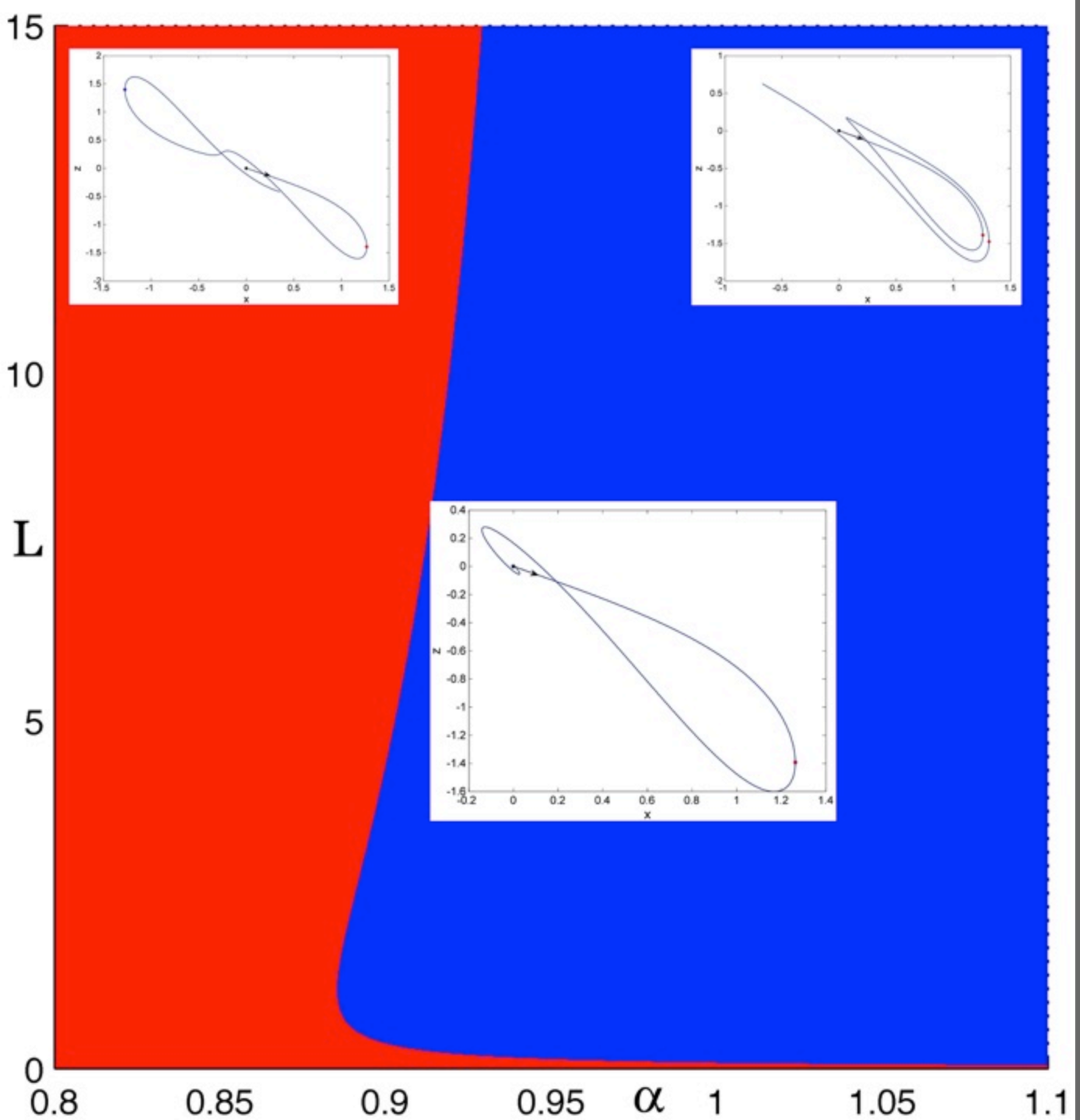
15
10
5
0
L
0.8
0.85
0.9
0.95
α
1
1.05
1.1

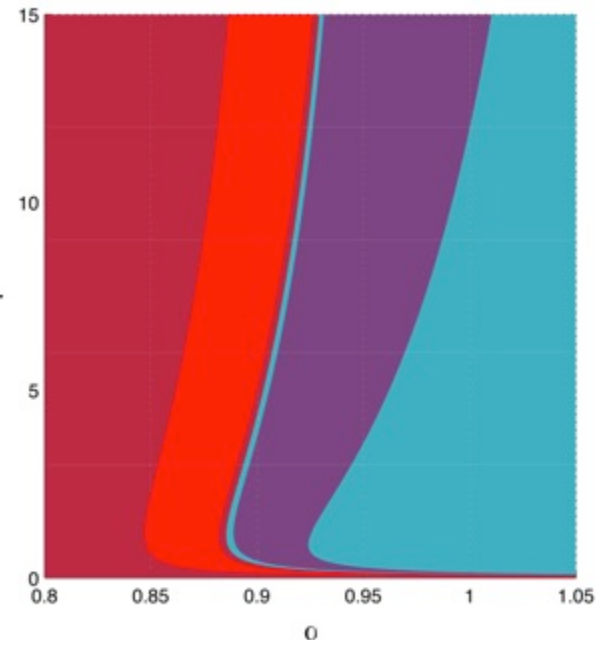
15
10
5
0
0.8
0.85
0.9
0.95
1
1.05
o

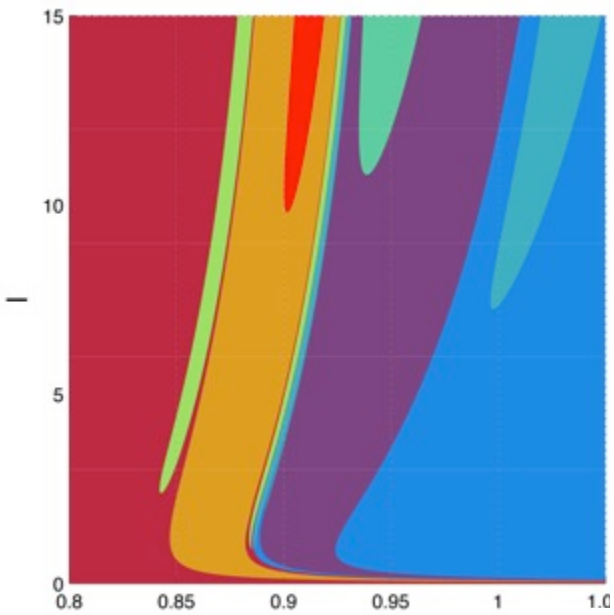
15
10
5
0
0.8
0.85
0.9
0.95
1
1.0
l

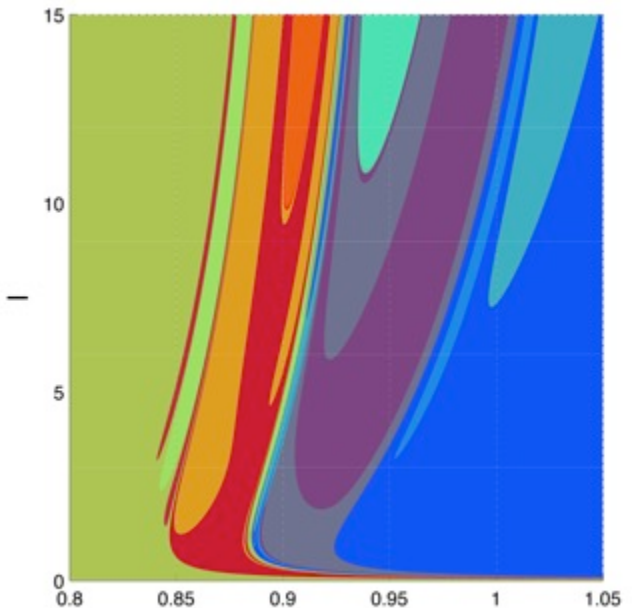
15
10
5
0
0.8
0.85
0.9
0.95
1
1.05
l

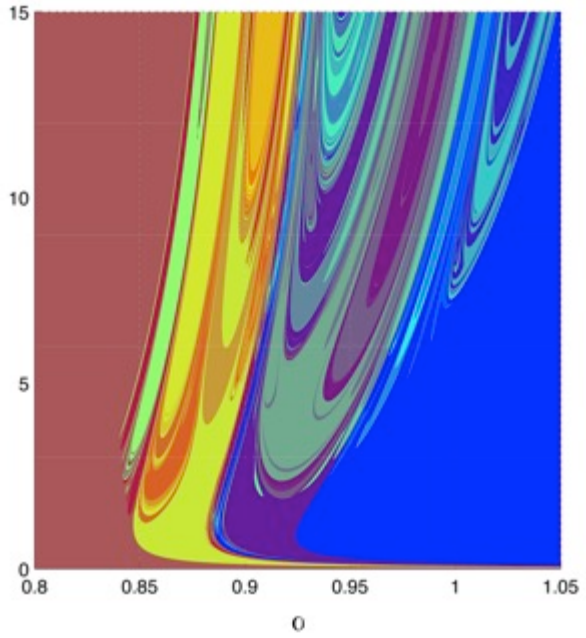
15
10
5
0
0.8
0.85
0.9
0.95
1
1.05
o

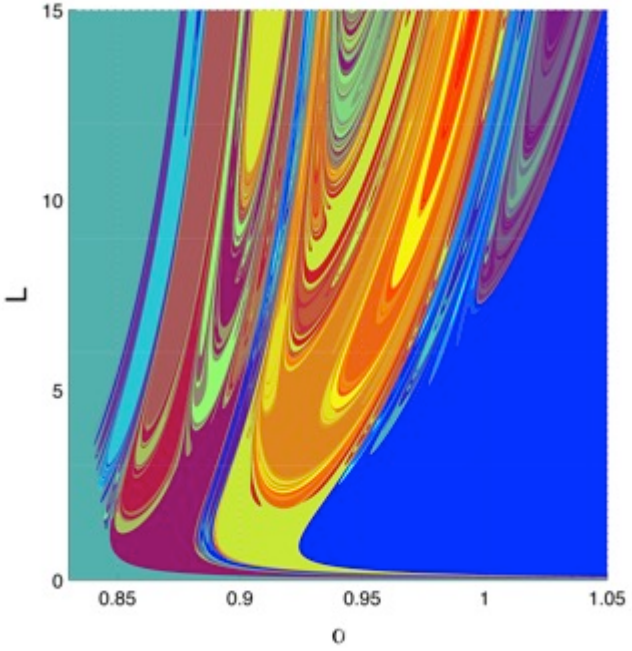
15
10
5
0
0.85
0.9
0.95
1
1.05
L
o

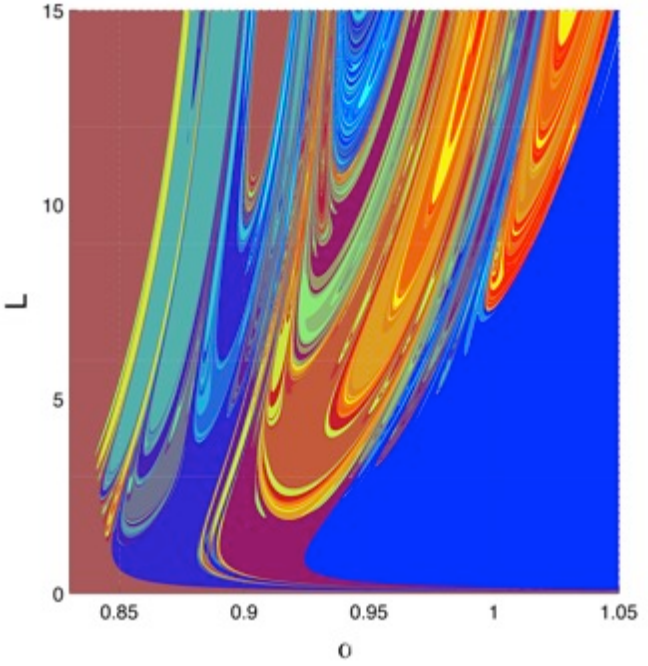
15
10
5
0
0.85
0.9
0.95
1
1.05
L
o

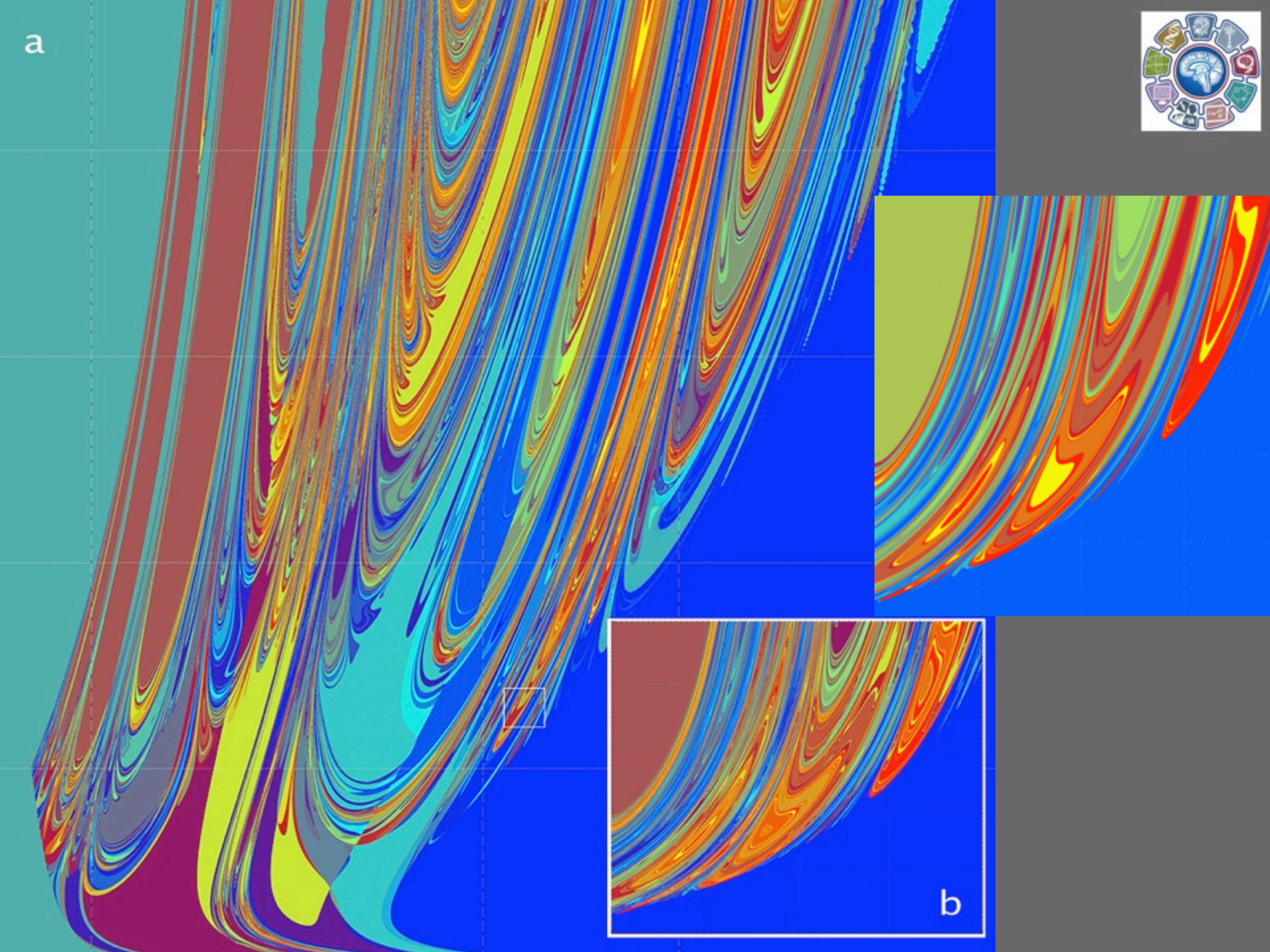
a
b

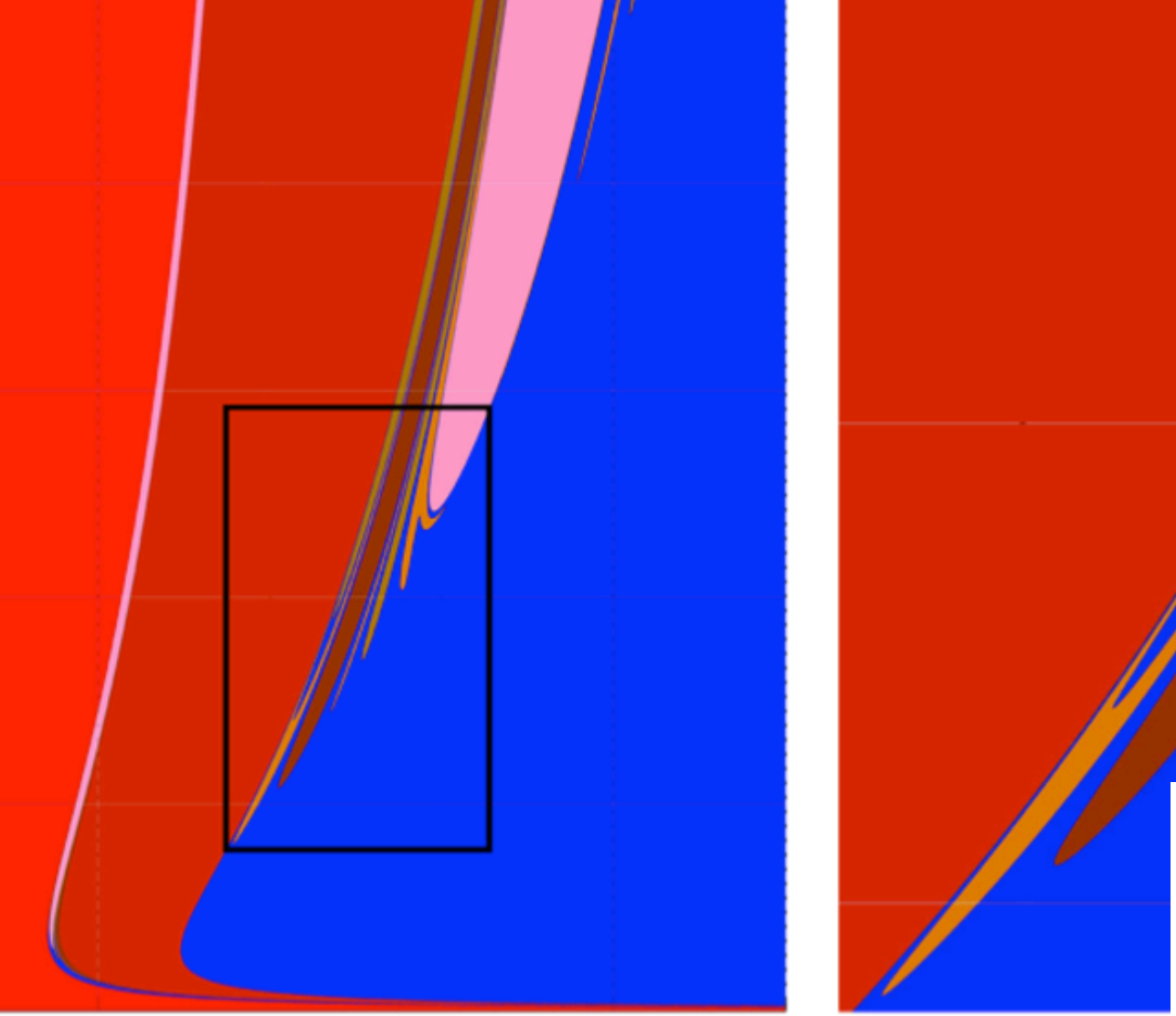

(a)

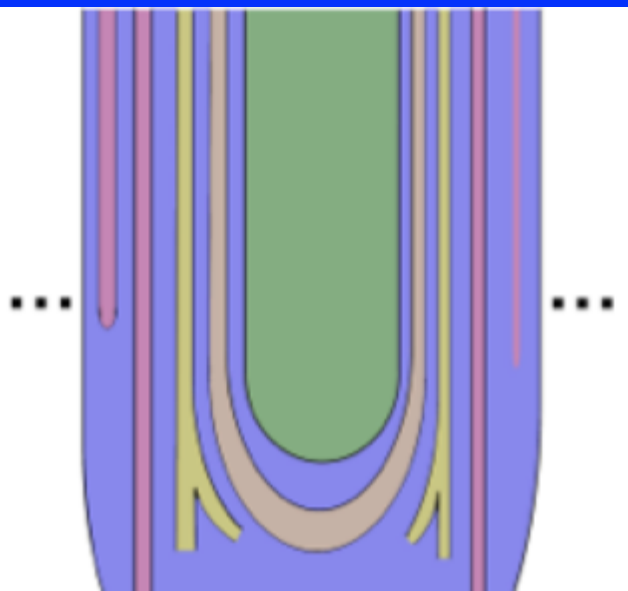

Bykov T-points

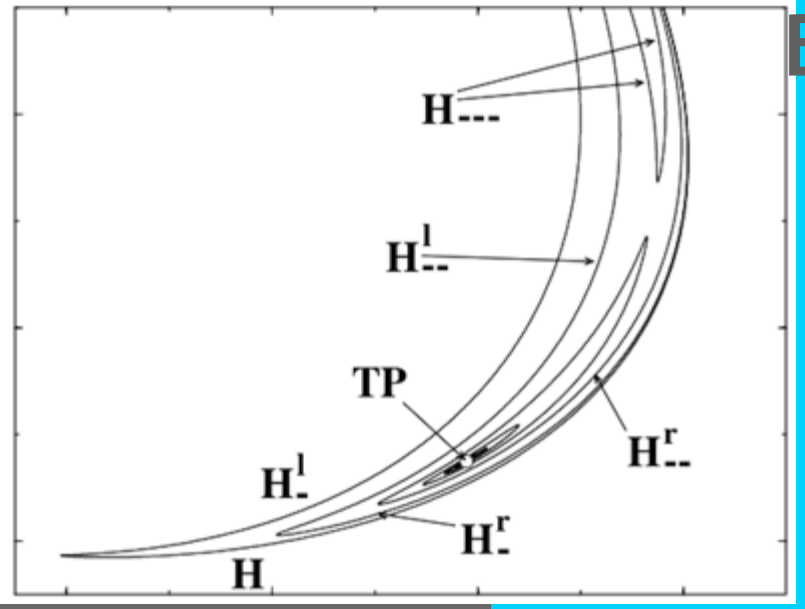

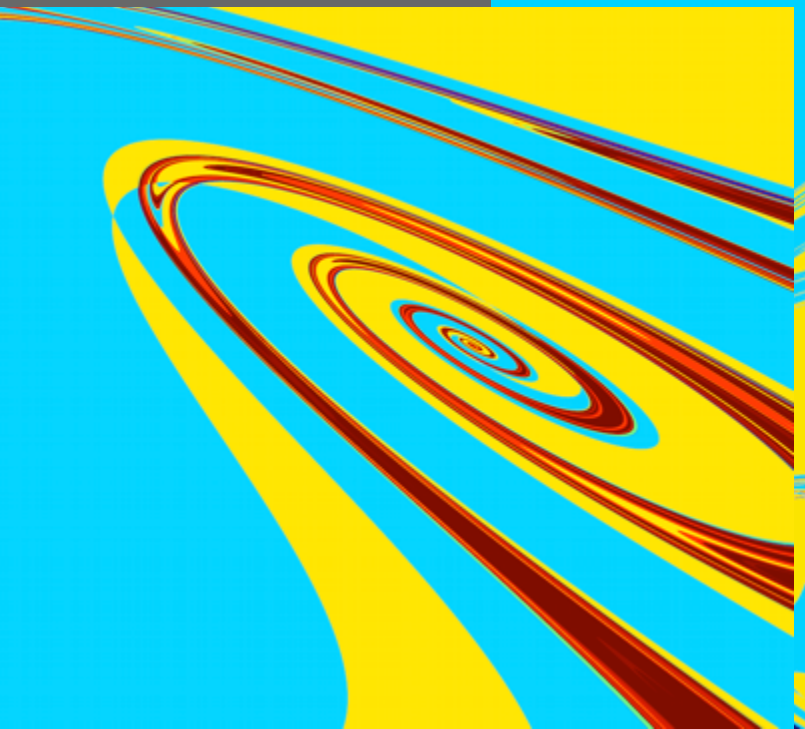

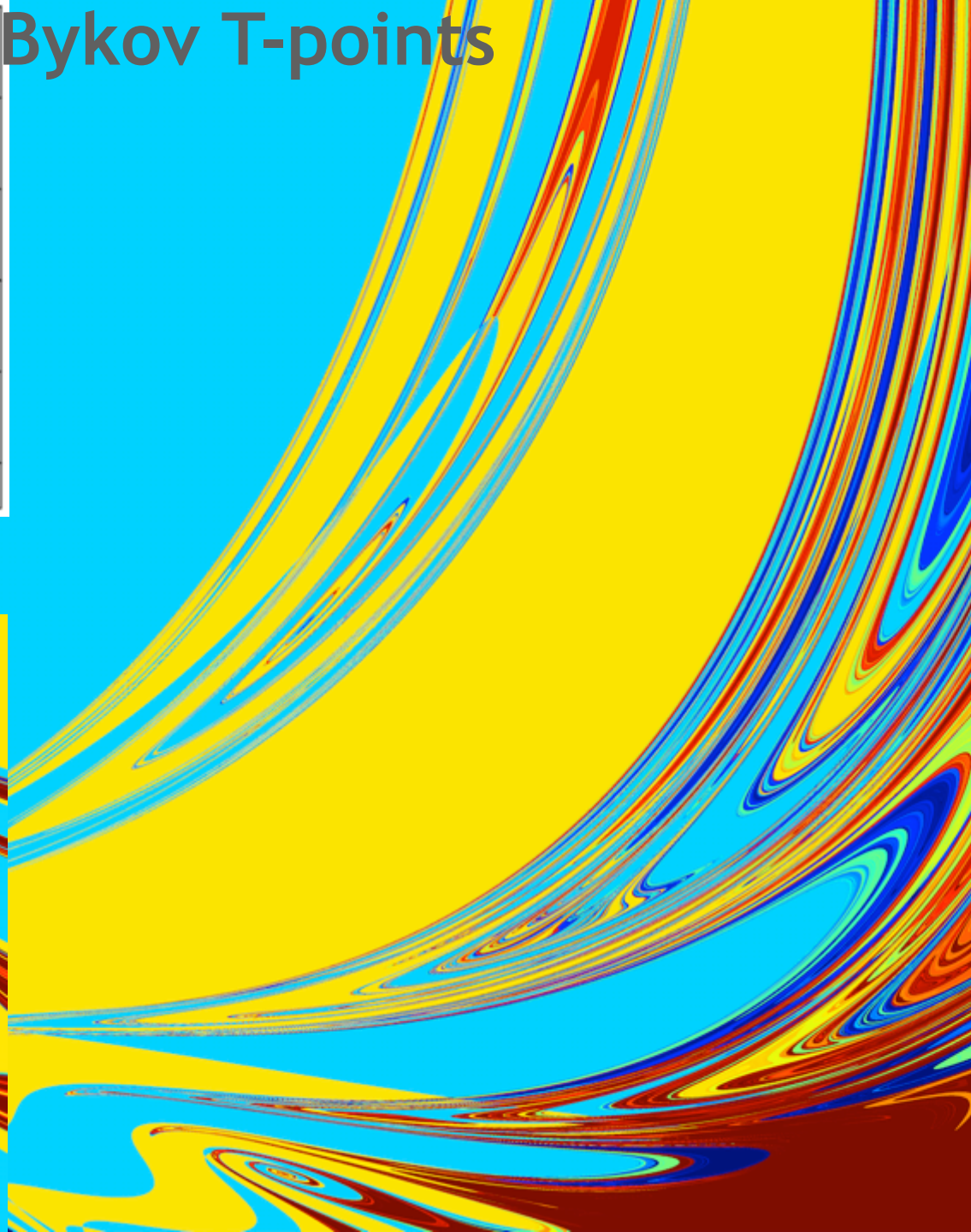

when Shilnikov meets Lorenz

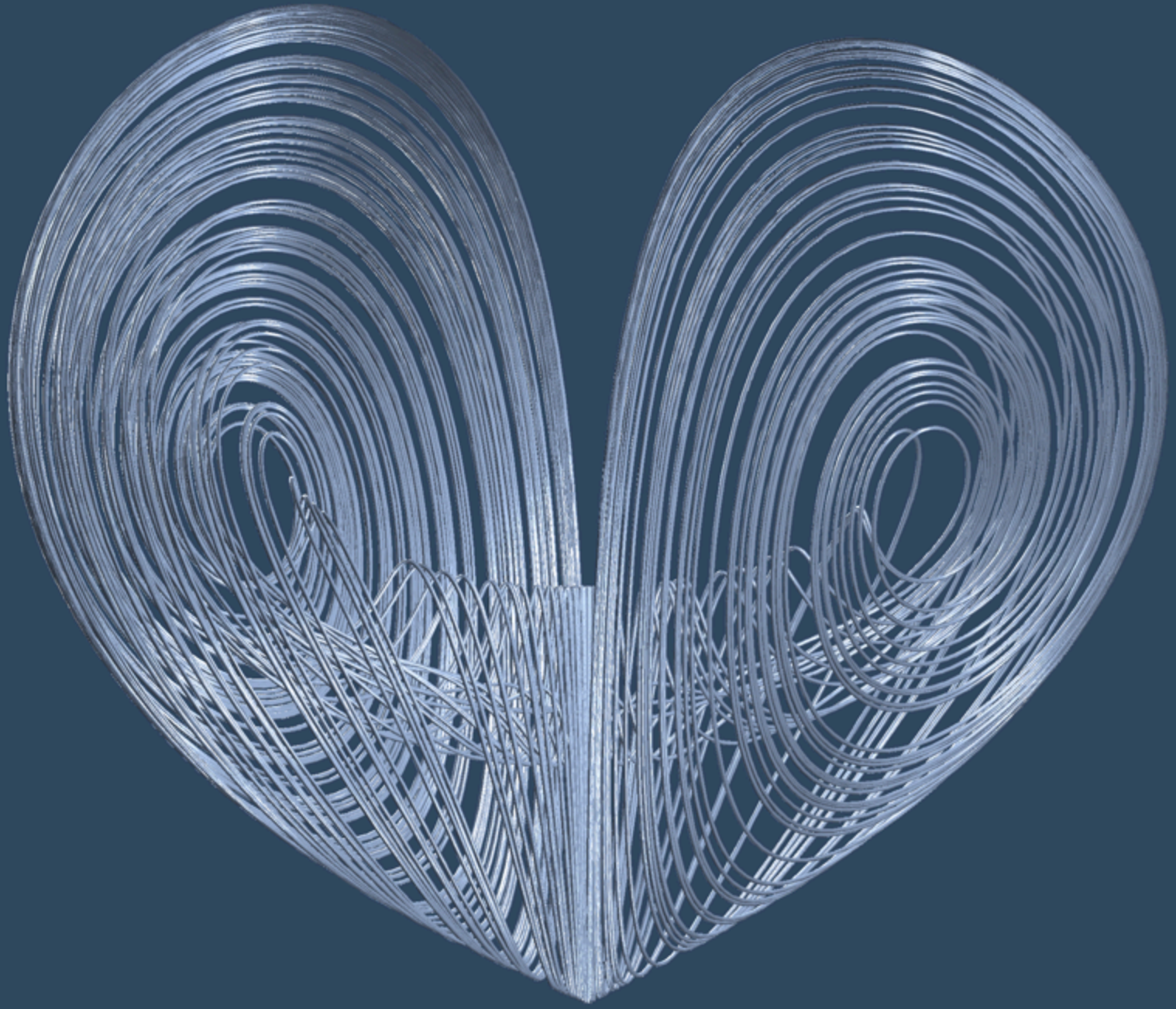

Shilnikov NeurDS lab

at 2015 Snowbirdie

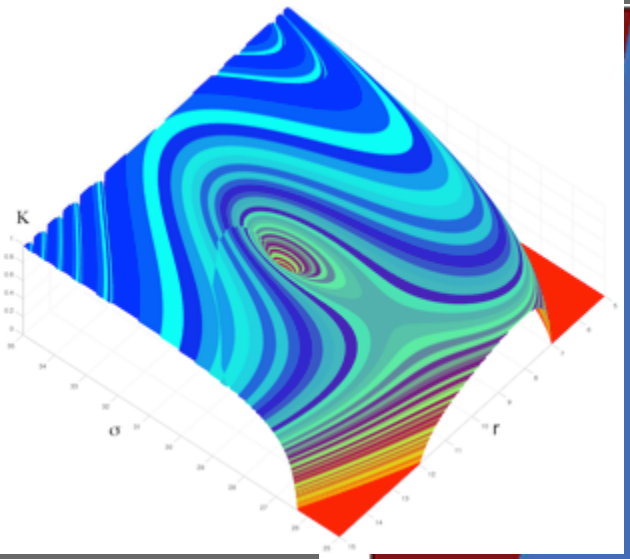
K
σ
r

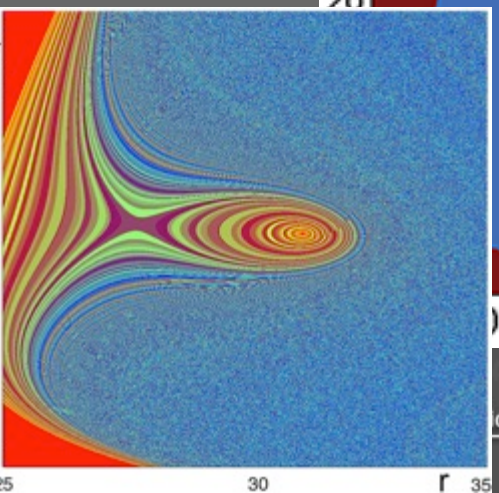
25
30
r
35

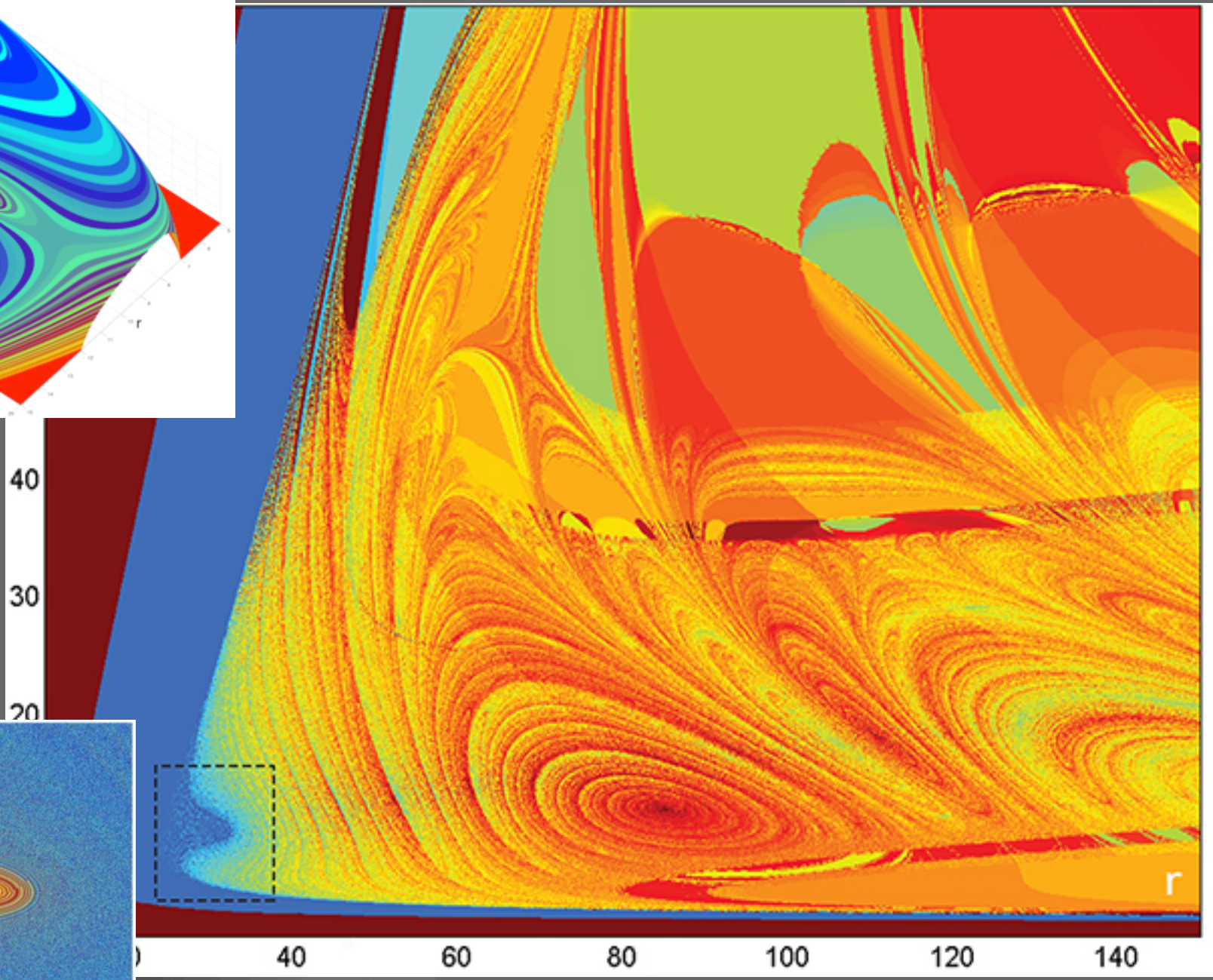
40
30
20
r
40
60
80
100
120
140

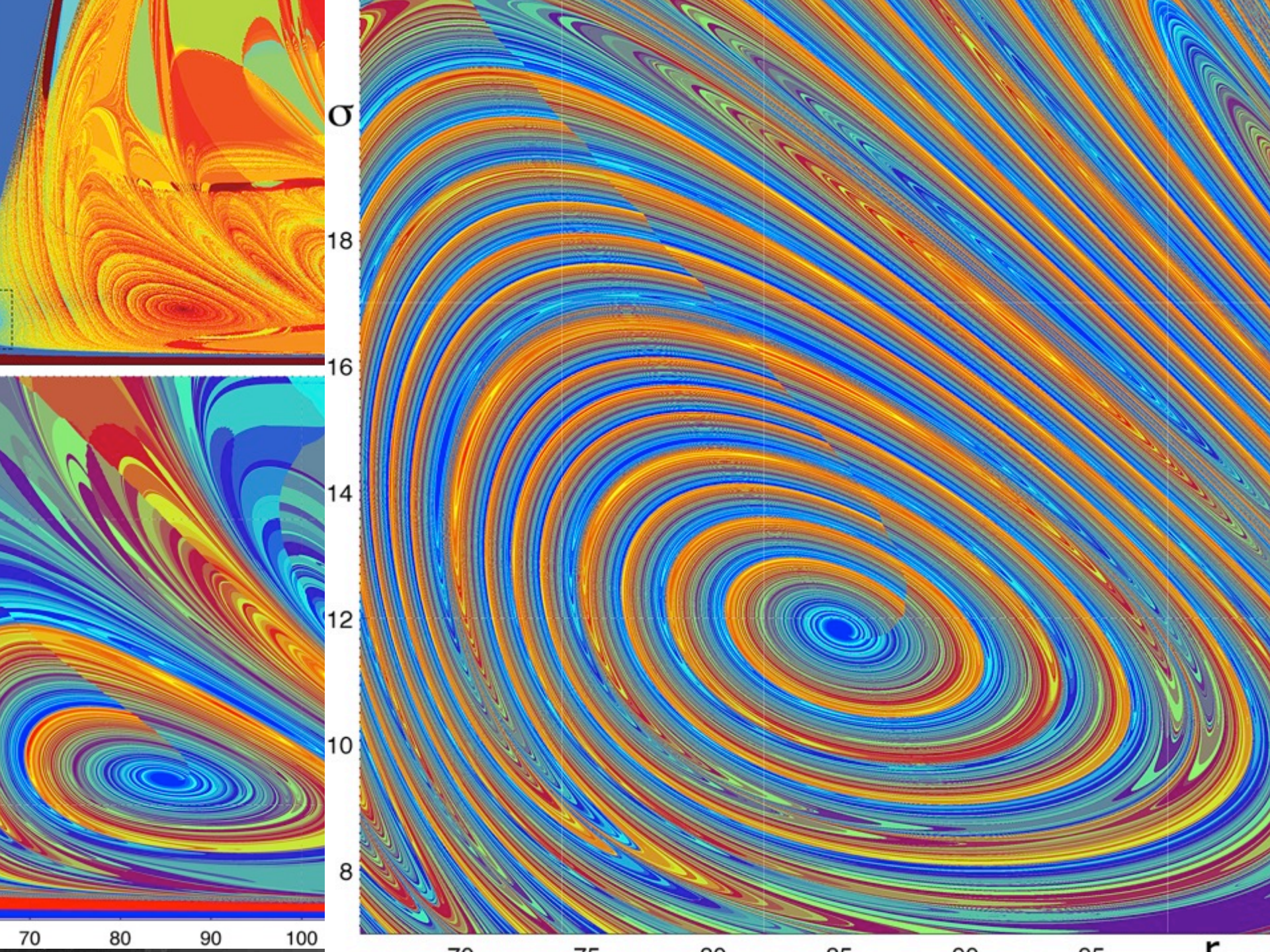
σ
18
16
14
12
10
8
70
80
90
100
r